The Impact of The Storage Facility on Performance Parameters of Aqueous Film-Forming Fire-Fighting Foam (AFFF) in Aviation Fire Protection

Nhlanhla Fortune Khanyi

Submitted in fulfilment of the academic

requirements for the degree of

MASTER OF ENGINEERING

in MECHANICAL ENGINEERING

in the

Department of Mechanical Engineering

Durban University of Technology

Durban

2023

DECLARATION

I, **Nhlanhla Fortune Khanyi**, declare that:

1. The research reported in this dissertation, except where otherwise indicated, is my original research.
2. The dissertation has not been submitted for any degree or examination at any other university.
3. This dissertation does not contain other persons' data, pictures, graphs, or other information unless specially acknowledged as being sourced from other persons.
4. This dissertation does not contain other persons' writing unless specially acknowledged as being sourced from other researchers. Where other written sources have been quoted, then:

a) Their words have been rewritten, but the general information attributed to them has been referenced.

b) Where their exact words have been used, then their writing has been placed in italics and inside quotation marks and referenced.

5. This dissertation does not contain text, graphics, or tables copied and pasted from the internet unless specially acknowledged, and the source is detailed in the dissertation and the reference sections.

May 2023.

Student: _____ 15 September 2023

Nhlanhla F Khanyi Date

Supervisor: _____ 15 September 2023

Pavel Y Tabakov

ACKNOWLEDGEMENTS

I would like to express my sincere gratitude to the following people for their assistance, guidance, and support during this study:

- My supervisor, Prof. P. Y. Tabakov for his continual guidance, advice, and mentorship throughout my research. His patience with my endless queries, extensive knowledge of engineering studies, and enthusiasm for the whole project were great motivations, and I am very thankful to him.
- My former colleague, Mapule Molabe for her continual assistance from the commencement of this report. You know this dissertation would have not even started without your technical expertise, and for that I thank you.
- My friend, Andile Ntanjana for his continual assistance in reviewing my report regularly and providing technical expertise was necessary.
- My friend, Yamkelani Mlunguza for her continual assistance in reviewing my report and guiding me in the right direction throughout the years.
- My brother, Siphesihle Mhlongo for his assistance with compiling the LaTeX version of this document. Although I did not finally submit it, but your effort is highly appreciated.
- I would also like to extend my sincere gratitude to my family members and my dearest friends for their unwavering support throughout my degree study.
- Special gratitude goes to National Research Foundation (NRF) for their funding (reference **MND200611530513**). It also brings me great pleasure to convey my appreciation to Columbus Stainless (Pty) Ltd for supplying the duplex stainless steel for experimental purposes. Lastly, the Durban University of Technology (DUT) for assisting with FTIR and DLS instruments.

DEDICATION

This dissertation is written in honor of my late brother, Sabelo ‘Spinza’ Mhlongo. You were always encouraging me to never stop learning; I know if you were still alive, you would’ve been far along with your academics. Your words of encouragement kept me going throughout this journey, and for that I dedicate this work to you, brother.

ABSTRACT

Aqueous Film Forming Foam (AFFF) has become a critical constituent within the aviation industry. It was declared by National Fire Protection Association (NFPA) as the sole optimum extinguishing agent for the suppression of hydrocarbon fires. Nevertheless, unexpected circumstances occur when AFFF is unable to perform as anticipated. In the aviation industry, this is normally noticed during periodic tests. As a consequence, it has become a necessity to monitor the performance of AFFF regularly.

This study aims to investigate the impact of the storage facility on the performance parameters of AFFF. The principal focus is on the materials that are commonly used to construct the storage tanks used for storing AFFF concentrate, namely mild steel, stainless steel, and high-density polyethene (HDPE). The aim focuses specifically on ascertaining if these materials affect the properties of AFFF concentrate, thus influencing its performance during firefighting. In this way, the optimization of these materials in such a way that they are compatible with AFFF concentrate becomes a feasible alternative.

A qualitative research approach was used to investigate the impact of the materials used to construct the storage tank for storing AFFF concentrate. Based on the aforementioned challenges, Fourier transforms infrared spectroscopy (FTIR), transmission electron microscopy (TEM), dynamic light scattering, and inductively coupled plasma atomic emission spectroscopy (ICP-AES) were all used for testing the materials. The findings from the primary research concluded that the three materials affect the foaming ability and foam stability of the AFFF solution, with the severity being the variance. HDPE was found to have a less severe impact, while stainless steel had a tolerable impact. The findings demonstrated that mild steel greatly affects the aforementioned performance parameters of AFFF. Based on these findings, it was concluded that mild steel is incompatible with AFFF concentrate.

The study recommends that mild steel should be heat treated to enhance its properties in such a way that it is innocuous to AFFF concentrate. The study further recommends that other materials, such as fibreglass and cross-linked polyethene (XLPE), be established as potential materials for constructing AFFF storage facilities.

RESEARCH OUTPUTS

Journal article:

Khanyi, N. F. and Tabakov, P. Y. 2023. The impact of mild steel, stainless steel, and HDPE on the foaming ability and foam stability of AFFF in aviation . FAM-23-0028 (Under review).

TABLE OF CONTENTS

LIST OF FIGURES

LIST OF TABLES

NOMENCLATURE

P	*Pressure*	*Pa*
V	*Velocity*	m/s
H	*Height*	*m*
G	*Gravitational acceleration*	m/s^2
ρ	*Density*	kg/m^3
Q	*Flowrate*	m^3/s
A	*Cross-sectional area*	m^2
M	*Mass*	*kg*
C_p	*Specific heat capacity*	$kJ/kg.℃$
ΔT	*Temperature difference*	℃
K	*Thermal conductivity*	$W/m.℃$
Δr	*Distance difference*	*m*
H	*Hydrogen*	
C	*Carbon*	
O	*Oxygen*	
OH	*Hydroxide*	
H_3O	*Oxonium*	

H_2O	*Water*	
R	*Aryl, Alkyl, or Acyl*	
Si	*Silicon*	
α, β	*Probability*	
$G(X)$	*Number of crosslinking*	
$G(S)$	*Number of scissions*	
F	*Force*	N
S_p	*Minimum proof strength*	Pa
k	*Stiffness*	N/mm^2
L	*Length*	m
S	*Welding speed*	m/s
η	*Efficiency*	%
D_T	*Translational diffusion coefficient*	m^2/s
R_H	*Hydrodynamic radius*	m
K_b	*Boltzmann constant*	J/K
T	*Temperature*	K
η	*Viscosity of the medium*	Ns/m^2
b	*Constant of the diffusing molecules*	

LIST OF ACRONYMS

AFFF	-	Aqueous film-forming foam
FAA	-	Federal Aviation Administration
NAA	-	National Aviation Authority
NFPA	-	National Fire Protection Association
FP	-	Fluoro protein foam
FFFP	-	Film-forming fluoro protein foam
AR-AFFF	-	Alcohol-resistant aqueous film-forming foam
AR-AFFFP	-	Alcohol-resistant film-forming fluoro protein foams
JP-4	-	Jet propellant
Ph	-	Potential for hydrogen
AHJ	-	Authority having jurisdiction
CAA	-	Civil aviation authorities
ICAO	-	International civil aviation authority
CAF	-	Compressed air form
NRCC	-	National Research Centre of Canada
NDT	-	Non-destructive testing
LLDPE	-	Linear low-density polyethene
FCC	-	Face-centred cubic

HCP	-	Hexagonal closed pack
BCC	-	Body-centred cubic
OSHA	-	Occupational Safety and Health Act
SAIW	-	The Southern African Institute of Welding
FEA	-	Finite element analysis
ACSA	-	Airports Company South Africa
Cr	-	Chromium
Ni	-	Nickel
Mo	-	Molybdenum
HSLA	-	High-strength low-alloy steel
RH	-	Relative humidity
OSD	-	On-site Stormwater Detention
UN/ECE	-	United Nations Economic Commission for Europe
TOW	-	Time of wetness
ISO	-	International Standardization Organization
TEM	-	Transmission Electron Microscopy
PE	-	Polyethylene
LDPE	-	Low-density polyethene
MDPE	-	Medium-density polyethene

HDPE	-	High-density polyethene
FTIR	-	Fourier Transform Infrared Spectroscopy
TEM	-	Transmission Electron Microscopy
DLS	-	Dynamic Light Scattering
ICP-AES	-	Inductively Coupled Plasma Atomic Emission Spectroscopy

CHAPTER 1: INTRODUCTION

1.1 Introduction

This chapter provides an overview of the research content structure and the background to the questions underlying this study. The aims of the study are exhaustively outlined in terms of the research outcomes it seeks to achieve. The motivations for this study are clearly stated. In addition, the format/layout of the entire dissertation is briefly discussed, and the content of the next chapter is outlined.

1.2 Background to the Problem

Fire protection is a critical sector in any aviation industry, which has given rise to differing opinions on compliance standards. Aviation accidents are devastating, given the loss of life and costly equipment to be expected. In aviation, fire-fighting foam, especially Aqueous Film Forming Foam (AFFF), is the optimum means of extinguishing flammable or combustible fires. Thus, any aviation industry must adhere to appropriate compliance standards and be fully equipped for any contingency in the event of unforeseen fire related accidents.

Periodic training is mandatory in all aspects of aviation fire protection to ensure that the industry's firefighting skills and resources meet Federal Aviation Administration (FAA), National Aviation Administration (NAA), and National Fire Protection Association (NFPA) standards for rapid response during accidents. The main priority of AFFF is to suppress the fire and give possible victims more time to escape during an accident. However, according to relevant compliance standards, all of this must be accomplished in one minute or less after arrival at the accident scene. Unforeseen circumstances often arise where the AFFF cannot perform as expected and takes a longer period of time to effectively suppress fires. This could result in the loss of life and damage to property. Thus, periodic testing of extinguishing foam performance parameters is a necessity to regularly monitor its capabilities. The reduction in performance of AFFF can be caused by numerous and varied factors such as dilution, contamination, extremes of temperature, and system failure [1]. However, this research focuses on the effects that are caused by the storage facility for AFFF concentrate.

1.3 Significance of the Study

Fatal fires have occurred in the aviation industry in recent decades, prompting researchers to further study the fire protection sector. Nevertheless, there are still notable gaps that haven't been addressed by previous research, in particular, the effects of the firefighting foam storage tank have been little studied. This is due to the nature and diversity of these problems. The difficulty of focusing on the optimization of fire foam in storage has always been a concern because of the complex engineering branches such as materials science, structural analysis, and thermal engineering.

In 1965, Meldrum et al. [1] published their study on the shelf life and usefulness of mechanical firefighting foam fluids. The study was instrumental in predicting the period for which firefighting foam can be stored before it deteriorates. It also highlighted gaps and limitations in previous studies and difficulties in optimizing the problem. Predictions depend on parameters such as temperature extremes, oxidation, evaporation, corrosion, dilution, and contamination of the storage facility. Much of this research work will be compared to [1]. Extensive research will be done on the effects of storage or reservoir on the AFFF.

Large tanks for storing AFFF concentrate are advantageous because the foam concentrate can be quickly pumped from one source (the tank) to the firefighting trucks during emergencies without the need for replenishment every so often. These critical considerations lead to storing foam concentrate for firefighting in a variety of tanks rather than the manufacturer's original recommended containers. Consequently, this research work is essential for evaluating the impact of storage facilities on the performance of AFFF and proposing possible solutions that might eliminate or mitigate these concerns.

1.4 Aims and objectives of the study

The aim of the present research work is to experimentally evaluate and assess the compatability of mild steel, stainless steel, and high-density polyethene (HDPE) storage tanks with AFFF concentrate. To achieve this goal, the objectives of this study are to:

1. Conduct a detailed study of the literature on class B firefighting foams and on mild steel, stainless steel, and HDPE.
2. Design an experimental programme that will determine the possible effect or impact of mild steel, stainless steel, and HDPE on the properties of AFFF concentrate.

3. Perform the experimental tests to evaluate and assess if any of mild steel, stainless steel, and HDPE degrade or deteriorate the properties of AFFF concentrate, and if so, determine the degree of severity.
4. Scientifically deduce if the degraded properties of AFFF concentrate affect its performance under firefighting circumstances.

1.5 Research question

1. What impact do mild steel, stainless steel, and HDPE storage tanks have on the properties of AFFF concentrate and, thus, on its performance during firefighting conditions?

1.6 Limitations of the study

The study is only concerned with the effect of the materials on AFFF concentrate. It does not investigate the causes of these effects, but this can be accomplished in future research. Furthermore, the study does not practically test the performance of AFFF, as would normally happen in the aviation industry during periodic tests or aircraft accidents. Rather, the study experimentally assesses the properties of AFFF concentrate and then draws conclusions based on scientific knowledge.

1.7 Dissertation layout

The study consists of six chapters structured as follows:

Chapter 1: Introduction

This chapter provides a brief overview of the organisation included in the study as well as thebackground to the problem underlying the research work. It outlines the aim and importance of the study. It explains the research objectives, formulates the research question, and discusses the format of the study.

Chapter 2: Literature review

Chapter 2 provides a comprehensive summary of the existing literature on AFFF that was consulted. It focuses on the broader knowledge of previous studies that relate to the problems of this study. The current and previous studies on the compatibility of engineering materials

with AFFF concentrate have been conducted. This is then validated by the experimental analysis in Chapter 4 based on the outcomes.

Chapter 3: Materials and Methods

This chapter documents the experimental method for the tests and analyses undertaken in this study. In addition, all the materials and equipment utilised during the testing are displayed and their relevance is briefly explained.

Chapter 4: Results and discussions

This chapter documents and discusses the results of the experimental tests conducted in Chapter 3. The results were recorded and benchmarked with the standard parameters. The discussions are drawn based on outcomes and the existing literature review and scientific knowledge.

Chapter 5: Conclusions and further work

This chapter concludes the study with a summary of research findings aimed at solving the research problem. The scope for future research areas is discussed, and the conclusion for the entire study is made.

1.8 Conclusion

Considering the devastation caused by hydrocarbon fires, the fire protection sector cannot be overlooked in the aviation industry. This chapter provided a brief overview of the entire study, which included background information on the problem, a statement of the problem, significance of the study, aims and objectives, research question and limitations of the study. The format of the study was also described. The next chapter explores the literature that is relevant to this study.

CHAPTER 2: LITERATURE REVIEW

2.1 Introduction

This chapter aims to provide an overview and foundation of the current knowledge of this study in literature as well as a theoretical base for the current work. The fundamentals of this study are presented. The techniques related to AFFF have been proposed and analysed by many researchers. All optimization problems are about maximising the effectiveness and efficiency of AFFF under firefighting circumstances.

The first section of the literature is a brief overview of the significant fundamentals of AFFF, focusing on evolutionary changes, characterization, foaming ability, mechanical stability, and critical application rates. This is followed by a review of current problems and difficulties related to environmental concerns pertaining to AFFF. Issues concerning the compatibility of various materials commonly used to construct storage facilities are discussed. Previous studies and experimental work aiming at the optimization of AFFF are discussed.

2.2 A brief overview of Class B fires

In the aviation industry, fire is of great concern due to the incidence of fires that are usually devastating to both human lives and properties. Since fire is of great significance in the present research, it is beneficial to understand the various classes of fire. Fire is usually classified into five classes. In fire science, fire is classified by the type of fuel it burns, namely: Class A, B, C, D, and K [2]. The classes are discussed in detail in Table 2.1. However, the present research work will only focus on Class B fire since AFFF is used to suppress this Class of fire.

It is essential to comprehend that Class B fires are an exothermic reaction as any other type of fire that relies significantly upon four (4) elements: fuel, air or oxygen, heat, and a chemical chain reaction [3]. However, this fire is normally caused by low-viscosity liquids. Removing one element will effectively halt the fire. The following four (4) suppression mechanisms are required for knockdown and burn-back resistance in Class B fires:

- The foam blankets the fuel surface, smothering the fire.
- The foam blanket separates the flames or ignition source from the fuel surface.
- The foam cools the fuel and any adjacent metal surfaces.

- The foam blanket suppresses the release of combustible fumes that can mix with air [3].

Table 2.1: Various classes of fire [2].

Class of fire	Type of fire	Commonly encountered
A	Common combustibles such as wood, paper, and rubber materials.	General places.
B	Flammable liquids such as fuel, petroleum greases, and flammable gases.	Airports and petroleum industries.
C	Energized electrical equipment and conductors.	Electrical distribution industries.
D	Combustible metals such as magnesium, titanium, and sodium.	Metal manufacturers.
K	Cooking oils, normal grease, and animal fat.	Production and FMCG industries.

In general, there are two different basic flammable or combustible fuel groups that yield to Class B fires. It is essential to identify which group you are exposed to, as it greatly assists in selecting the suitable extinguishing agent (type of firefighting foam). The two groups are divided as follows:

- Standard hydrocarbon fuels such as gasoline, diesel, kerosene, jet fuel, etc. do not blend with water or are not miscible in water, they usually float on top of the water, and, for the most part, they do not intermix.
- Polar solvents, or alcohol-type fuels, are fuels that mix readily with water or are miscible in water [3].

2.3 Evolution of AFFF for effective extinguishment of Class B fires

In the aviation industry, firefighting foam was declared by the FAA as the sole optimal extinguishing medium used for the suppression of Class B fires during emergency conditions [4]. Originally, five types of firefighting foams were commonly used: fluoroprotein foams

(FPs), aqueous film-forming foams (AFFFs), film-forming fluoroprotein foams (FFFPs), alcohol-resistant aqueous film-forming foams (AR-AFFFs), and alcohol-resistant film-forming fluoroprotein foams (AR-AFFFPs) [5]. All of them were designed to be effective in handling precise fire conditions and contain one or more fluorinated surfactants as key ingredients.

It is well known that water has long been a universal agent for the suppression of fires; however, it is not exceptional in all instances [4]. For instance, water is regularly incapable of suppressing combustible fluids and can be perilous. Protein-based foams, which presented a drastic improvement over water for combating liquid fuel fires, were initially developed and used. These protein-based foams are thick and form a heavy, heat-resistant covering over a burning liquid surface [6]. These properties made protein-based foams constrained, as they were not able to spread rapidly over the fuel surface. This was a concern for a long time, as protein-based foams were not very effective in low-viscosity fuels such as kerosene, which is commonly used in the aviation industry.

In general, foam is made by first mixing foam concentrate with water to create a foam solution. This aqueous concentrate is then blended with air using standard aspirating nozzles to generate foam [4]. Fire-fighting foam is an extinguishing agent composed of numerous bubbles formed mechanically or chemically from the liquid, as shown in Figure 2.1. These are commonly used to reduce the spread and extinguishing of Class B fires and to prevent re-ignition, while in certain situations they may be implemented to extinguish Class A fires [2]. AFFF is a low-viscosity foam, consequently, it spreads easily on the surface of the flammable liquid. This enables the formation of a dense and stable foam layer that acts as a physical boundary against heat and mass transfer, thus exhibiting excellent cooling and covering effects in hydrocarbon fires [7].

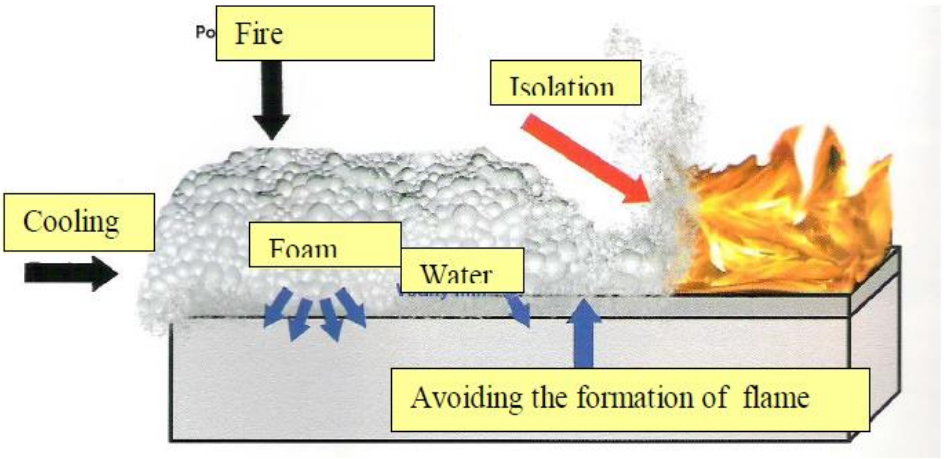

Figure 2.1: Scheme of the extinguishing mechanism by using firefighting foam [5]

Synthetic-based foams were developed and introduced in the mid-1960s to optimize protein-based foams [8]. These firefighting foams included AFFF and AR-AFFF. AFFF concentrates are made by blending fluoro-and hydrocarbon-surfactants; modest quantities of salts and foam stabilizers are regularly included [9]. The AFFF concentrate is then mixed with a specific level of water to form a foam solution. The proportioning rate is usually 1%, 3%, or 6% of foam concentrate to water. Furthermore, an additional feature of 'aqueous film' is formed on the surface of a flammable liquid by the foam concentrate as it drains from the foam blanket [3]. This film is very fluid and floats on the surface of most hydrocarbon fuels, hence providing AFFF with tremendous speed during extinguishing conditions. This made AFFF further developed and predominant in most firefighting foams. Moreover, the introduction of AFFF represented a significant increase in firefighting performance in terms of more rapid control and extinguishment of fuel fires, especially in industries that are involved with low-viscosity fuels. The vital chemical composition of AFFF is depicted in Figure A.1 in the appendices.

All firefighting foams were developed for the suppression of specific combustible fuels. It is vital to identify which fuel group is involved when flammable fire conditions occur. This is to ensure timely and effective extinguishment during fire conditions. As a consequence, firefighting foam may be ineffective when used on unsuitable fuel, which may yield unexpected or unfavourable outcomes.

To date, AFFF has been widely used in aviation fire protection for the suppression of hydrocarbon fuels (a part of Class B fires). This synthetic-based foam has a low viscosity and spreads quickly across the surface of most hydrocarbon fuels. Initially, AFFF was developed for the aviation industry due to the fuel (kerosene) they are involved with, and it has proven to be effective in several cases. However, they can also be relatively utilized for extinguishing Class A fires. During firefighting, a water film forms underneath the foam, which cools the liquid fuel, halting the formation of combustible fumes [6]. Consequently, this gives a sensational fire knockdown, which is a critical aspect of crash rescue firefighting.

2.4 Foam generating devices and processes

Foam, in general, is created by mechanical action (dispensing equipment); hence, the generation of firefighting foam is a mechanical process that comprises numerous prior steps. There are various methods of generating firefighting foam; each method relies on the type of fire involved and the foam concentrate used. To date, there are three methods of generating

firefighting foam from a foam concentrate, namely: aspirated nozzle, compressed air foam (CAF), and chemical reaction method [10]. The distinctions in these methods yield unique characteristics of the foam produced, with noticeable contrasts in the size and uniformity of the bubbles produced using each method [10]. Such differences may lead to significant variations in foam performance during fire conditions. However, the aspirated nozzle is a traditional and widely used method of generating firefighting foam, particularly in aviation fire protection.

Aviation fire protection has adopted the technique of an aspirated nozzle when generating foam. Due to the type of environment and aviation standards that the National Fire Protection Association (NFPA) developed and oversaw, this technique is more useful for aviation fire protection. Technically and according to the research, the aspirated nozzle is suitable for low-expansion foams such as AFFF and AR-AFFF [11]. Aviation fire protection utilizes AFFF for fire suppression due to the class of fuel (Jet A-1) they are involved with. Subsequently, the aspirated nozzle technique has been compatible with AFFF. However, during the periodic tests in aviation, the functionality of this technique is tested, and according to the reports, there are still concerns when using it [10]. Moreover, gaps exist in the optimization of this foam generation.

Comprehending various foam generation methods is essential in the present research work to evaluate and deduce if any other method can yield any benefits. Most of the research has been focused on the aspirated nozzle and CAF generation methods, aiming to optimize or implement new methods. Optimization of these methods requires complex mathematical analysis as there are numerous parameters involved. Besides, the complexity further relies on the variation of chemicals involved in the chemical reaction technique. The experimental work conducted by Laundess et al. [10] shows that foam generated by the CAF technique displays uniformly small bubbles; the aspirated nozzle produces a greater spread of bubble sizes; and the chemical (nitrogen) reaction displays the most uniform size distribution of bubbles, as shown in Figure 2.2. In addition, the CAF method has the advantage of being environmentally friendly. With the aspirated nozzle technique having environmental concerns, a new technique or optimization has emerged as an alternative in aviation fire protection.

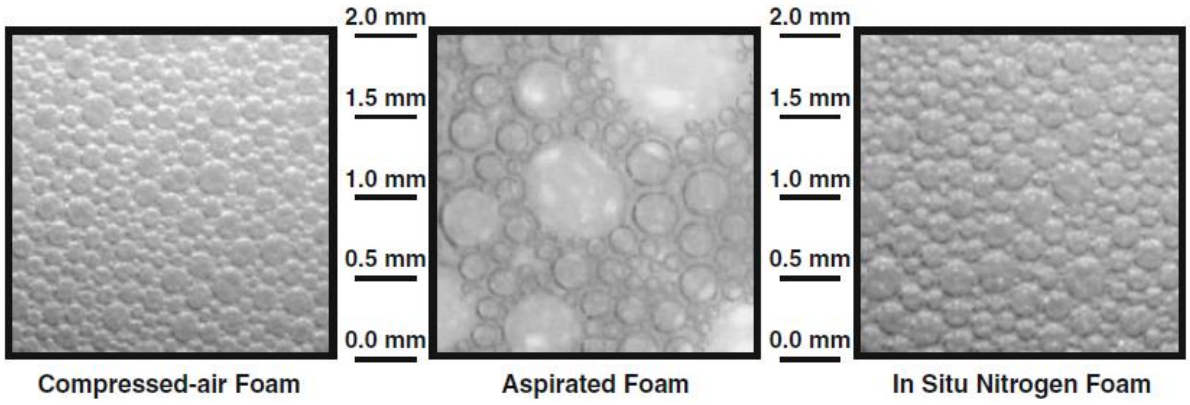

Figure 2.2: Bubble characteristics for different generation methods [10].

2.4.1 Aspirated nozzle

The technique has been extensively used and is the traditional way of generating firefighting foam. In this method, foam is generated by extracting air into a jet of foam concentrate inside a nozzle [11]. Most firefighting foam nozzles are specially designed with convergent geometry. In this way, parameters such as pressure, velocity, and flow rate are carefully controlled. As shown in Figure 2.3, foam solution at high pressure and low velocity enters the orifice at 1 and exits as finished foam at low pressure and high velocity at 5, at a constant flow rate. During stages 2, 3, and 4, air is drawn by a jet and blended with foam concentrate, resulting in strong mixing and agitation [12].

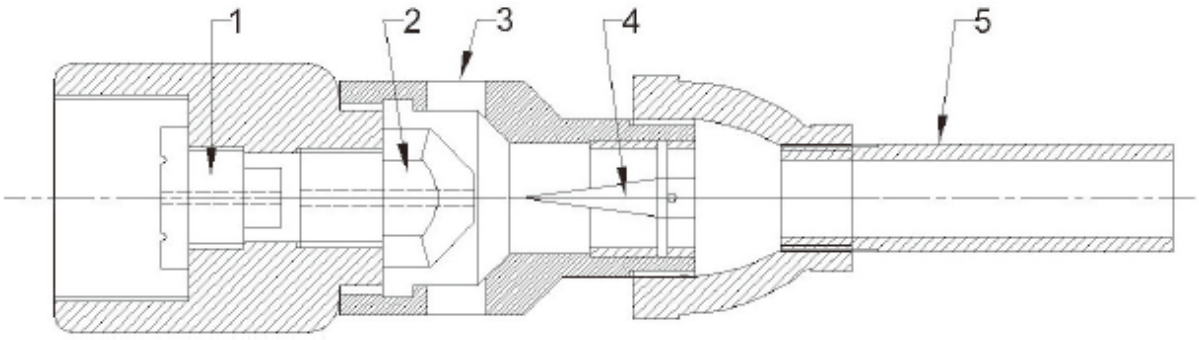

Figure 2.3: Nozzle for generating foam [12].

The governing equation for critical parameters during the foam generation is usually Bernoulli's equation, which is given as:

$$P_1 + \frac{1}{2}\rho {v_1}^2 + \rho g h_1 = P_5 + \frac{1}{2}\rho {v_5}^2 + \rho g h_5 \quad (2.1)$$

As seen in Equation 2.1, in case where the potential energy at the elevation 1 ($\rho g h_1$) equals the potential energy at elevation 2 ($\rho g h_5$), then the equation can be simplified and written as:

$$P_1 + \frac{1}{2}\rho {v_1}^2 \quad P_5 + \frac{1}{2}\rho {v_5}^2 \tag{2.2}$$

Where,

p_1 *is the pressure at elevation* 1 *in Pa*

v_1 *is the velocity at elevation* 1 *in* $^m/_s$

h_1 *is the height at elevation* 1 *in m*

P_5 *is the pressure at elevation* 2 *in Pa*

v_5 *is the velocity at elevation* 2 *in* $^m/_s$

h_5 *is the height at elevation* 2 *in m*

v_5 *is the velocity at elevation* 2 *in* $^m/_s$

g is the acceleration due gravity in $^m/_{s^2}$

ρ *is the density offuid in* $^{kg}/_{m^3}$

Since convergent nozzles are used to increase the outlet velocity (v_5 *in figure* 2.3) due to the conservation of mass, while critically maintaining the inlet flowrate during firefighting. Therefore, the following assumptions can be made:

$$A_1 > A_5$$

$$V_1 < V_5$$

$$P_1 > P_5$$

When the areas of the inlet and outlet are known and the flow rate that must be achieved is also known, then velocities can be calculated using the following equation:

$$Q = VA \tag{2.3}$$

Where,

$Q\ is\ the\ flowrate\ in\ \ {}^{m^3}/_{S}$

$V\ is the\ velocity\ of foam\ solution\ is\ \ {}^{m}/_{S}$

$A\ is\ the\ area\ of\ the\ nozzle\ at\ a particular\ point\ in\ m^2$

2.4.2 Compressed air foam (CAF)

The CAF method is commonly used for generating any kind of firefighting foam and was initially developed by the National Research Centre of Canada (NRCC) in the late 1990s [13]. The technique has offered several benefits in fire protection since the prohibition of halogen-based agents due to some environmental impacts. This technique is similar to the aspirated nozzle method in that it also consists of a divergent nozzle for discharging foam. The distinction is that, in the CAF system, the air is pressurized using an air compressor and then fed or injected into an aqueous foam solution. As the foam expands, it discharges and is guided through a nozzle.

2.4.3 Chemical reaction

Laundess et al. [10] discovered the chemical reaction technique, aiming to eliminate the foam generation problems. The method has not yet been recognized in fire protection standards but certainly has several benefits. With other generation methods extensively used to produce much heavier carbon dioxide bubbles, it was of great practical significance to evaluate other methods that would produce lighter, uniform bubbles. Consequently, nitrogen gas bubbles were the empirical and realistic alternative. In this way, the chemical reaction between foam solution and nitrogen creates numerous, uniformly sized bubbles of nitrogen gas within the foam.

The method has been reviewed by many researchers. The only concern is the need to optimize foam formulations to prevent surfactants from being affected by nitrogen generation and the presence of salts formed during chemical reactions [10]. For this reason, aviation fire

protection will need to examine this as an alternative to possibly eliminating the aspirated nozzle method.

2.5 Foaming ability and Mechanical stability

Foams are typically described in terms of their foamability and stability. Foamability is defined as the capacity of the surfactants to form foam regardless of the special foam properties, while foam stability describes the variations in foam height or volume with time, immediately after foam generation. The two concepts are interrelated; the greater the stability of the foam films, the greater the foamability of the solution. Modern firefighting foams are primarily of the mechanical type. This means that before being utilized, they should be proportioned (mixed with water) and aerated (blended with air). Four elements are necessary to produce a quality and stable foam blanket, and they include foam concentrate, water, air, and aeration (mechanical agitation) [2].

In recent years, mechanical stability has been a concern for most firefighting foams. Many researchers have approached this challenge with the aim of optimization. Foaming ability is a key factor in advancing the mechanical stability of firefighting foams. The rate at which air bubbles are produced during the foaming process is essential for evaluating the mechanical stability of the foam [2]. Stability properties, as well as the effectiveness of firefighting foams, are determined by their physical and chemical properties, as described by Turekova and Balog [5]. These properties may include: viscosity, foam frost resistance, the content of the sediment, foam stability, half-life of foam, pH, foaming concentrate, spreading factor, etc. [5].

The mechanical stability of AFFF depends upon the structure of the surface films from the so-called foaming agents. During firefighting conditions, the foams are continuously disrupted by the influence of the heat of ignition, the internal force of the foam, and the hot surface of burning liquid [5]. Foaming ability is thus a fundamental procedure as it directly affects the quality, hence the performance, of the foam. The important parameters affecting a foam's ability to extinguish hydrocarbon fuel fires were addressed by Joseph et al. [6] with theoretical modelling to further evaluate the challenges and limitations of the current methods used. Figure 2.4 shows the parameters that affect the foaming ability of AFFF under firefighting circumstances.

Xiaoyang Yu et al. [14] studied the formation of stable aqueous foams. They experimentally demonstrated that the presence of sodium and sulphur within the aqueous solution is responsible for the stable foam formation. As a matter of fact, for stable foam formation, there must be less surface tension in the water. This is mostly accomplished by increasing the sodium alkyl sulfate concentration. As a consequence, sodium and sulphur are the primary elements of interest when optimizing the AFFF concentrate.

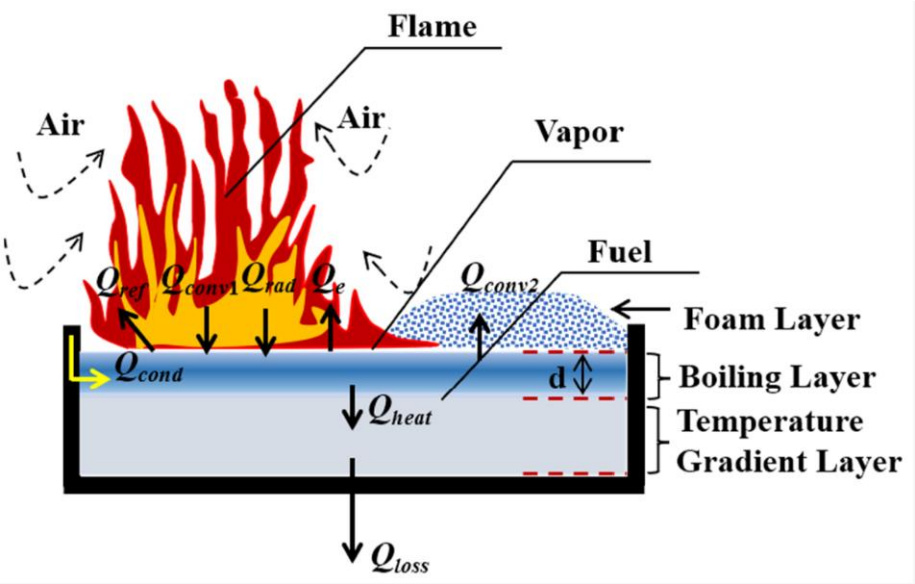

Figure 2.4: Important parameters affecting a foam's ability to extinguish hydrocarbon fuel fire [14].

Oguike [2] conducted experimental tests intending to assess the foaming ability of various foams. The analysis comprised eight (8) empty bottles that were filled with constant foam concentrate but different volumes of water. The bottles were shaken vigorously at a steady rate in each case, and the foam height was recorded. The foams were left to stand for some time, and their heights were measured again. Foams were left to stand for further days, and height was measured again. Finally, the foams formed were left to stand until they collapsed, and time was recorded for each foam solution. This experiment set a benchmark for most researchers, as most of the other foaming ability experiments have been based on it.

The current challenge is to develop small-scale test methods that measure these parameters in such a way that they can be used to predict large-scale foam performance. Persson [15] described optimization techniques and results to investigate foam mass loss by evaporation as a function of radiant heat from a fire. The finding was that foam viscosity and spreading are

areas requiring further investigation. In addition, further investigation of mass loss by evaporation must be done in order to develop solutions that will mitigate these foam mass losses by evaporation.

2.5.1 AFFF blanket stability/drainage time

Drainage time is a measurement of the rate at which foam concentrate drains out of finished foam and hence indicates the stability of the foam blanket [7]. Drainage time is often used to analyze the stability of various foams; however, according to Mukunda and Dixit [12], it does not provide a reliable indication of the firefighting capability of foams. High expansion foams usually maintain stability and heat resistance due to their long drainage time and, hence, slow loss of water from the finished foam.

In recent years, most researchers have concluded that the drainage times of finished foams do not solely depend on foam concentrate but also on the type of foam generation [16]. In most cases, drainage time for low expansion foams such as AFFF is often expressed as 25% drainage time, while for medium and high, it's usually 50% drainage time. This is the time taken for 25% or 50% of the original foam solution content (by volume) to drain from the finished foam, as shown in Figure 2.5.

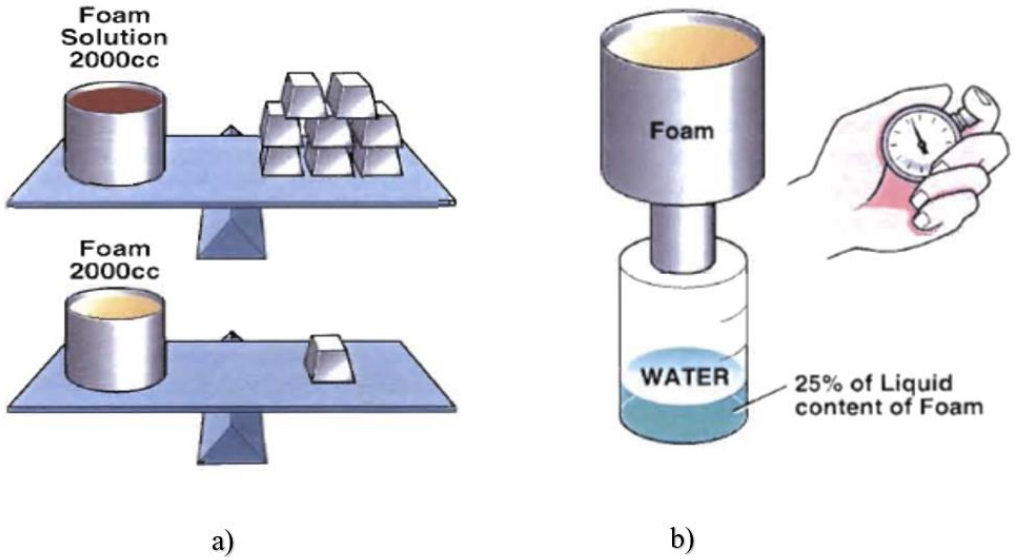

Figure 2.5: Low expansion test (a) and drainage test (b) [7].

Researchers have been working on optimizing the foaming ability, hence the stability of foams, particularly for low expansion foams. An experimental work to analyze and compare the drainage time and bubble size distribution of various firefighting foams was described by Mark et al. [10]. Table 2.2 shows the results of [10] comparing the 25% drainage times at an expansion ratio of 7:1 for two different foam concentrates.

Table 2.2: Comparison of 25% drainage times at 7:1 expansion [10].

		Mean Drainage time (s)			
Foam concentrate	Generation system	Mean	Max	Min	Standard Deviation
Telomet 6%	ISNF	342	450	264	93
	CAF	488	533	430	53
	Aspirated	N/A	N/A	N/A	N/A
FC-600 3%	ISNF	539	725	450	126
	CAF	1060	1281	844	288
	Aspirated	N/A	N/A	N/A	N/A

The findings show that the drainage rates for the various foam types were quite different, which may be due to variations in the bubble size distributions as discussed below in Figure 2.6. To explain the differences in foam drainage rates between the three foam types, they studied the bubble size distributions for each foam type. As shown in Figure 2.6, the drainage time is profoundly dependent upon the type of foam generation. Also, the aspirated foam generation method produced larger bubbles in terms of size. These bubbles contributed to shorter drainage times, as seen in Table 2.2, hence the reduction of foam quality and stability. This correlation technique was benchmarked by Oguike [2], and most researchers, such as Laundess et al. [10], have concluded the same.

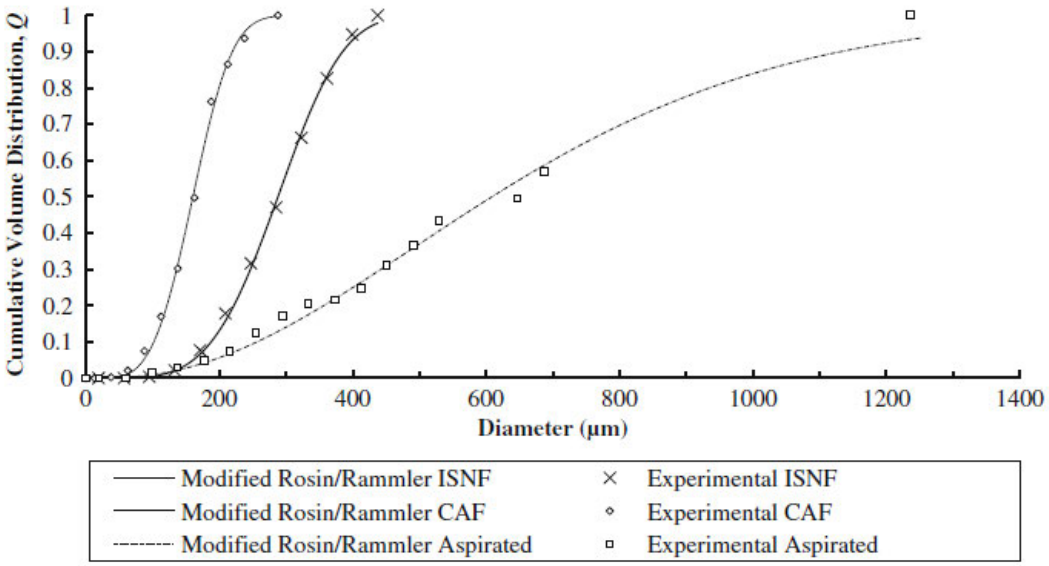

Figure 2.6: Cumulative bubble size distributions for various foam generation methods [10].

Mukunda and Dixit [12] developed a model of foam drainage based on momentum flux balance and conducted experiments with a device that simulated foam drainage through a fuel layer. According to their theoretical predictions, their findings revealed a linear relationship between 25% drainage time and height. A recommendation made by [10] indicates that there is a need for further research to develop new surfactant formulations immune to the oxidation reaction that generates nitrogen bubbles. This foam generation method will simultaneously increase the drainage rates and stability of low-expansion foams due to nitrogen bubbles.

2.6 Critical application rates

In the most recent decade, most researchers have been interested in the application rates of various firefighting foams. The number of studies on effective application rates has increased significantly, and most of these studies have been based on protein- and synthetic-based foams. The underlying motivation for considering diverse critical application rates was to identify the compatibility of foams with various classes of fire. With the original motivation behind the development of synthetic-based foams being economic issues, the application rates were thus critical.

Most of the research on firefighting foams is based on optimization aiming to provide the necessary effectiveness and efficiency in performance. In 1972, Geyer [17] conducted tests with protein and AFFF concentrates that provided the foundation for the present minimum application rates. These "modelling" tests involved jet propellant (JP-4) pool burns of 21, 30,

and 43 metres in diameter. In addition, they comprised large-scale verification experiments with a B-47 aircraft and simulated shielded fires done with a JP-4 pool fire 34 metres in diameter and 43 metres in diameter, with all tests undertaken using the air-aspirating foam generation method. The outcomes by [17] showed that PF and AFFF have an application rate with a ratio of 1.49:1, respectively, as shown in Figure 2.7. This difference in application rate acknowledges the intrinsic benefit of utilising AFFF to extinguish hydrocarbon pool flames and reflects the fact that AFFF has been shown to extinguish pool fires more rapidly than PF at equal application rates. For equivalent extinguishment timeframes, AFFF requires lower rates than PF [6].

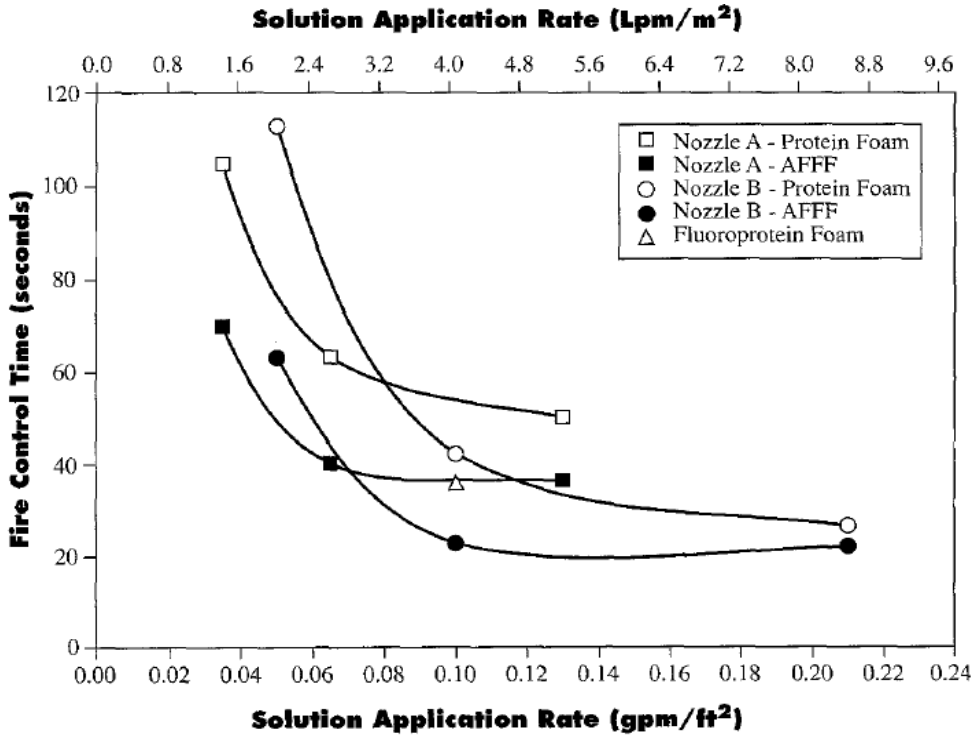

Figure 2.7: Fire control time as a function of concentrate application rate using protein foam and AFFF on JP-4 pool fires [17].

Many researchers have carried out numerous experimental tests to validate these application rates. Geyer et al. [18] further conducted tests on critical application rates for validation. The experimental tests conducted were focused on fire control time as a function of solution application rate for PF, AFF, and FPF for Jet A fuel fires, and the results are shown in Figure 2.8. These were aimed at employing more foam generation methods and different fire types to make necessary analyses of outcomes and compare with [17]. Based on Figures 2.7 and 2.8, the application rate is greatly dependent on the type of foam generation device and the

type of foam concentrates used. There have been numerous challenges regarding the critical applications of firefighting foams. The proliferation of performance guidelines and specifications for firefighting foams has created divergent opinions, especially on aviation industry fire protection standards [6].

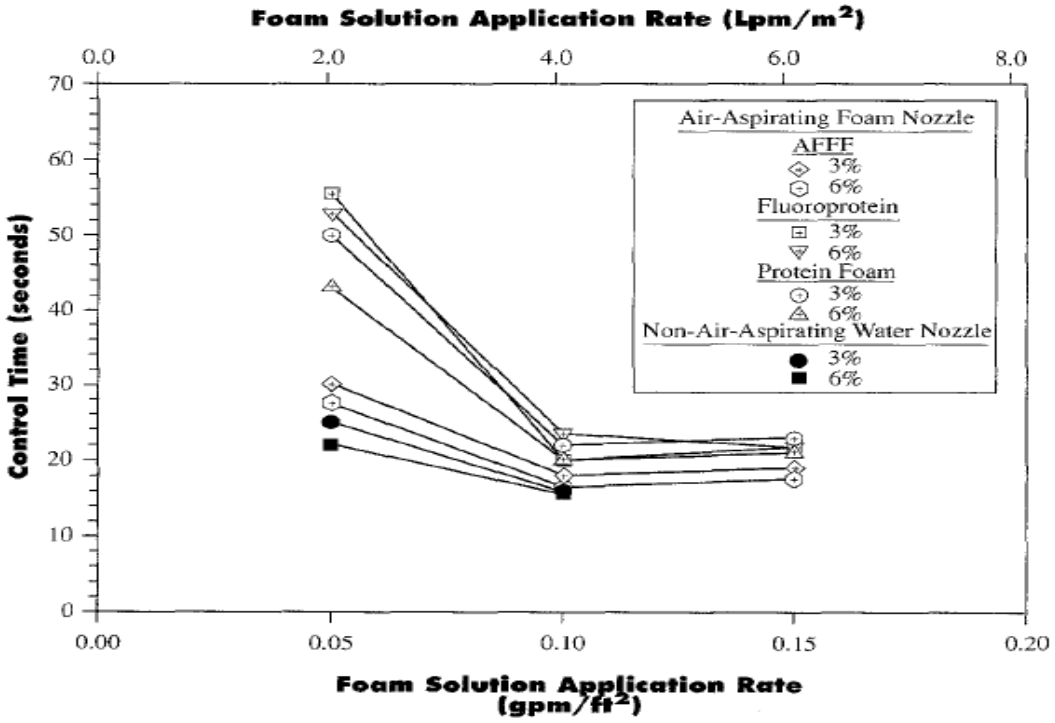

Figure 2.8: Fire control time as a function of concentrate application rate for AFFF, fluoroprotein, and protein foams for Jet A fuel fires [17].

2.7 Effect of degradability

Firefighting foams naturally degrade over time due to several factors, such as liquid drainage driven by gravity and coarsening. Firefighting foam degradation is defined by Hinnant et al. [19] as a reduction in foam layer thickness regardless of any changes in foam density or ‘quality’. Aviation periodic training is the only platform for testing foam performance parameters, hence foam degradation. Foam degradation can substantially diminish foam's efficacy. Consequently, foam deterioration can be affected by numerous circumstances, including hot fuel, fire, and foam formulations containing surfactants and chemicals necessary for foam generation [19]. Even though these components are recognised, others, such as fuel and fire, are difficult to regulate.

During the firefighting process, foam is continuously interacting with fuel and flame. The interaction may immensely destroy the thick layer of foam [20]. In this way, the ability of foam will be reduced, and its performance may be compromised. However, foam degradation may suddenly increase dramatically during this process. The causes of this are not well understood due to a lack of research on foam degradation. Furthermore, the individual effects of fire and fuel on degradation are inseparable due to the presence of fire [19].

Previous research on foam degradation has mostly focused on the natural ageing process of foam [21] and the effect of the interaction of hydrocarbon liquids with foam [20]. The natural ageing of foam can be mainly influenced by the storage tank utilised. Hinnant et al. [19] studied the influence of fuel on foam degradation for fluorinated and fluorine-free foams. The study outcome showed that the fuel temperature is by far the major factor contributing to foam degradation, followed by the effects of surfactant formulation, type of fuel, and bubble diameter or expansion ratio. Figure 2.9 shows the percentage change in AFFF thickness versus time at room temperature at 35, 50, 75, and 90 °C.

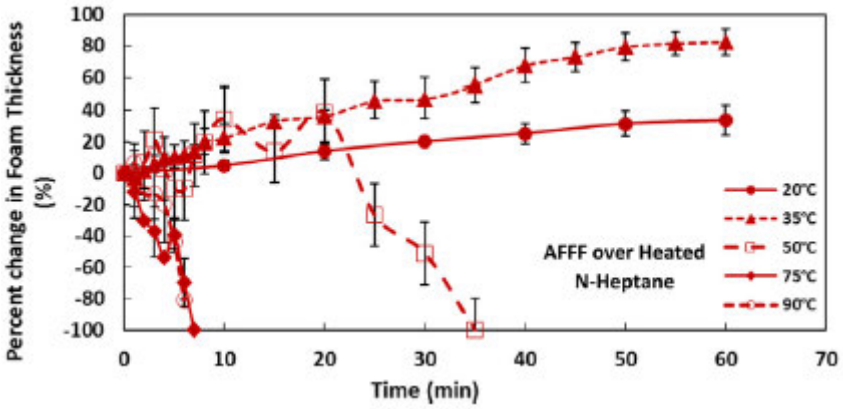

Figure 2.9: AFFF foam degradation versus time over n-heptane fuel at different temperatures [19].

Parameters such as bubble diameter or expansion ratio are highly dependent on the foam generation method, which is discussed in Section 2.4. Larger bubbles cause a faster drainage rate than smaller bubbles, and according to [19], the increased drainage rate can cause the foam to degrade rapidly. In this way, the storage facility may indirectly affect foam degradation. This is due to the sediments or sludge that may accumulate in the storage facility during the ageing process. Consequently, sediments may affect foam characteristics, particularly bubble distribution, during the foam generation process; this is shown by

employing a flow process in Figure 2.10. The optimization of a storage facility by reducing the accumulation of sediments will prove to extensively reduce foam degradation.

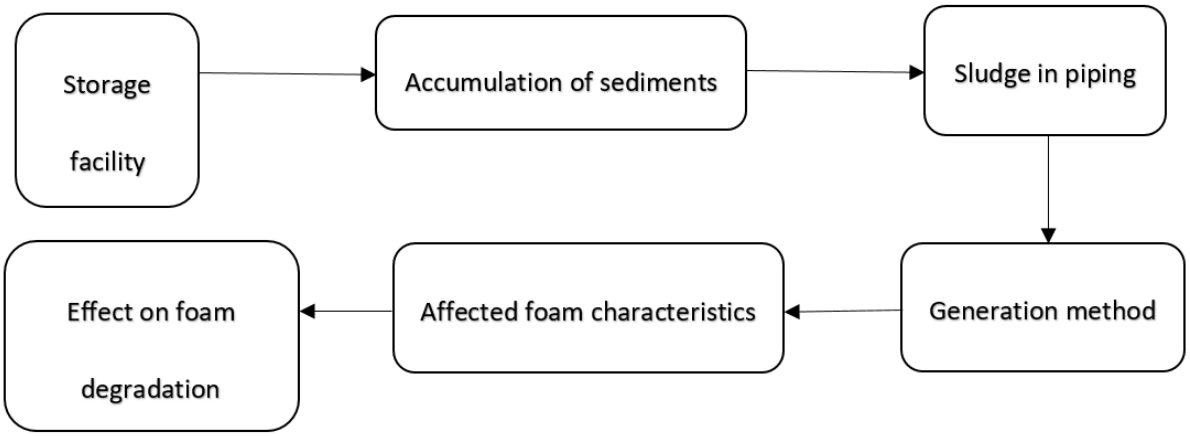

Figure 2.10: Effect of AFFF degradation.

There have been fewer studies on the effect of surfactant formulation on degradation, further research should be conducted to detect the effect of this parameter on foam degradation. Furthermore, other parameters that may affect foam degradation should be extensively investigated in the future, as foam degradation may regularly affect the performance of the foam.

2.8 Environmental issues

Modern firefighting foams can be considered sensational in terms of fire extinguishing capabilities, but, in recent years, the new Registration Evaluation Authorization and Restriction of Chemicals (REACH) legislation has drawn attention to their ecotoxicological properties [5]. While AFFF is the most widely used firefighting foam in aviation fire protection, it still has some disadvantages, of which one is the environmental impact [22]. Due to growing concerns about the environmental impact of firefighting foams, measures must be taken to correct the situation. To date, few studies have examined the environmental impact of AFFF. Initially, AFFF contained substances such as perfluoroalkyl and polyfluoroalkyl (PFAS). Previous research shows that PFAS has significantly caused the contamination of soil, groundwater, and surface water, including water stream animals, as a result of AFFF being released during aviation periodic training [23]. As shown in Figure

2.11, this poses acts of negligence and is hazardous to the environment, as foam detoxifies naturally in soil.

Figure 2.11: Used AFFF during aviation periodic training.

Initially, PFAS were not previously known or recognized as being harmful to the environment. This was due to the complexity of AFFF mixtures utilized and previous significant gaps in the thorough comprehension of PFAS, including their toxicity, bioaccumulation, occurrence, transport, and transformation mechanisms [23]. However, PFAS's impact on the environment was then recognized in the late 1990s, and several jurisdictions offered guidance with a limited range or amount of PFAS that could impact the environment [19].

Elimination of PFAS in AFFF was a challenge for every manufacturer and the aviation industry, as these chemical substances were key during fire suppression. AFFF was able to suppress fire rapidly due to the presence of PFAS. With environmental regulations enforcing the elimination of PFAS, manufacturers had no other alternative but to cooperate in the elimination of PFAS. Consequently, PFAS were phased out in 2002 by all the manufacturers due to their environmental impact [24]. Fluorinated surfactants replaced PFAS instantly, intending to reduce the environmental impact while still being compatible with AFFF.

According to the research, fluorinated surfactants were also found to have an impact on the environment [16]. As a result, samples that were analyzed in 2010 indicate that AFFF manufacturers have begun to gradually reduce or even eliminate fluorinated surfactants in their

formulations [23]. Moreover, this process of eliminating present surfactants is critical, as the transition should be carefully analyzed, in order to prevent the possible negative influence it might pose on the performance parameters of firefighting foam. To date, fluorinated surfactants that are present in AFFF are continuously bio-persistent in the environment and pose health hazards to humans.

In recent years, researchers have been investigating effective ways of mitigating environmental issues. While the progress of this optimization has been held back by the difficulties stated above, the NFPA committee, which is responsible for NFPA 11, *low expansion foams,* has made a significant effort by tasking a group to address the environmental concerns around low expansion foams [6]. The outcome of the task group has been recently published with full guidance for end users [6]. Alternatively, researchers have managed to implement new surfactants that are environmentally friendly. However, commercial firefighting foams without fluorinated surfactants developed to date have not been able to extinguish the fire as rapidly as AFFF [19]. In the future, researchers will need to conduct an extensive investigation to implement environmentally friendly surfactants that will be compatible with AFFF.

2.9 Constructing materials of AFFF concentrate storage tanks

This section details an in-depth understanding of the engineering materials commonly used to construct the storage facility for AFFF concentrate. The scope of this section includes a brief overview of these materials to thoroughly understand how they are classified. It further details the properties of interest for each material and why they opted for storage facilities. The fundamental literature concerning the evolution of these materials is detailed in this section. Furthermore, an understanding of the metallic bonding and cross-linking of these materials is vital. To improve the properties of these materials, the behaviour of these materials when reacting with AFFF concentrate must be better understood.

2.9.1 A brief overview of construction materials

As the economy becomes increasingly global, the importance of materials increases. Storage facilities/tanks can be constructed using a variety of materials. The selection of the material can be a challenging, systematic process that is commonly dependent on cost, reliability, availability, ease of fabrication, material properties, and environmental impacts [25]. The main goal to be achieved in this process is to minimize the cost while meeting the product's

performance efficiently. However, for storage facilities, it may largely depend on the type of product to be stored. The product to be stored may vary in state or phase of matter, which is critical to evaluate before any process commences. To date, there are five (5) different states of matter that are known: solids, liquids, gases, plasma, and Bose-Einstein condensate [26]. The classification of engineering materials is shown in the form of a flow chart in Figure 2.12.

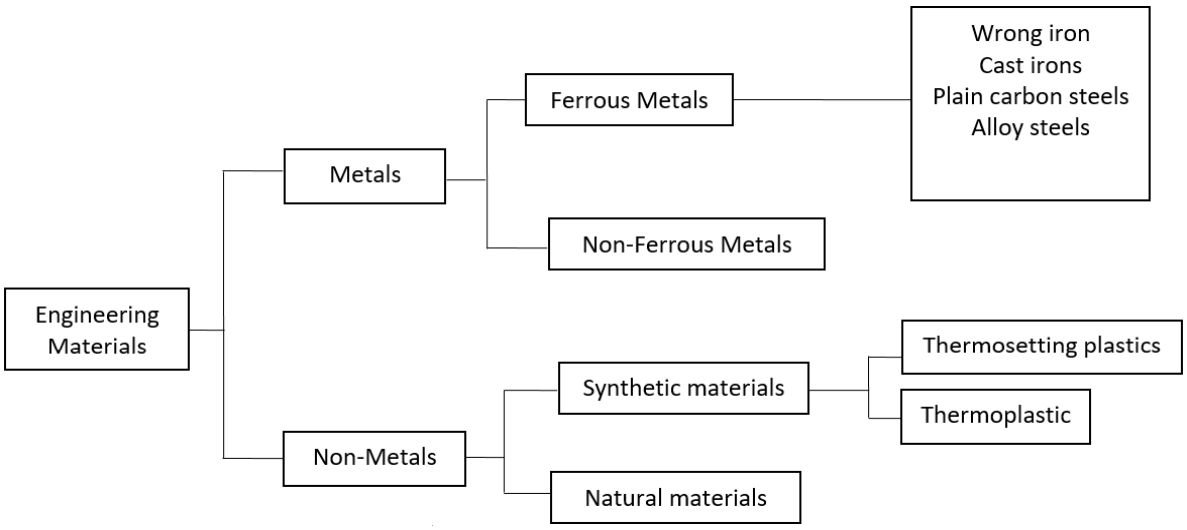

Figure 2.12: Engineering materials classification [27]

Material selection is not a new era; it is a large and traditional branch of engineering materials. Moreover, it requires technical expertise. Material properties can be decisive when evaluating the storage facility's material of construction. Material property is defined as an intensive property of a material that is not influenced by the amount of the material [28]. Typically, these are the properties we can measure or test. These properties can continuously interfere with the product stored in the storage tank; hence, it is crucial to thoroughly comprehend them.

It is vital to decide whether you are investigating the properties of the material or an object, as this could cause a contradiction. For example, you should decide whether you are identifying the properties of the storage facility or the properties of the material it is constructed of. Properties such as the shape and mass of the object (storage facility) may vary, even when they are constructed of the same material. In other instances, material properties can be improved by processes such as mixing, heating, and cooling (heat treatment). This may be useful, as the improved properties may yield better performance.

Traditionally, storage facilities were constructed using metallic materials. However, in the last decade, researchers have developed specialized non-metallic materials in the form of composite materials to enhance materials that are utilized to construct storage facilities [25]. These exceptional materials have diverse and combined properties that produce even better performance for storage facilities. Nevertheless, these advanced materials have some limitations and challenges that are notable during the specialized manufacturing technique.

2.9.2 Metallic materials

Metallic materials are a significant part of engineering materials and have been extensively studied and used for a variety of purposes. In material sciences, metallic materials are inorganic substances that usually contain a combination of metallic elements, which may also contain small amounts of non-metallic elements [29]. The typical combination of metallic elements could be metals such as gold, iron, titanium, aluminium, etc. The small amount of non-metallic could be elements such as carbon, nitrogen, oxygen, etc. [25]. In the physical sciences, there are 118 elements on the periodic Table, and 86 of these belong to the metallic group [29]. All these 86 metals have diverse characteristics, and a limited number of them can be significantly used for engineering and other purposes.

In the last century, scientists have been working tirelessly to significantly understand these types of materials and develop efficient techniques that will aid in the optimization of metallic materials [28]. With that being said, over the last 70 years, scientists have developed new techniques for producing various materials with enhanced properties compared to those of natural materials [29]. To date, numerous metallic materials, such as gold and copper, mostly rely on these new techniques to yield effective performance. Consequently, metallic materials are rarely utilized as authentic elements, so they are usually blended with other elements to form an alloy [25]. Many storage facilities are constructed using alloy metals due to their distinctive characteristics.

The metallic materials are broadly classified as ‘ferrous and non-ferrous’ [29]. Ferrous metals are those that contain iron (Fe) elements within them, while non-ferrous metals do not contain any iron elements. In the present study, only ferrous metals will be discussed. Mild and stainless steels are regarded as ferrous metals due to the presence of iron in their structures. Usually, ferrous metals suffer from the ‘corrosion phenomenon’ due to the presence of iron. Ferrous materials constitute more than 50% of the metallic materials section

[29]. Furthermore, these materials (ferrous) are useful in numerous applications as they meet the various service requirements of our modern and complex society.

While scientists have managed to develop efficient techniques for producing metals, it is of great importance to understand the relationship between the structural elements of the materials and their properties. In the textbook Engineering Materials Science by Mcarthur and Spalding [28], the microstructure is defined as the arrangement of crystals (or grains) of the different phases. When a polished segment of the material is inspected under a microscope at high magnification, it is therefore identified [30]. The chapter on metallic materials has been studied extensively. As a consequence, it has been experimentally proven over the past decades that the properties of metallic materials are interrelated with the microstructure of the material itself. This is evidence that the properties can be enhanced by altering the relative proportions of the micro-constituents (or phases). Phases are distinguished by their distinct crystal shapes, chemical compositions, and physical properties [28].

Liquid storage facilities are critical to ensuring that the properties of the stored products are well maintained. Metallic materials have offered numerous and diverse benefits when utilized as liquid storage facilities. However, in other instances, horrible incidences that result in catastrophic failure of storage facilities occur. This proves that although metallic materials are beneficial, there are still gaps that exist, probably in metal production optimization, enhancement of natural properties, and relevant material selection. There are relatively three factors that may influence the choice of metals and alloys when used as an AFFF storage facility:

- Mechanical, physical, chemical, and thermal properties.
- Degradation of the material.
- Compatibility with the product to be stored, which is AFFF for the present study.

2.9.3 Metallic bonding

In general, the term ‘bonding’ can be described as the action of joining two or more things firmly, especially employing adhesive, heat, or chemical bonds [31]. In materials and science, there are three types of bonding: covalent, ionic, and metallic bonding. Paul Drüde developed the hypothesis of metallic bonding by modelling metals as a mixture of atomic cores (positive

nuclei + inner shell of electrons) and valence electrons in the early 20th century [32]. Metallic bonding is the type of chemical bond established between positively charged atoms in which the free electrons are distributed throughout a lattice of cations [33]. In contrast, covalent and ionic connections are formed between atoms that are separate from one another. Metallic bonding is the predominant kind of chemical bonding between metal atoms. Figure 2.13 depicts the formation of a metallic bond.

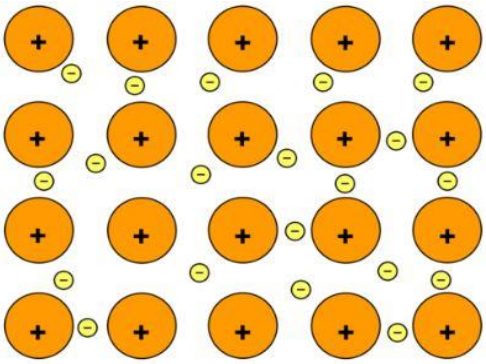

Figure 2.13: Metallic bonding: Positive atomic nuclei (orange circles) surrounded by delocalized electrons (yellow circles) [31].

Metallic bonds are commonly noticed in natural metals, alloy metals, and some metalloids. For instance, graphene (an allotrope of carbon) usually reveals two-dimensional metallic bonding [33]. Metals, including natural ones, are not limited to metallic bonding. Thus, they have the capability of forming other types of chemical bonds within their atoms. Atoms have a tiny nucleus made up of neutrons and protons, and electrons are in orbit around it [25]. Significantly diverse atomic models can be employed to describe various aspects of the overall material. As noted previously, one advantageous model of a metal is a repeating structure of metallic ions surrounded by a "sea" of electrons (see Figure 2.13). Critically determining the thermal and physical properties of a metallic substance are the "free electrons" [25]. Instead, certain mechanical features of metallic materials can be better comprehended if atoms are viewed as "hard spheres" [25].

When atoms behave like hard spheres, they are relatively bonded together by an attractive force [33]. However, this type of bonding is very weak, which is why metals have a crystalline structure where atoms are significantly arranged in a dense, regular, and repeating manner. The atoms of various metals are significantly arranged in various crystal structures [25]. Atoms in metallic materials can be relatively arranged in four (4) different ways: face-

centred cubic (f.c.c.), hexagonal closed pack (h.c.p.), body-centred cubic (b.c.c.), and tetragonal. A typical example may include a pure metal such as aluminium (Al), in which atoms are relatively arranged in f.c.c. at room temperature [25], as shown in Figure 2.14.

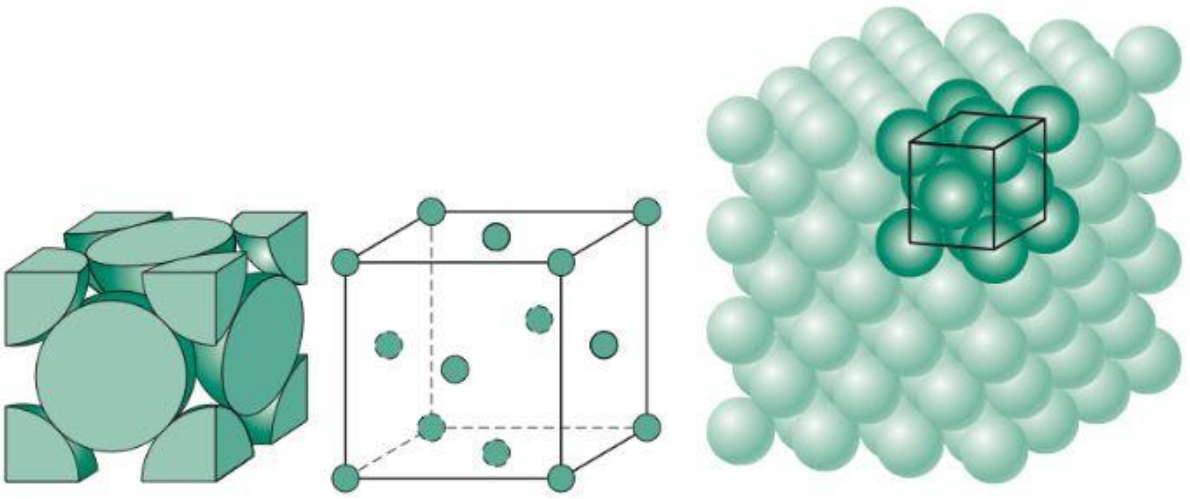

Figure 2.14: Crystal structure of aluminium metal (Al) at room temperature [25].

The mentioned crystal structures are determined at room temperature. However, the transition in the crystal structure is much more possible in several metals. This transition varies with the temperature to which the metal is exposed [34]. For example, metals such as pure iron may reveal two different crystal structures. At room temperature, it reveals b.c.c., but when the temperature is constantly increased towards a melting point (912–1394 °C), its crystal structure changes to f.c.c. Further increasing the temperature to about 1538 °C will result in reverting the crystal structure to b.c.c [29–30]. For alloy metals, the transition in the crystal structure can be achieved by adding an element with a different crystal structure. Table 2.3 shows the atom arrangement in the crystal structure of some commonly used pure metals.

The metallic bonds and the placement of the atoms in the crystal structure affect a number of a material's physical and mechanical properties. For example, when metallic material is heated to a melting point, the atoms have to gain sufficient energy to break free from the crystal structure [25]. This is evidence that the properties of materials can be altered by altering the arrangement of atoms in a crystal structure. Moreover, the crystal structure significantly determines the ability of atoms to slip over one another during the deformation

of metals [34]. This is especially true of ductile metals due to their ability to deform without easily breaking. These types of materials are commonly used to construct liquid storage facilities due to their crystal structure that yields exceptional properties.

Table 2.3: Crystal structure for popular metals, at room temperature [25].

Metal	Crystal structure
Aluminum	FCC
Chromium	BCC
Copper	FCC
Gold	FCC
Iron	BCC
Silver	FCC
Nickel	FCC

2.9.4 Mild steel the material

Mild steel is a ferrous metal that contains a relatively low content of carbon, which usually ranges from 0.05% to 0.25% by weight [34]. Thus, it is also known as 'low-carbon steel. Low-carbon steels consist primarily of ferrite rather than perlite [35]. Metals containing carbon content ranging from 0.30 to 2.0% are typically referred to as higher carbon steel [27]. The addition of carbon content increases the strength of the steel. Consequently, steel materials having a carbon content higher than 2% are often regarded as ‘cast iron' [34]. Mild steel is a popular metallic material that has been extensively used for many applications, including industrial storage facilities.

Although mild steel contains carbon, iron, and other elements in its composition, it nonetheless cannot be regarded as alloy steel. This is due to the extremely low amount of carbon and other alloying elements it contains; thus, these elements are insufficient to produce alloy steel. The relatively low amount of carbon and other alloying elements in the

composition of mild steel results in diverse properties when compared to higher carbon and alloy steels [27]. The high content of iron and ferrite in the composition of mild steel means that it is magnetic [35]. Low-carbon steels are generally useful in liquid storage facility construction due to their compatible properties. In particular, mild steel is one of the most commonly used tank construction materials. It is popularly known for its ductility and can be made from readily available natural materials. The low cost of this metal makes it beneficial to numerous industries in terms of economics.

To date, the low-carbon steel setback has been corrosion, which causes more serious deterioration problems in storage facilities [36]. Various coatings have been developed over the past decade, aiming to mitigate this problem. The other major concern regarding low-carbon steels is that it is nearly impossible to alter some of their mechanical properties through heat treatment [34]. Moreover, low carbon content means that mild steel has very few alloying elements to prevent dislocation in the crystal structure, resulting in less tensile strength than high-carbon and alloy steels [34].

2.9.4.1.1 Useful properties

As previously stated, the material property is a comprehensive property that is not dependent upon the amount or size of the material [37]. These are the quantitative parameters that are measurable, tested, and observed when a load is applied. As a consequence, these properties are significantly determined by the composition and crystal structure of the material. Thus, it is vital to understand the arrangement of atoms in the crystal structure.

Mild steel has a variety of properties that make it beneficial for several applications, and these are detailed in Figure B.2 in the appendices. These properties can be broadly grouped into mechanical and physical properties [37]. These two properties are vital determinants of whether a metal is considered compatible with a given application. In almost every instance, mechanical properties are interdependent, meaning high performance in one category may be achieved by lowering performance in other categories [37]. For example, the low content of carbon in mild steel means that this metallic material is more ductile when compared to alloy steel.

For low-carbon steels, ductility indicates that they can be formed into the desired shape at any temperature without major difficulties [38]. Figure 2.15 shows how the carbon content of

plain carbon steel affects the properties of the steel. Referring to Figure 2.15, it can be observed that altering the carbon content of plain carbon steels has an impact on their properties. Consequently, when the carbon content has increased, the ductility of the steel materials has relatively decreased. Moreover, strength and hardness are remarkably increased, which results in the transition from ductile to brittle [39]. For liquid storage facilities, ductility is one of the significant properties. This property means that the storage facility can be rolled or joined using various mechanical fabrication methods without major concerns.

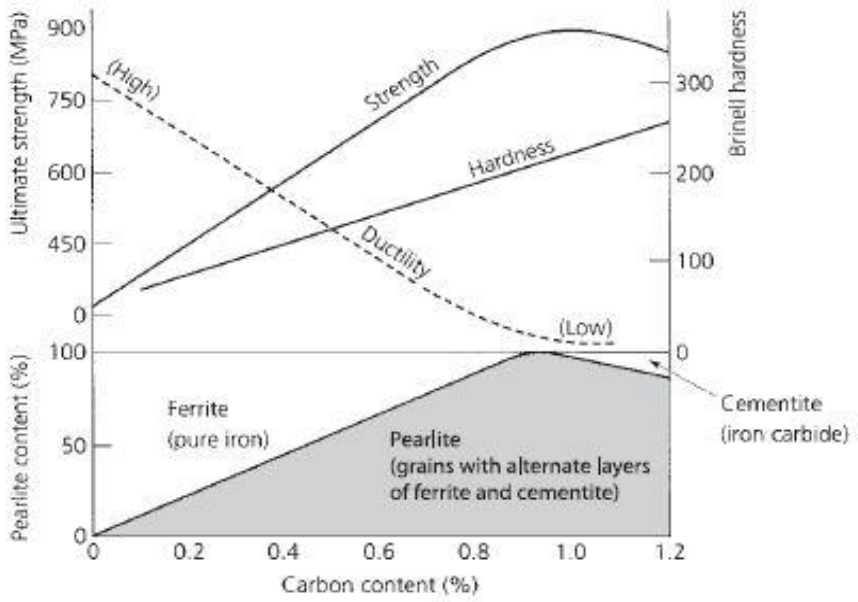

Figure 2.15: Effect of carbon content on the properties of plain carbon steel [27].

Another critical parameter for storage facilities constructed of mild steel is thermal conductivity, which falls under physical properties. In the textbook Heat Transfer: A Practical Approach by Cengel [40], thermal conductivity is defined as a measure of the quantity of heat that flows through a material. In the present study, the storage facility does not necessarily need to be constructed with materials that have a high thermal conductivity. However, achieving this is somehow difficult due to the diverse properties a material can have.

Mild steel has a thermal conductivity of 64.86 $^{W}/_{m.K}$ at most [40]. This is quite low when compared to other steels but can be considered high for applications that do not require heat transfer. At extremely high temperatures, heat may be transferred to the product inside the storage tank and may influence the viscosity of the product. When the storage facility is

continuously exposed to high-temperature environments, heat can be gradually transferred until it causes some notable problems with the liquid stored. To reduce heat transfer, insulating materials are usually utilized, but they do not eliminate the problem completely [28]. As a consequence, it is vital to understand the environmental factors that may be associated with the properties of the material at the location of the storage facility.

There are normally three means of transferring heat: conduction, convention, and radiation [37]. Heat transfer through solid materials is known as conduction; heat transfer between a moving gas or liquid and a solid surface is known as convention; and radiation is the energy that matter emits in the form of electromagnetic waves [40]. For the worst situation, the total heat energy that can be transferred to the storage facility, hence the liquid stored as a result of the surrounding atmosphere (radiation), can be calculated using the energy balance equation as follows:

$$Q_c = m \times C_p \times \Delta T \tag{2.4}$$

Where,

Q_c *is the amount of net heat transfer to the system in* J

m *is the mass of a material in* kg

C_p *is the specific heat capacity in* $^{kJ}/_{kg.℃}$

ΔT *is the temperature difference of surfaces in* ℃

When the total heat energy that is being transferred to the storage tank holding liquid is known, it is now vital to estimate the rate at which this heat energy is transferred. This is critical in predicting whether the composition of concentrate is being affected by the heat that is transferred to the storage facility by conduction. The equation for the calculation of conduction heat transfer rate is known as Fourier's Law of Heat Conduction and is given by:

$$Q_C = -k \times A \times \frac{\Delta T}{\Delta r} \tag{2.5}$$

Where,

Q_c *is the conductive heat transfer rate in* W

k *is the thermal conductivity of the material in* $^{W}/_{m.\,°C}$

A *is the cross − sectional area in* m^2

ΔT *is the temperature difference of surfaces in* °C

Δr *is the distance separating the surfaces in* m

Positive heat conduction indicates that heat is entering the body, whereas negative heat conduction indicates that heat is exiting the body. Many study domains have utilised heat transfer primarily to raise the heat transfer rate, decrease the heat transfer rate, and maintain a specific temperature range [40]. The attentiveness is to reduce the rate of heat transfer so that it does not abruptly alter the composition of the concentrate, thereby affecting its properties.

2.9.5 Stainless steel the material

Stainless steels are ferrous metallic materials that contain a minimum of 10.5% chromium and about 8% nickel as the main alloying element [42]. All the alloying elements have a significant role in the stainless steel family. The chromium element forms a protective self-healing oxide film, which greatly improves the corrosion resistance of stainless steel [30]. Large amounts of nickel contribute to both heat and corrosion resistance [43]. However, depending on the percentage of nickel added, it also contributes to high strength and excellent toughness. Additional relevant components are frequently added to stainless steel to improve its capabilities. These alloying components are what make stainless steel more expensive than carbon steel in general.

The classification of stainless steel is determined by its metallurgical structure [44]. As aforementioned in Section 2.9.1, the metallurgical structure is the arrangement of the atoms that make up steel grains. The microstructure of steel is formulated based on its chemical composition. Stainless steels can be entirely austenitic, fully ferritic, fully martensitic, or a mixture of ferrite and austenite (duplex) if the alloying elements are combined in a way that

results in a unique microstructure [44]. Figure 2.16 depicts these probable four microstructure phases. Several types of stainless steel are produced under particular cooling conditions, and they are all advantageous for a multitude of applications [44].

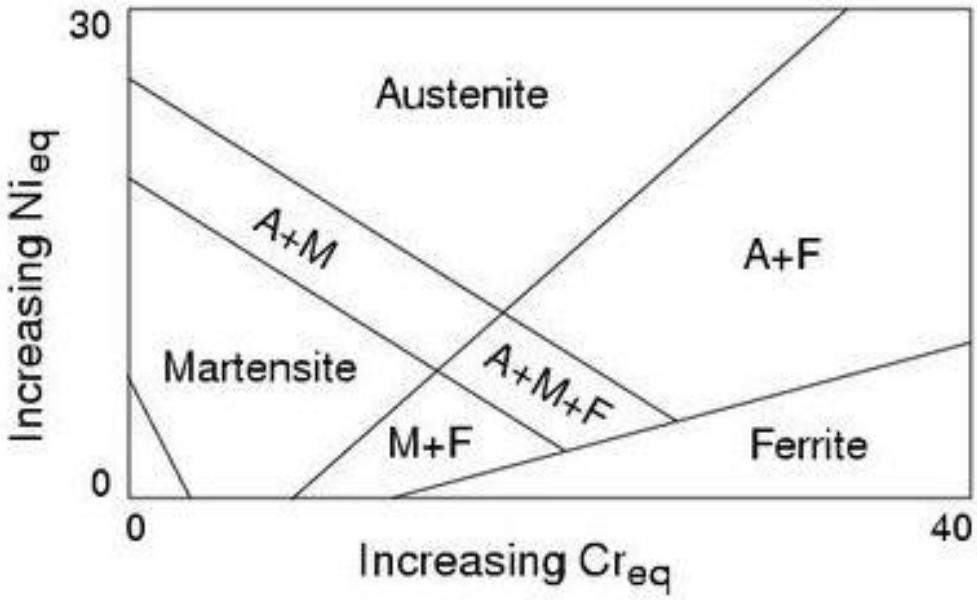

Figure 2.16: Stainless steel phase diagram as a function of chromium and nickel equivalents at room temperature [44].

As can be seen in Figure 2.16, the duplex contains a combination of austenite and ferrite, approximately 50% of each. It is more beneficial and extensively used in liquid storage facilities, as it yields a combination of properties. This is due to a large amount of chromium and a lower nickel content, which results in corrosion resistance, high strength, and excellent toughness [45]. The weighed composition of duplex stainless steel is detailed in Figure B.3 in the appendices. The lower content of nickel in duplex stainless steel implies that duplex is relatively inexpensive compared to other classes [42]. The two-phase mixture also reduces the risk of intergranular attack; for the same reason, they are not prone to solidification cracking during welding [42]. Figure 2.17 shows the comparison of the weight percentages of chromium (Cr), nickel (Ni), and molybdenum (Mo) in duplex and austenitic stainless steel.

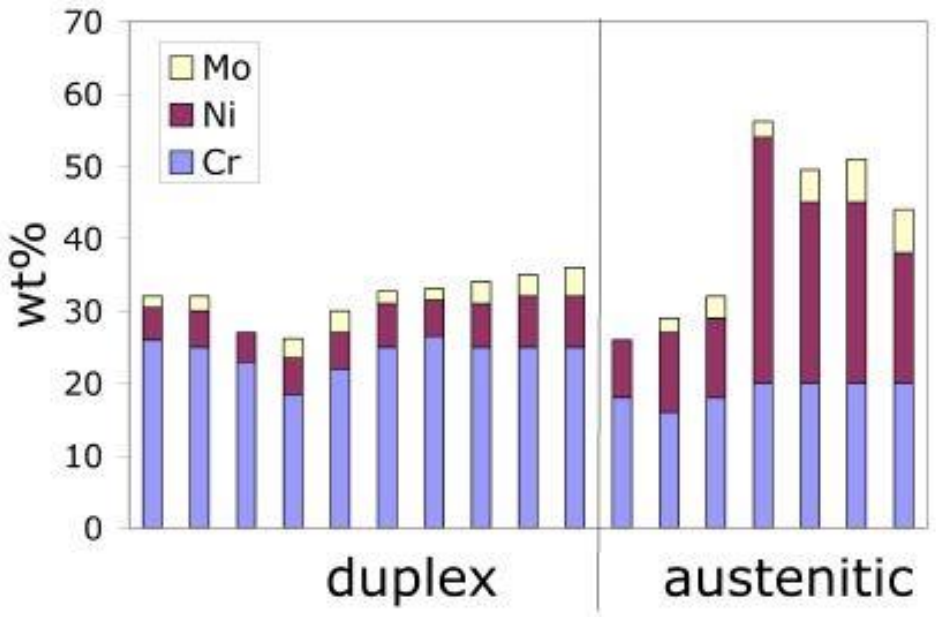

Figure 2.17: Weight percentage of Cr, Ni, and Mo in duplex and austenitic steels [42].

In general, stainless steel is an excellent metallic material that has several useful properties, which are shown in Figure B.4 in the appendices. Consequently, this type of steel offers numerous benefits for various applications. Although stainless steel is popularly known for excellent corrosion resistance, reports in recent years have suggested otherwise [46]. Corrosion in stainless steel often occurs unexpectedly on the welded joints, which then affects the product that is stored, particularly in welded storage tank applications. Another concern for stainless steel is the difficulty of machinability [47]. Fabricating or manufacturing stainless steel is not an easy task due to the elements it contains.

2.9.6 Polyethene plastics

Plastics, also known as polymers, have become a major class of engineering materials. Polymers are substances whose molecules have high molar masses and are composed of a relatively large number of repeating units. There are both naturally occurring and synthetic polymers [48]. They offer several beneficial properties (mechanical, physical, chemical, and optical) when utilised for certain industrial applications [49]. In contrast to metals, polymers are generally characterised by lower density, strength, elastic modulus, thermal and electrical conductivity, high corrosion resistance, and cost [48]. Thus, this is the reason for the rapid increase in plastic processing on an annual basis. In addition, they are the preferred materials over metals nowadays for numerous industrial applications. However, their setback to date is

that they are a waste that affects the environment if they are no longer in use. Nonetheless, there have been developments over the years that aim to rectify this issue, with recycling being the most notable.

Many plastic materials fall under the polymer tree. However, for the present study, polyethene (PE) plastics will be discussed. This is due to the growing demand for this material for manufacturing liquid storage facilities. PE is undoubtedly the most popular plastic material in the world. It is a commodity material that statistically accounts for about 70% of the plastic family [48]. PE is thermoplastic in nature, so it can be reprocessed repeatedly. This is why it is easily available at a relatively low cost and can be easily processed [50]. Moreover, it can be utilised for diverse industrial applications. PE is often classified by the density it contains. Therefore, there is low-density polyethylene (LDPE) ($0.910 < \text{density} < 0.925$), Medium-Density Polyethylene (MDPE) ($0.926 < \text{density} < 0.940$), and High-Density Polyethylene (HDPE) [51]. Consequently, changing the density of the PE will alter its properties. The effect of changes in density, melt index, and molecular weight distribution on the properties of PE is tabulated in Figure E.7 in the appendices.

HDPE is commonly used in the manufacturing of chemical or liquid storage facilities due to the seamless final product that is produced for greater strength and corrosion resistance; thus, it is of great importance in the present study. HDPE is a thermoplastic material composed of mainly carbon and hydrogen atoms joined together to form a high molecular weight product, as shown in Figure 2.18 [51]. Methane gas is converted into ethylene, which, with the application of heat and pressure, is further converted to polyethene. The polymer chain may be 500,000 to 1,000,000 carbon units long. The longer the main chain, the greater the number of atoms [51]. As expected, the properties of HDPE or any plastic material depend on the arrangement of the molecular chains.

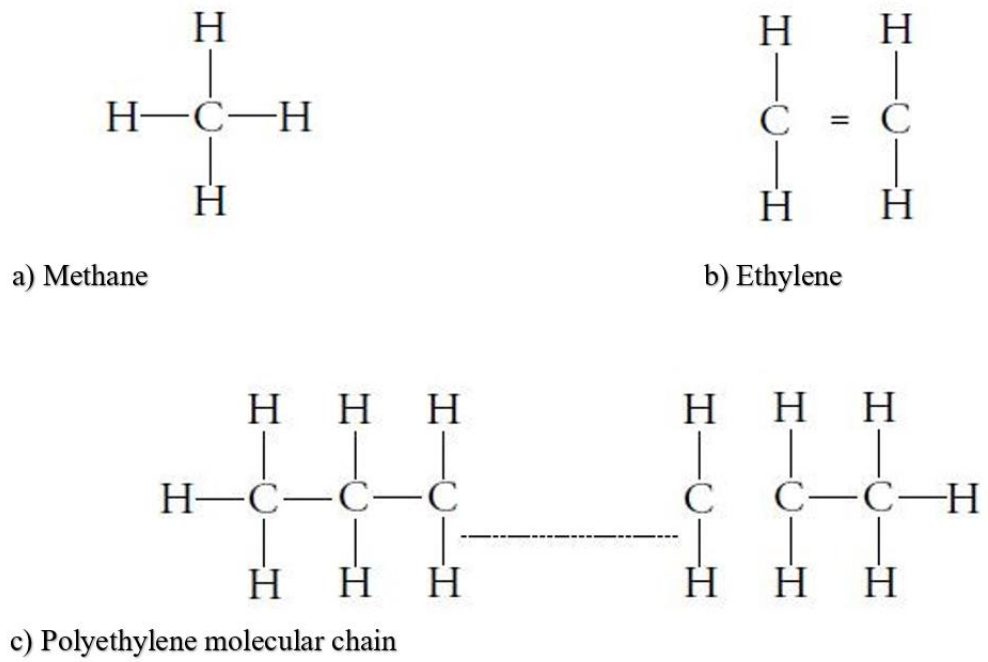

Figure 2.18: Methane gas (a), ethylene (b) and polyethene (c) [51].

2.9.7 Cross-linked polyethene (XLPE) material

Many researchers have been making efforts to obtain a PE with specific chemical, mechanical, and thermal characteristics for the fabrication of complex-shaped products or for use in adverse environmental conditions [50]. In general, plastic is a light and weak substance that easily melts when exposed to heat. However, altering the carbon atoms within the structure changes this perspective. To be precise, cross-linking the carbon atoms within the structure usually transforms such material into a superior material that may be resistant to temperature, pressure, and corrosion, and that can be used in a variety of applications [52]. Crosslinking is known as a process in which carbon atoms of the same or different polyethene chains are joined together to form a three-dimensional network structure [50].

The crosslinking technique was first discovered in the late 1960s by the European scientist known as Engel [52]. The introduction of cross-linked polyethene (XLPE) was another milestone in the plastic era. As a consequence, when PE is cross-linked, it is advantageously employed in the manufacturing of storage facilities due to the advanced resulting properties. The fundamental way to enhance material properties such as impact strength, chemical resistance, and thermal characteristics is via cross-linking [53]. Cross-linking will, however, change the nature of the polymer from thermoplastic to thermosetting polymer, thus yielding

a non-melting and more durable polymer matrix [54]. Crosslinking is easily achieved in branched polymers. With the branched HDPE, it is convenient to crosslink the polymer. However, this is a long and tiring process as compared to LDPE. Since HDPE has a linear molecular structure, crosslinking this type of polymer requires special attention as compared to LDPE. Figures 2.19 and 2.20 show the process of branching HDPE and LDPE, respectively.

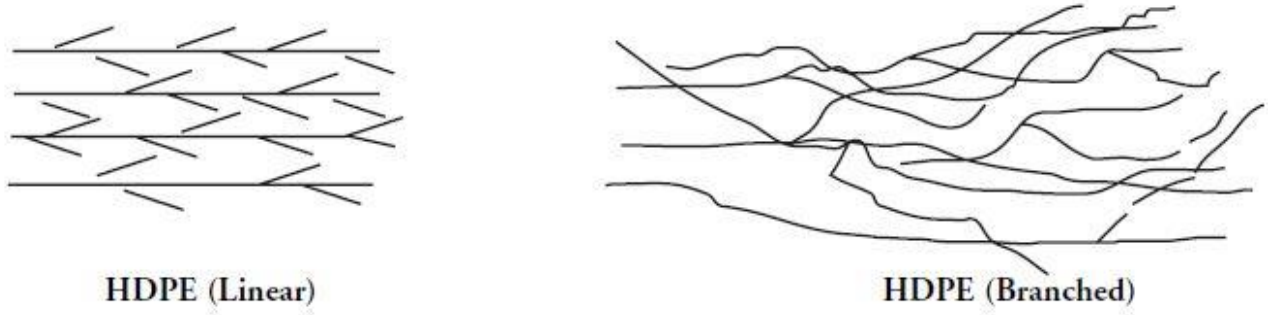

Figure 2.19: Linear and branched HDPE [51].

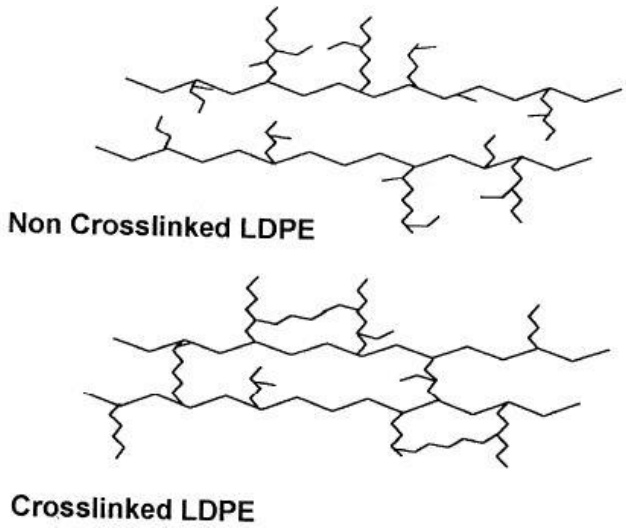

Figure 2.20: Crosslinked and non-crosslinked LDPE [50].

Over the past decades, several crosslinking methods have been developed. However, to date, two tested methods have been used to crosslink polymers: chemical and radiation (physical) methods [51, 53]. These two methods are unique in their own way and are often utilized for a specific purpose. They usually depend on the state (molten or solid) of the polymer during crosslinking and the type of activator used to promote crosslinking [50]. Figure 2.21 illustrates the available crosslinked methods in detail, as discussed above.

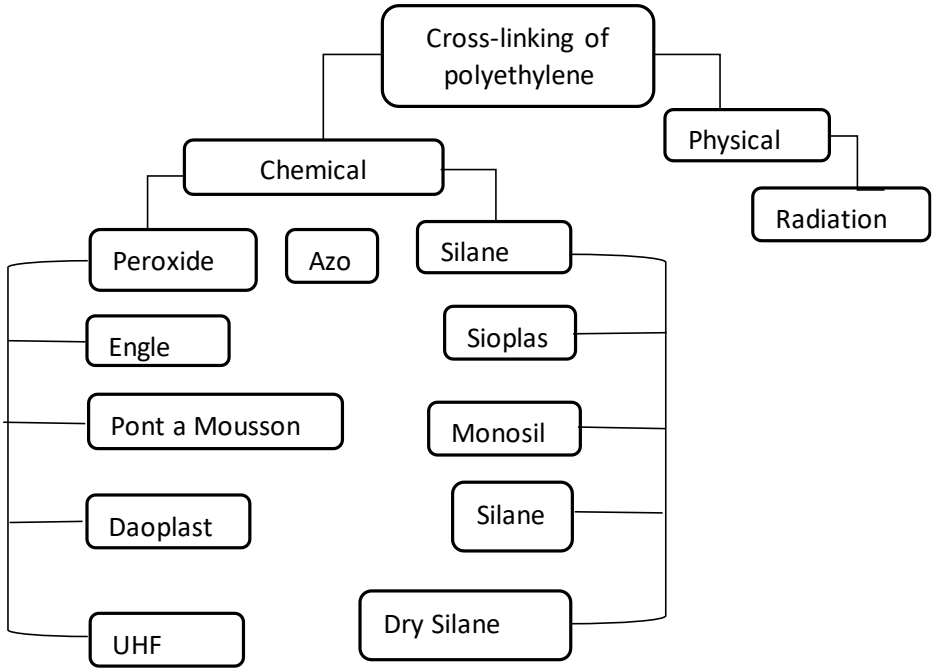

Figure 2.21: Methods available for crosslinking polyethene [54].

2.9.8 Chemical processes

This is an extensively used method for crosslinking polymers. For the method to work as desired, a chemical substance, usually peroxide or silane, is required to significantly activate the links in the polymer chain; thus, it is known as a chemical process [52]. During the chemical process, crosslinking takes place through direct carbon-to-carbon bonds. An alternative may be through the chemical bridges that connect various polyethene molecules [50].

In recent years, most researchers have been interested in knowing the crosslinking method that yields quality thermoplastic. The recent relevant literature suggests that the intensity of crosslinking in thermoplastic resin usually varies with the crosslinking process. Chemical crosslinking using peroxide significantly results in the highest and most uniform degree of crosslinking as compared to the radiation process [52, 54]. Tamboli et al. [54] experimentally investigated the difference in the degree of crosslinking polymers using chemical and radiation processes. The outcome was that radiation crosslinking yields a degree of crosslinking between 34 and 75%. In the chemical crosslinking method, peroxide gives a much higher degree of crosslinking (up to 90%), while silane-based crosslinking can have a 45-70% degree of crosslinking.

2.9.8.1 **Peroxide processes**

The Peroxide crosslinking process has been used for nearly 40 years and is the most common crosslinking process for thermoplastics, especially polyethene. In this method, organic peroxide is used as the initiator. In most cases, an organic peroxide is used in its original, unprocessed structure [54]. It is important to note that this process only occurs when the thermoplastic is in a molten state. In addition, the process is a carbon-based chemical that includes a minimum of two oxygen atoms that are bonded together (-O-O-). The general formula is:

$$R^1 - O - O - R^2 \tag{2.6}$$

Where R1 and R2 values can be aryl, alkyl, or acyl groups, and O is the two oxygen atoms that are bonded together. The alkyl peroxides significantly produce the most reactive free radicals; thus, they are the most commonly used peroxides for crosslinking [50]. Figure 2.22 shows the entire schematic representation of crosslinking polyethene using the peroxide substance. The peroxide process has the advantage of producing products with high thermal stability due to the C-C bonds; however, this is achieved at relatively high costs [54].

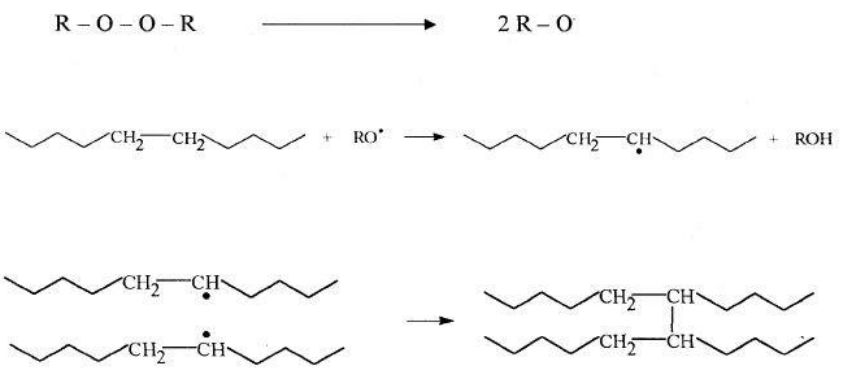

Figure 2.22: Process of crosslinking using the organic peroxide as the initiator [52].

2.9.8.2 **Silane processes**

Silane coupling agents, which react with many chemicals, including polymers, through typical organic chemistry reactions, significantly activate crosslinking, making this process possible. The organ silane molecule critically includes a central silicon atom (Si) bound to two different categories of groups (vinyl and alkoxy), which usually display different

reactivity [52]. Both of these groups are vital in the process of cross-linking. The vinyl groups usually allow silane grafting to the PE, and the alkoxy groups generate a three-dimensional network of siloxane linkages in the presence of water or moisture (through condensation or hydrolysis).

In contrast to the peroxide process, the PE is cross-linked in the crystalline state in the silane process. Thus, the use of silanes results in the formation of siloxane (Si-O-Si) bridges, which are less rigid than carbon-to-carbon (C-C) bonds produced in the peroxide process. The silane process is shown in Figure 2.23 as a two-step process, starting from the grafting of silane on PE to condensation (cross-linking). At first, silane is grafted on PE, and then condensation takes place, yielding cross-linking. One of the advantages of the silane process is that it can be achieved at room temperature and at a relatively low cost.

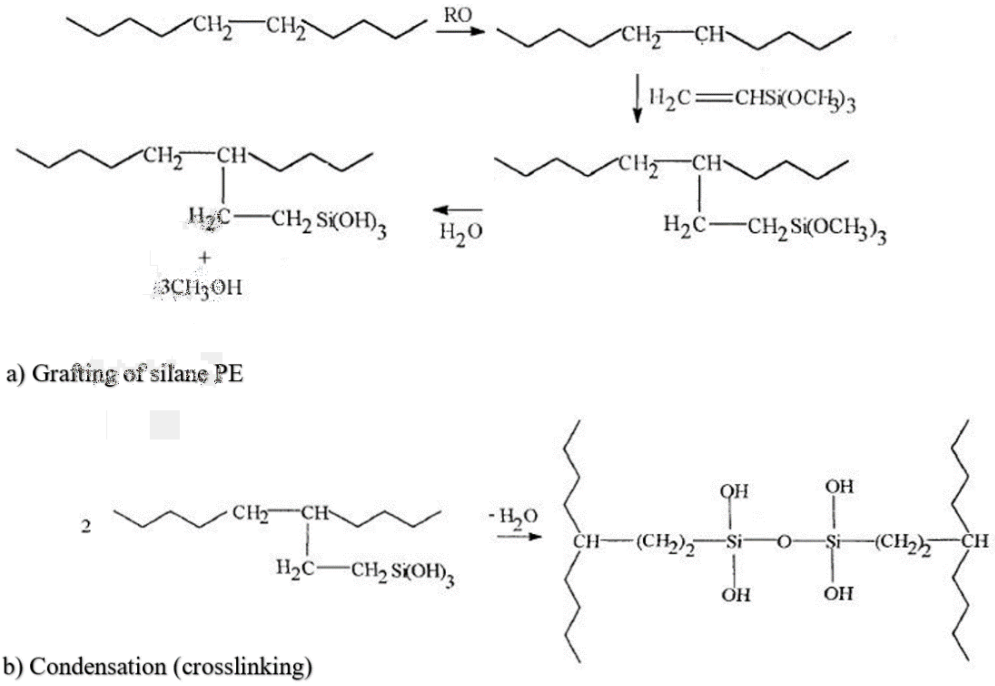

Figure 2.23: Silane grafted polyethene crosslinking reaction [52].

2.9.8.3 **Radiation (physical) processes**

In contrast to chemical processes, radiation processes do not necessarily require the addition of any sort of chemical to the original compound of PE. In the radiation method, crosslinking

is significantly achieved by the free radical mechanism, which is generated in a radiation polymer chain using high energy [52]. As a consequence, two or more chains will join together where the free radical is generated. Figure 2.24 shows the schematic process of crosslinking PE by radiation.

The involvement of high-energy radiation on polymeric materials can critically produce crosslinking or cause a degradation in the main chain, which is termed ‘scission’ [55]. In this way, both chain scission and crosslinking occur simultaneously and competitively. However, the dominance of one or the other may significantly depend upon several factors, such as the sensitivity of the polymer to radiation, the irradiation dose, and the polymer radiation environment [55]. To be precise, in the presence of oxygen (O2), scission is relatively dominant over crosslinking, while in an environment that contains other gases such as nitrogen (Ni), crosslinking is normally dominant [52]. However, the changes and chemical properties of the finished product depend mostly on the efficiency of the crosslinking reaction and its relative ratio with degradation [55].

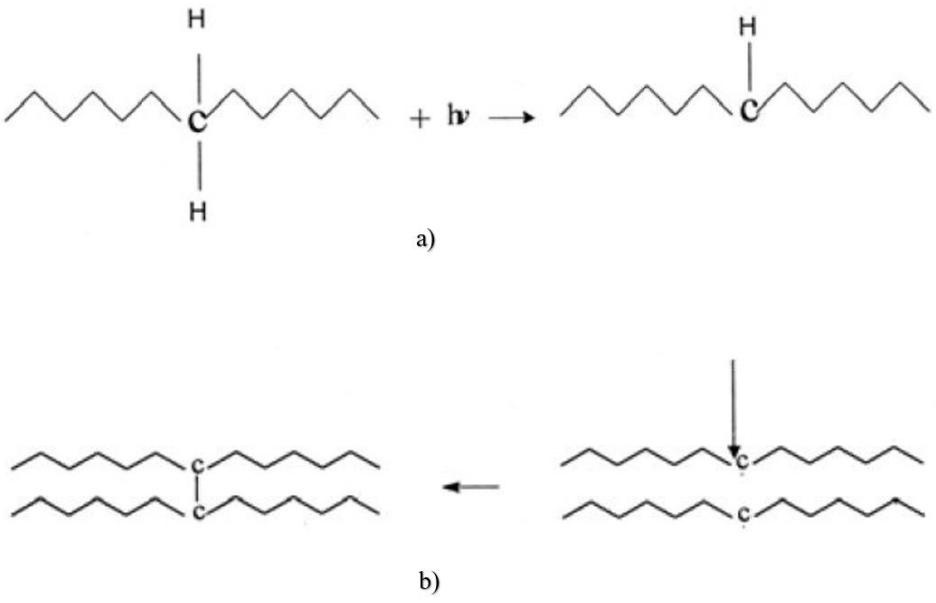

Figure 2.24: Polyethylene energy radiation (a) and the resulting crosslinked PE (b) [52].

Mathematically, the scission and crosslinking can be related to estimating the probability between them. This probability can be expressed as a ratio that is given by the following equation.

$$\frac{\beta}{\alpha} = \frac{1}{2}\frac{G(S)}{G(X)} \tag{2.7}$$

Where,

$\alpha\ is\ a probability\ of c\ rosslinking o\ f chains\ after\ one\ electron\ volt\ of energy$

$absorbed.$

$\beta\ is\ a probability\ of chain\ scission\ after\ one\ electron\ volt o\ f energy\ absorbed.$

$G(X)\ is\ a number\ of\ crosslinking\ per\ 100eV\ of\ radiant\ energy\ absorbed.$

$G(S)\ is\ a number\ of\ scission\ per\ 100eV\ of\ energy\ absorbed.$

The typical G(X) and G(S) values are listed in Figure E.9 in the appendices.

According to several scientists, the bond energy for breaking the C-H bond is typically 364 Kj/mol [52]. Therefore, an electron beam having sufficient energy to break the C-H bond is normally suitable for crosslinking rather than scission [56]. The technique of crosslinking PE by radiation normally involves four main variables.

- The type of radiation and its sources.
- The nature of PE structure to irradiate.
- Mechanisms and theories of reaction.
- The properties of the network formation, especially physical, chemical, and mechanical.

2.9.9 Environmental Stress Crack Resistance (ESCR)

With liquid materials that contain sensitive chemicals within their composition, under certain temperature and stress conditions, the PE material may begin to crack sooner than expected. It has been experimentally proven that storage facilities containing chemically free liquids do not suffer from cracks as much as those containing chemical liquids [57]. This phenomenon is known as the environmental stress crack (ESC). The test methods that are usually used to evaluate ESC and other substances are provided in Figure E.8 in the appendices.

All engineering materials that are suitable for storing liquids containing chemicals are critically evaluated against ECS. For PE, normally the stress-cracking agents are polar materials such as alcohols, detergents, halogens, and aromatics [53]. The property of a material to resist ESC is called environmental stress crack resistance (ESCR) [58]. Researchers have been working on understanding the mechanism of ESCR; however, to date, it is not entirely understood. In most instances, failures of PE polymers that are caused by ESC tend to be due to the development of cracks in the area of tensile stress, which gradually grow and propagate over time [52].

Over the past years, there have been several efforts made to avoid ESC [59]. Therefore, using an appropriate resin formulation of ESCR materials, designing the geometry appropriately, carefully using the manufacturing controls that prevent the occurrence of severe stress risers, and limiting stresses and strains during the storage facility installation are usually sufficient to avoid ESC [53]. Moreover, PE polymers may be cross-linked to improve their chemical properties and thus resist cracking. With this regard, it is vital to test the compatibility of PE, especially XLPE, with AFFF concentrate to avoid unexpected circumstances during fire conditions. To date, there are over 40 different ESCR test methods that are used to determine the chemical resistance of various materials. The standard test that is currently used in the polyethene industry is the bent-strip test [60]. The method is normally used to assess the performance of polyethene cable insulation but can be cautiously used to evaluate the performance of XLPE storage facilities in the presence of AFFF concentrate. The bent-strip test is shown in Figure 2.25. Where the specimen is immersed in a surfactant of interest and the time to failure is noted. The results are reported using the notation, where xx is the percentage of samples that have been tested.

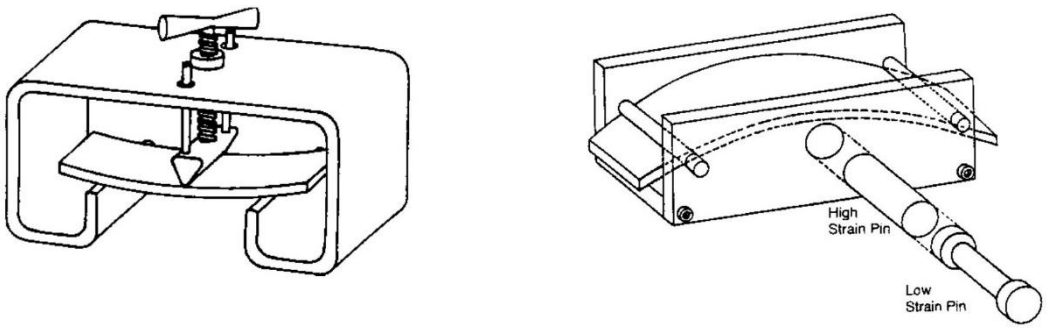

Figure 2.25: Three-point bending apparatus for testing ESCR under constant strain [60]

Research shows that the density of the PE polymer plays a critical role in ESCR [61]. For PE resins of the same molecular weight, the lower the density, the greater the ESCR. The greater the proportion of crystals, the greater the density and brittleness of the resin, which causes rapid crack initiation [54]. However, since the phenomenon of ESC is not fully understood, density alone is inadequate to predict ESCS.

2.10 Infrared spectroscopy overview

Early in the study of organic compounds, chemists observed that certain groups of atoms and associated bonds, known as functional groups, impart distinct reactivity patterns to the molecules to which they belong [62]. Although the properties of each of the several million organic molecules whose structures are known are unique in some sense, all molecules containing the same functional group have a similar pattern of reactivity at the site of the functional group. Consequently, functional groups are a central organising principle in organic chemistry. By focusing on the functional groups present in a molecule (most molecules contain more than one functional group), it is possible to predict and comprehend a number of the reactions that the molecule will undertake [63].

For researchers, Fourier transform infrared (FTIR) is one of the most essential analytical techniques. This method can be used to characterise liquids, solutions, pastes, granules, films, fibres, and gases and reveal their functional groups [64]. It employs infrared light to scan test samples and observe chemical properties. As a matter of fact, a change in the characteristic pattern of transmittance or obsorption bands clearly indicates a change in the composition of the concentrate or material. FTIR is the most popular characterization analysis when compared to other analyses due to its rapidity and relative sensitivity [64]. Throughout the FTIR analysis procedure, samples are exposed to infrared (IR) radiation. The IR radiations influence the atomic vibrations of a molecule in the sample, resulting in the absorption and/or transmission of energy. This makes FTIR a useful tool for determining the molecular vibrations of a sample.

Understanding the significance of the FTIR spectrum is the primary insight garnered from the FTIR analysis. The spectrum can provide "absorption versus wavenumber" or "transmission versus wavenumber" information. However, the "trasmission versus wavenumber" curves are are more reliable and accurate as they are also used in inductively coupled plasma atomic emission spectroscopy (ICP-AES) analysis [65]. The IR spectrum is divided into three

wavenumber regions: the far-IR spectrum (400 cm^{-1}), the mid-IR spectrum (400-4000 cm^{-1}), and the near-IR spectrum (4000-13000 cm^{-1}). The mid-IR spectrum is the most commonly used and provides thorough information for sample analysis, but the far- and near-IR spectra also contribute to providing information about the samples that have been analysed [66]. The mid-IR spectrum is divided into four regions:

1. The single bond region (2500-4000 cm^{-1})
2. The triple bond region (2000-2500 cm^{-1})
3. The double bond region (1500-2000 cm^{-1})
4. The fingerprint region (600-1500 cm^{-1})

The schematic IR spectrum is depicted in Figure 2.26, and the specific frequency of each functional group is also shown.

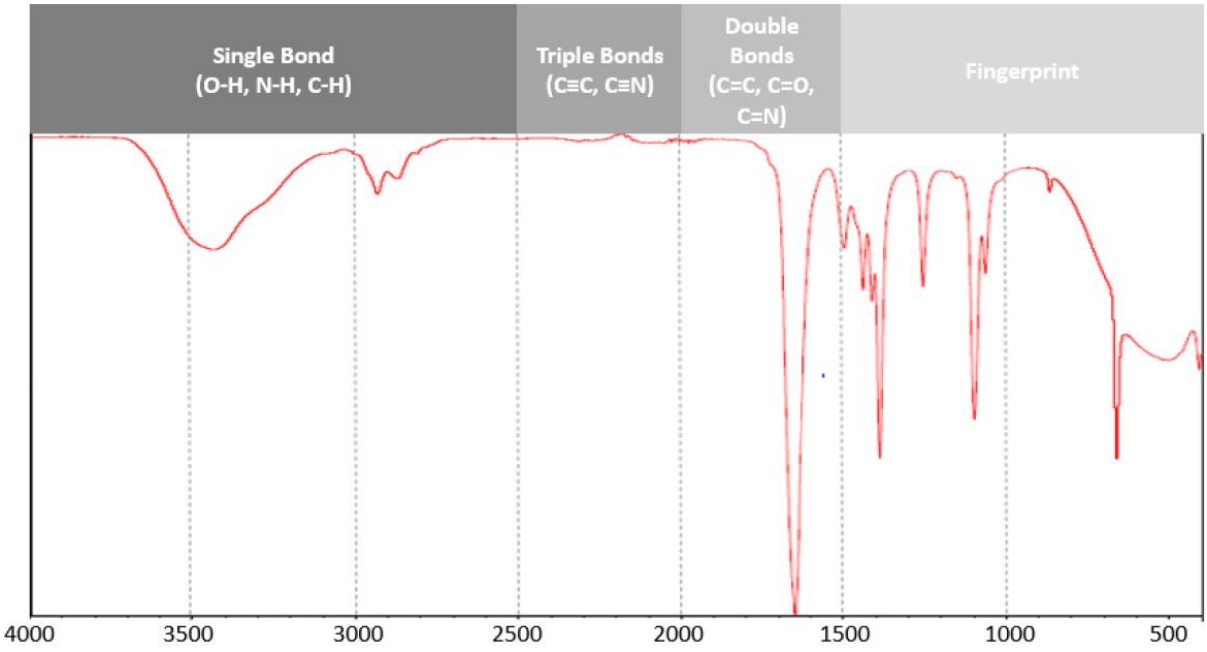

Figure 2.26: Functional group and its quantified frequencies [67].

In Figure 2.26, the x-axis is the wavenumber and the y-axis is the transmittance. All the wavenumbers have the corresponding functional groups. Coates [67] explains that these functional groups could shift when the material has undergone a chemical reaction or is contaminated. For instance, an H-bonded OH stretch in the single bond region may appear at 3000 cm^{-1} in a pure sample, but could shift to a lower or higher wavenumber, depicting that there have been alterations in functional groups of molecules. This, thus, demonstrates that the reaction has taken place within the analysed sample. Kolb et al. [68] conducted a study

that analysed the functionality of organic materials in terms of stability, oxidation, and reactivity. They concluded that the functional group analysis of a sample does not provide conclusive and sufficient information, but it can be primarily used to deduce if there is any reaction within the sample.

2.11 Conclusion

This chapter reviewed the relevant literature to gain a better and more in-depth understanding of the various firefighting foams. The focus was diverted to AFFF, where the evolution of this type of foam was studied. Various foam generation processes and their impacts on the poor performance of AFFF were discussed. Based on the previous studies, the aspirated nozzle is suitable for generating AFFF. The equations involved during this process were analysed, with some recommendations to optimize this process being detailed. The importance of foaming ability and mechanical stability were addressed, and the findings of previous studies were discussed. It was then found that stability directly affects quality, hence the performance of the foam.

The chapter further discussed the engineering materials investigated in the present study. Both metal and plastic materials were closely assessed. The previous research was studied; this was used as a benchmark in this research. The atomic bonding, cross-linking methods, and properties of interest were discussed. The properties of most materials depend on their microstructure. The environmental stress-cracking resistance of the plastics was also discussed. The basics and concepts of infrared spectroscopy were concisely discussed in order to serve as a basis during the results analysis and discussions. The next chapter discusses the experimental design method used for this study. It further discusses the suitability of the chosen research method.

CHAPTER 3: MATERIALS AND METHODS

3.1 Introduction

This chapter describes succinctly the purpose of the experiment, the experimental procedure, the materials, the sample analysis, and the specific experimental procedures used. Below are presented analyses of the methodologies and testing standards used. All the parameters used are discussed and shown, and the safety precautions are followed throughout the experiments. After the AFFF concentrate has been reacted with various engineering materials, the functional groups, particle shape and size, particle size distribution, and elemental composition are critically analyzed.

3.2 Aim of the experiment

The experimental work aims to evaluate and assess the impact and compatibility of the materials used to construct the storage facility with the AFFF concentrate. The incompatibility of these materials can greatly influence the performance parameters of an AFFF solution.

3.3 Methodology

Samples of stainless steel, mild steel, and HDPE, together with AFFF concentrate, were carefully prepared. These are the materials that they commonly use as storage for AFFF concentrate in the aviation industry. A guillotine machine was used to cut the material sheets into the desired shapes and sizes. All the material sheets were cut to the same sizes and shapes for a fair comparison. A total of three samples were used during the experiments. These sample materials were exposed to natural environmental conditions for 3 months. All the samples were then immersed and soaked in a 3% proportion of AFFF concentrate for 5 months. Fourier transform infrared spectroscopy (FTIR), transmission electron microscopy (TEM), dynamic light scattering (DLS), and inductively coupled plasma (ICP) wet analysis were performed on samples of AFFF concentrate. This was done to analyze any critical changes in the parameters, composition, or properties of AFFF concentrate after being in reaction with these three materials.

These are widely accepted methods to evaluate the hydrodynamic size of particles, functional groups, and particle size of the concentrate. For the DLS, the particle size results can be

represented using volume, number, and intensity. However, as stated in the international standard (ISO 22412:2017), intensity-based results are the most reliable parameters provided by DLS to describe particle size and particle size distribution (PSD) [69]. As a consequence, intensity-based results were opted for in the present research work to analyze the PSD of pure AFFF concentrate and AFFF concentrate after the three materials were immersed. A comparison in size distribution is then made to understand the influence of each material on the properties of AFFF concentrate. All the findings were carefully recorded and analyzed. However, it should be noted that the objective was to analyze the AFFF concentrate, not the engineering materials. The experimental procedure followed for all the samples is presented in the flowchart in Figure 3.1.

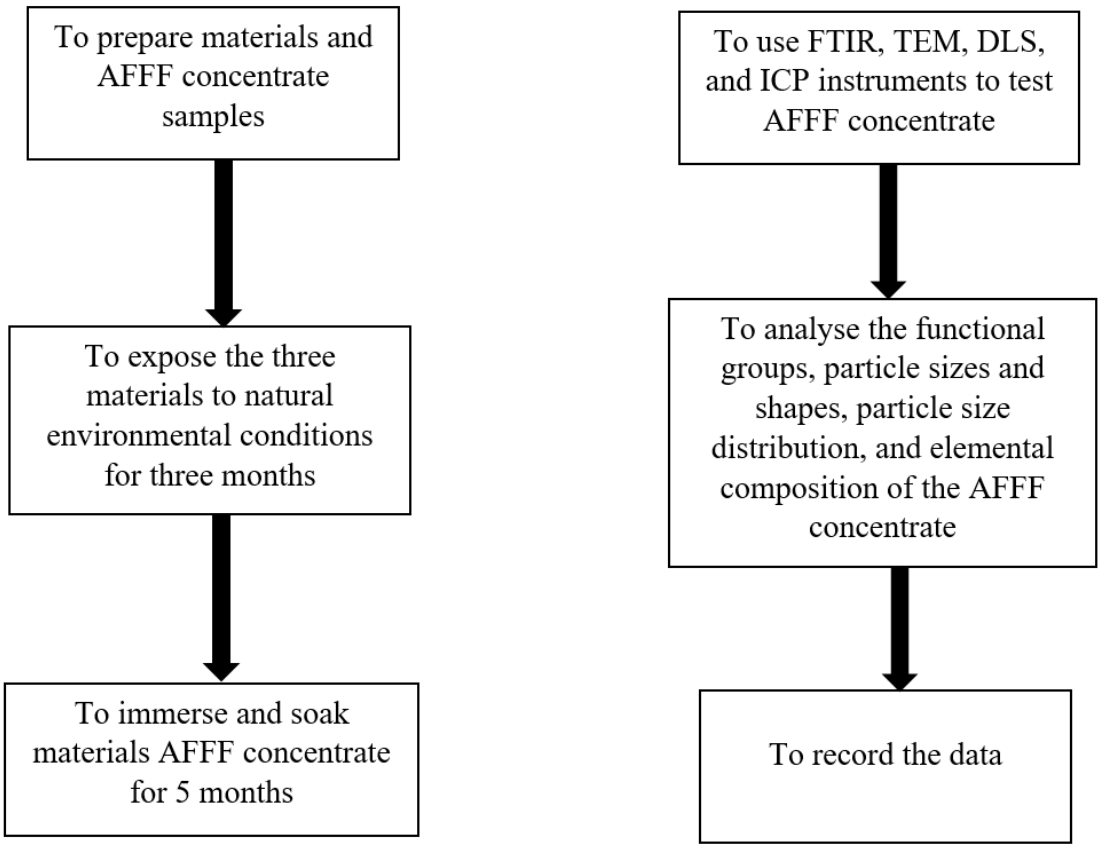

Figure 3.1: Typical experimental procedure.

3.4 Sample preparation

3.4.1 Material plates

The material sheet sizes are based on the common thickness of the storage tanks that contain the AFFF concentrate, as investigated by P. Marcus and E. Protopopoff [70]. Consequently, the thicknesses of 3, 4, and 5 mm for the sheets of mild steel, stainless steel, and HDPE, respectively, were carefully prepared for the experiments. The stainless steel was provided specially by Columbus Stainless (Pty) Ltd., while mild steel and HDPE were collected from the local suppliers in Durban.

These sheets were required to be cut to the desired shapes and sizes so that they could fit in 800 ml beakers filled with AFFF concentrate. The scriber was used to scribe the precise sizes and shapes to be cut. This was done at the Durban University of Technology (DUT) manufacturing workshop using a guillotine-cutting machine. The prepared material samples can be seen in Figure 3.2 (a–c).

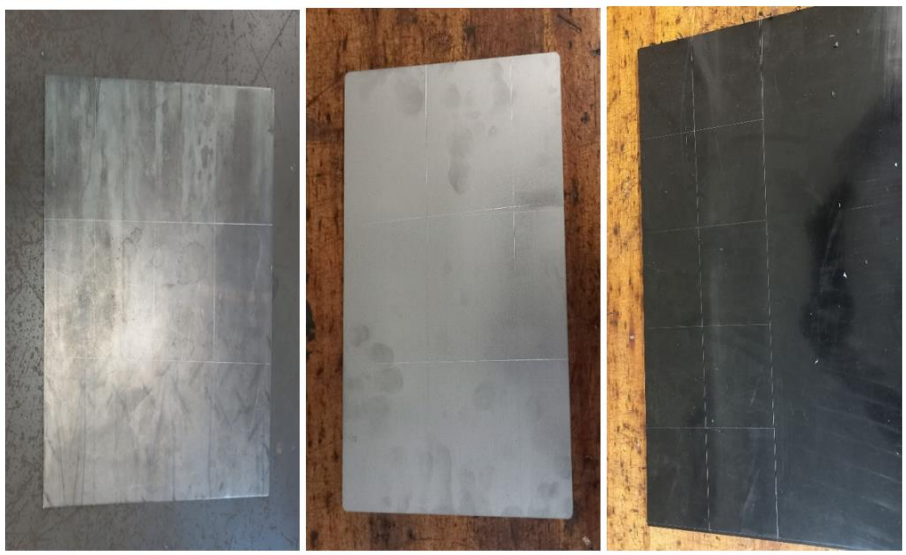

Figure 3.2: Mild steel (a), stainless steel (b), and HDPE (c).

3.4.2 The cutting process

The prepared samples were cut to sizes of 60 mm by 100 mm using a guillotine machine. It can be seen in Figure 3.2 (a-c) that the samples were first scribed before being cut to ensure precision. Mild steel and stainless steel were cut using a guillotine that can cut up to a thickness of 5 mm. In contrast, HDPE was cut with a guillotine that can cut up to 3 mm of thickness, as

it is not as hard as the two sheets of steel. Figure 3.3 (a-b) shows the two guillotine machines that were used to cut the samples.

a) b)

Figure 3.3: Guillotine machines that cut up to 5mm (a) and 3mm (b) thickness, respectively.

As aforementioned, the samples were cut into numerous pieces in the desired shapes and sizes to fit in the 800 ml glass beakers. Figure 3.4 shows the samples after the cutting process.

Figure 3.4: Samples after being cut to the desired sizes, mild steel, stainless steel, and HDPE (left to right).

The samples were polished and cleaned using the rectangular file. This was done to remove the roughness and dangerous chips, to avoid any possible injuries during the experimental setup. Figure 3.5 shows the tools used when cleaning and polishing the samples.

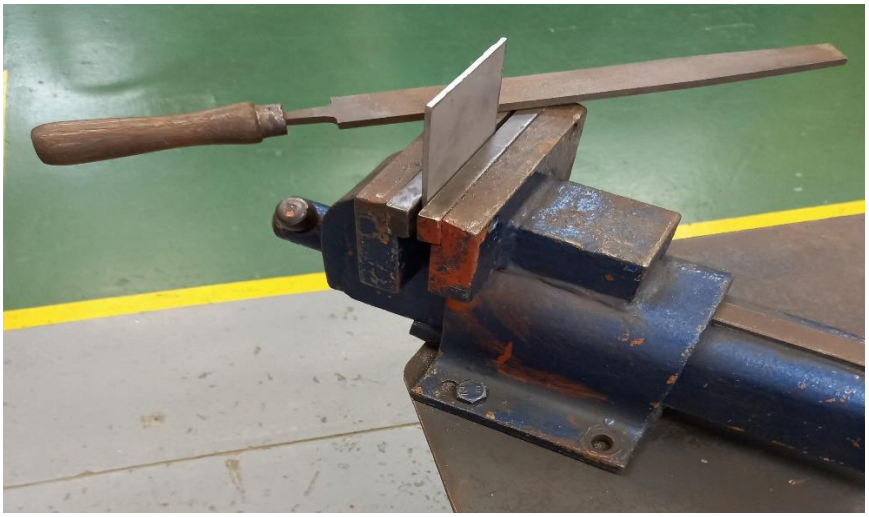

Figure 3.5: Rectangular file and bench vice.

3.4.3 AFFF concentrate samples

The 3% AFFF concentrate samples were prepared in 20-litre batches and kept at room temperature in the DUT laboratory. These were carefully stored in their original containers until the material sheet samples were available and ready. Figure 3.6 shows the AFFF concentrate from the supplier in its original 20-litre container.

Figure 3.6: Pure AFFF concentrate from the supplier.

To immerse various material samples, AFFF concentrate was filled in respective glass beakers. Figure 3.7 shows the three glass beakers used to immerse the three materials of interest.

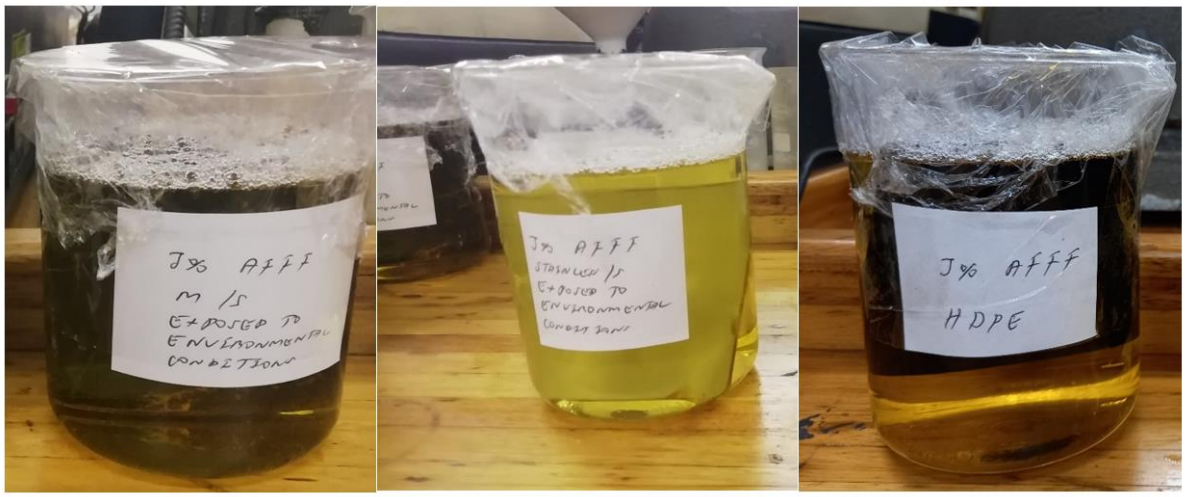

Figure 3.7: Mild steel, stainless steel, and HDPE (left to right) samples immersed in AFFF.

In Figure 3.8 below, samples 1, 2, and 3 are AFFF concentrates when mild steel, stainless steel, and HDPE, respectively, have been immersed (see Figure 3.7). Sample 4 is a pure AFFF concentrate for benchmark and comparison purposes.

Figure 3.8: Samples used during the DLS analysis.

3.4.4 Experimental matrix

The concise experimental matrix is depicted in Table 3.1. This provides a better understanding of which materials were analysed, using what instruments, and which analyses were performed. It can be seen in Table 3.1 that only AFFF concentrate (material) was analysed to deduce if any changes within its properties could be noticed. This was done using four distinct instruments and analysing various parameters (see Table 3.1) for conclusive information.

Table 3.1: Experimental matrix with AFFF concentrate.

Material	Instrument	Analyses
AFFF concentrate	FTIR	Functional groups
	TEM	Particle size and shape
		HR imaging
		Electron diffraction images
	DLS	Particle size
		Particle size distribution
	ICP	Elemental identification

3.5 Testing

The different tests that were performed after the experiments are discussed in this section. The apparatus and various instruments used to conduct the tests are concisely described. Moreover, the characteristic and capabilities of each equipment and its suitability for this study are thoroughly described.

3.5.1 Fourier Transform Infrared Spectroscopy (FTIR)

All the AFFF concentrate samples were analyzed using the FTIR Spectrophotometer (F520), as can be seen in Figure 3.9. This instrument is equipped with a spectral range of 7800–400 cm^{-1} and a resolution better than 0.5 cm^{-1}. The wavenumber precision of +/- 0.01 cm^{-1} makes it a reliable instrument for analysing molecular structure and functional groups. Its rapidity is characterised by a scanning speed of 0.2–2.5 cm/s. The FTIR analyses were accomplished by comparing the manufacturer's pure AFFF concentrate to others that had reacted with mild steel, stainless steel, and HDPE.

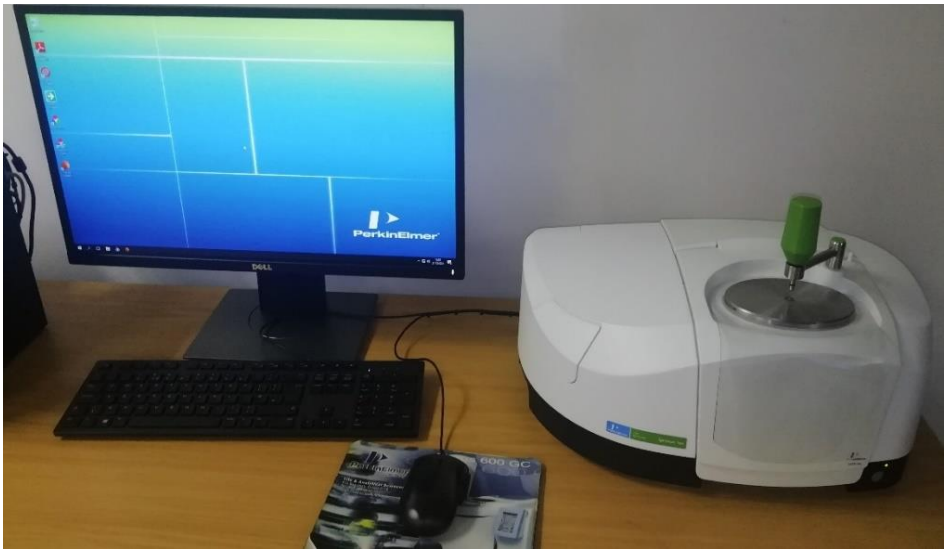

Figure 3.9: FTIR instrument used to identify the functional groups.

3.5.2 Transmission Electron Microscopy (TEM)

To analyze the overall particle shape and the visual overall size of the AFFF concentrate particles, a JEOL JEM 1010 transmission electron microscope (TEM) was used. This instrument is the 100 kV electron microscope shown in Figure 3.10. It is currently equipped with a 1k x 1k Gatan CCD camera (MegaScan model 794) and uses a tungsten filament as its electron source. The 1010 TEM generates very high-contrast images due both to its optics (the design of the pole piece) and to the 80 or 100 kV operating voltage. Moreover, it was designed to be an extremely robust instrument and is capable of high-throughput TEM materials science applications [71]. The JEOL JEM TEM used is limited in such a manner that it does not provide sufficient information on how the particles are distributed within the sample and does not convey precise particle sizes. Consequently, the other relevant tests were necessary.

Figure 3.10: TEM instrument used to analyze AFFF concentrate particles.

3.5.3 Dynamic Light Scattering (DLS)

The AFFF concentrate samples were subjected to particle size distribution and precise particle size tests using the DLS (Zetasizer Advance) shown in Figure 3.11. DLS is a noninvasive technique that depends on the particles moving randomly as a result of collisions with the solvent molecules (Brownian motion). As a result, only particles suspended in a liquid may be categorized [72]. This instrument is multi-angle, as it has improved resolution and provides angularly independent particle size results. It has the potential for particle size measurement ranging from 1nm to 10µn. However, it only requires low sample volumes, which range from 0.5–2 ml. These tests were achieved by measuring the hydrodynamic diameter (Z-average) of any present particles in units of nm within the AFFF concentrate.

Figure 3.11: DLS instrument used to analyze particle size and distribution of AFFF concentrate.

3.5.4 Inductively Coupled Plasma Atomic Emission Spectroscopy (ICP-AES)

The ICP-AES tests were performed using the Shimadzu ICPE-9820 shown in Figure 3.12. This instrument consists of a source, or plasma, optics to split the light into its various wavelengths, and a detector to measure each specific wavelength and its intensity. The continuous wavelength coverage is from 120 to 800, which makes it a very sensitive and accurate technique for the identification and quantification of elements in a sample.

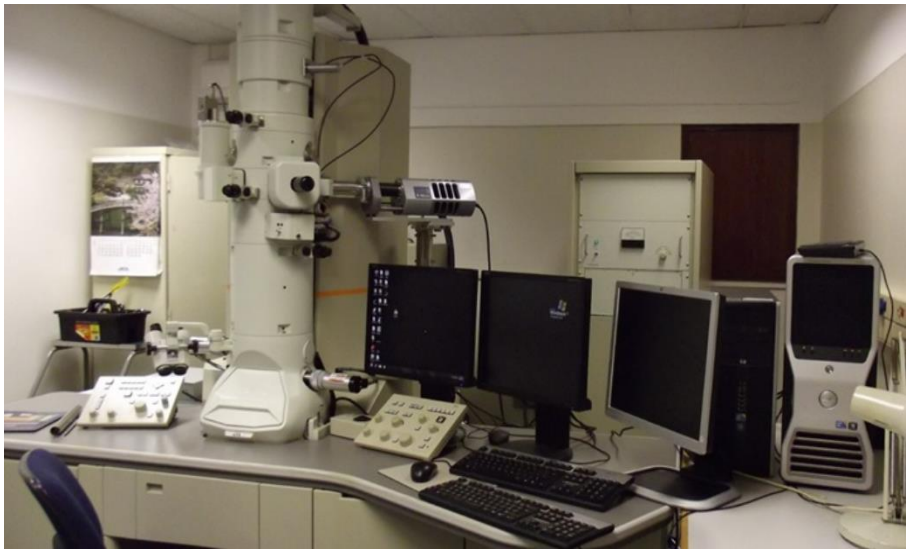

Figure 3.12: ICP-AES instrument used for elementary analysis.

3.6 Conclusion

This chapter discussed the objectives of the experiment, the materials employed, sample preparation, the procedures used to test the samples, the testing equipment and standards, and the sample preparation techniques. The equipment used to analyse the AFFF concentration samples were described in detail, along with the aim and technicality of each test. Moreover, the experimental approach utilised in this study was described. The findings and analysis of the study are described in Chapter 4.

CHAPTER 4: RESULTS AND DISCUSSIONS

4.1 Introduction

In this chapter, the results of the experimental tests conducted during this study are concisely presented and discussed. The variation and correlation observed are also presented. This chapter builds from the materials and methods (Chapter 3). Four tests were conducted as shown in the previous chapter, this was done to validate the objectives of the present study, which is to investigate the effect of mild steel, stainless steel, and HDPE on the properties AFFF concentrate, thus on the performance.

4.2 AFFF concentrate infrared spectroscopy

Figure 4.1 shows the FTIR spectra of the pure AFFF concentrate compared to the AFFF concentrate that has been exposed to the materials of interest. Their functionality in terms of stability, oxidation, and reactivity was revealed. Unsurprisingly, most of the chemical and functional groups appear within the group frequency of 4000–1500 wavenumber 4000-1500 cm^{-1}, since most of the organic compounds normally reveal their functionality in this region.

Referring to Figure 4.1, it can be observed that at the single bond region, broadband appears at 3355 cm^{-1}, which has been associated with a hydroxy group, the H-bonded OH stretch [73]. This functional group is responsible for enhancing the ability of the AFFF concentrate surfactants to dissolve in water [74]. Medial alkyne C≡C stretch appears as a weak band at 2120 cm^{-1}; this is a vital distinguishing tool since very few organic compounds reveal an absorption in this region [75]. The medium band detected at 1637 cm^{-1} can be assigned to alkenyl C=C stretch vibration. Interestingly, the fingerprint region also revealed quite a few functional groups. However, the methylene C-H bend and skeletal C-C vibrations can be disregarded since they appear in most organic compounds. Furthermore, the fluoro-compound C-F stretch at 1083 cm^{-1} confirms the presence of fluorosurfactant in AFFF concentrate. This C-F compound slightly shifted when the materials were immersed in AFFF concentrate, with the largest shift observed when mild steel was immersed.

Referring to Figure 4.1, which compares the FTIR spectra of pure AFFF concentrate with AFFF concentrate that has been exposed to materials of interest to deduce the significant shifts

of functional groups in the single-bond region, a hydroxy group, H-bonded OH stretch, still appears in all the FTIR spectra. However, there is a strange absorption peak of aldehyde C-C stretching that appears in AFFF concentrate after HDPE and stainless steel were immersed at bands 2710 and 2697 cm^{-1}, respectively [76]. This may indicate an interaction between the AFFF concentrate and these two materials. Moreover, there is a significant shift that can be observed in the triple bond region at bands 2056 and 2060 cm^{-1} for exposed HDPE and stainless steel AFFF concentrate, respectively. Consequently, this shift confirms the presence of isothiocyanate N=C=S stretching, which is a very unusual functional group, especially in organic compounds [74].

It can be clearly observed that there are minor shifts in the functional groups. However, these minor shifts can be subsequently used to predict the reaction of the materials with the AFFF concentrate in the long term. This is a very useful prediction technique since, in the present study, these materials were immersed in AFFF concentrate for only five months. Furthermore, the major reaction in the real world could take years. Figure 4.2 (a-c) in Section 4.3 compares the FTIR spectra of pure mild steel, stainless steel, and HDPE to others that have been immersed in AFFF concentrate. This was done to further examine and validate the functional group shifts on the exposed materials of interest.

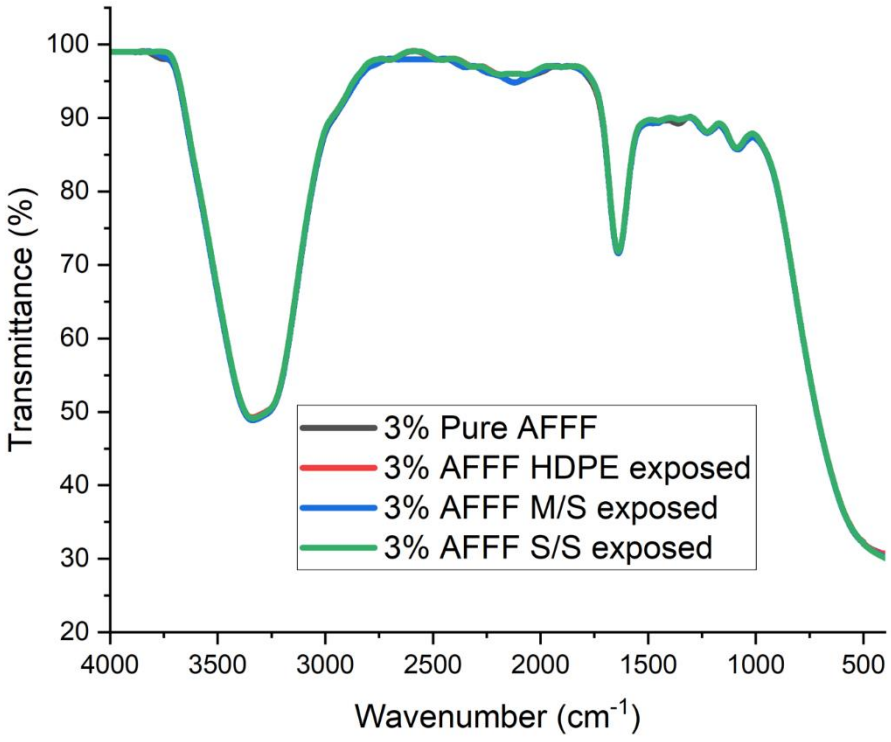

Figure 4.1: Comparisons of pure AFFF spectra with the other after materials were immersed.

4.3 Infrared spectroscopy of Mild steel, and Stainless steel, and HDPE

The FTIR spectra of the materials of interest were conducted to substantiate the minor shifts of the functional group on the exposed AFFF concentrate. Figure 4.2 (a-c) shows the FTIR spectra of the materials of interest. The reactivity of AFFF concentrate with the materials was of particular interest. It can be observed from Figure 4.2 (a-c) that there are significant shifts in functional groups. In Figure 4.2 (a), the O-H stretching, which can be observed at 3583 cm^{-1} in pure HDPE, shifted to a wavenumber of 3817 cm^{-1} when the materials were immersed in AFFF concentrate [77]. In pure HDPE, a strong amine N-H stretching at 3358 cm^{-1} can be seen, which shifts to a broad band at 3406 cm^{-1} in immersed concentrate [78].

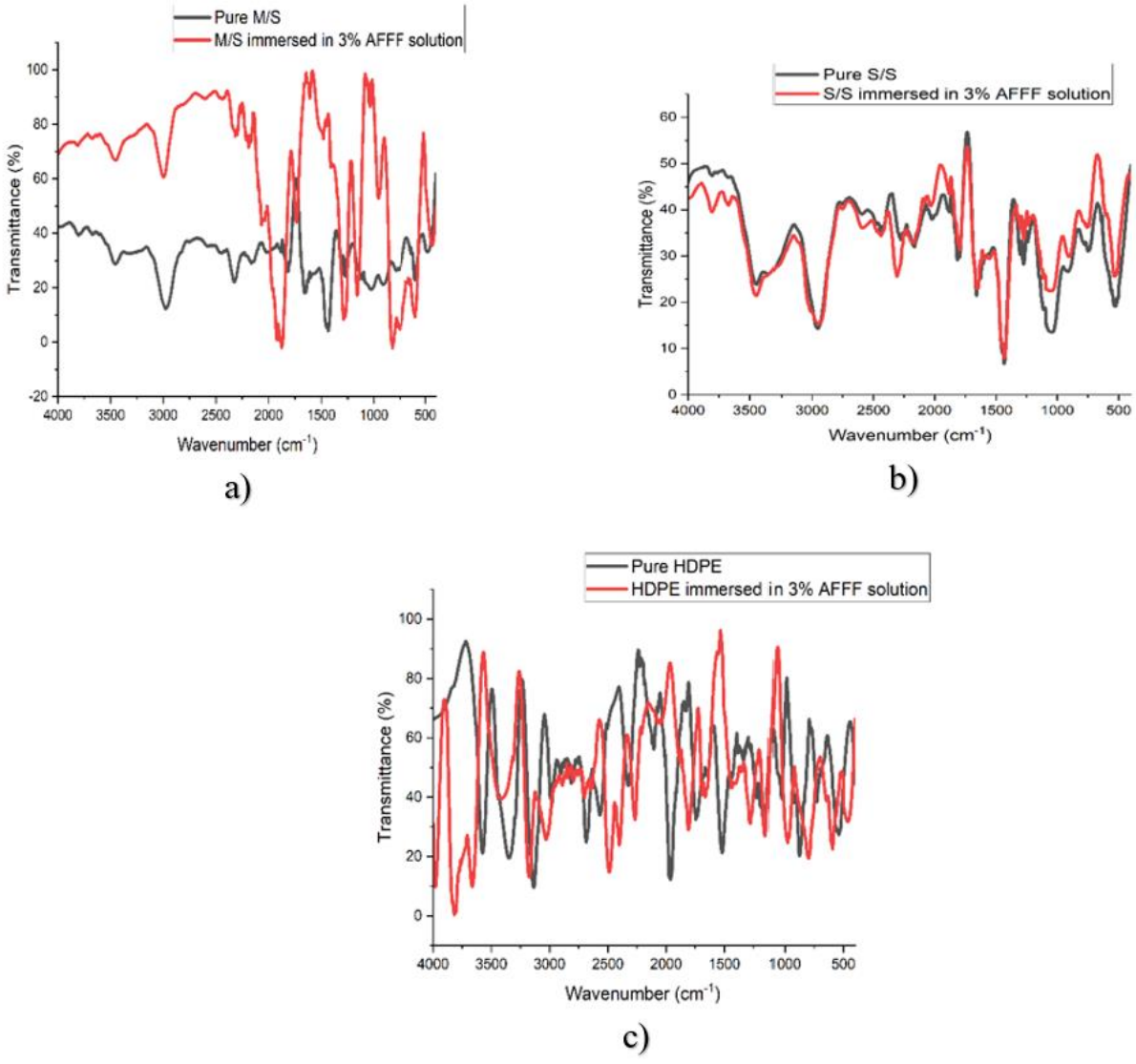

Figure 4.2: FTIR spectra, comparing various materials.

4.4 Transmission Electron Microscopy (TEM)

Figure 4.3 shows the TEM images of pure AFFF concentrate which depict the HR and electron diffraction images in various distinct parts.

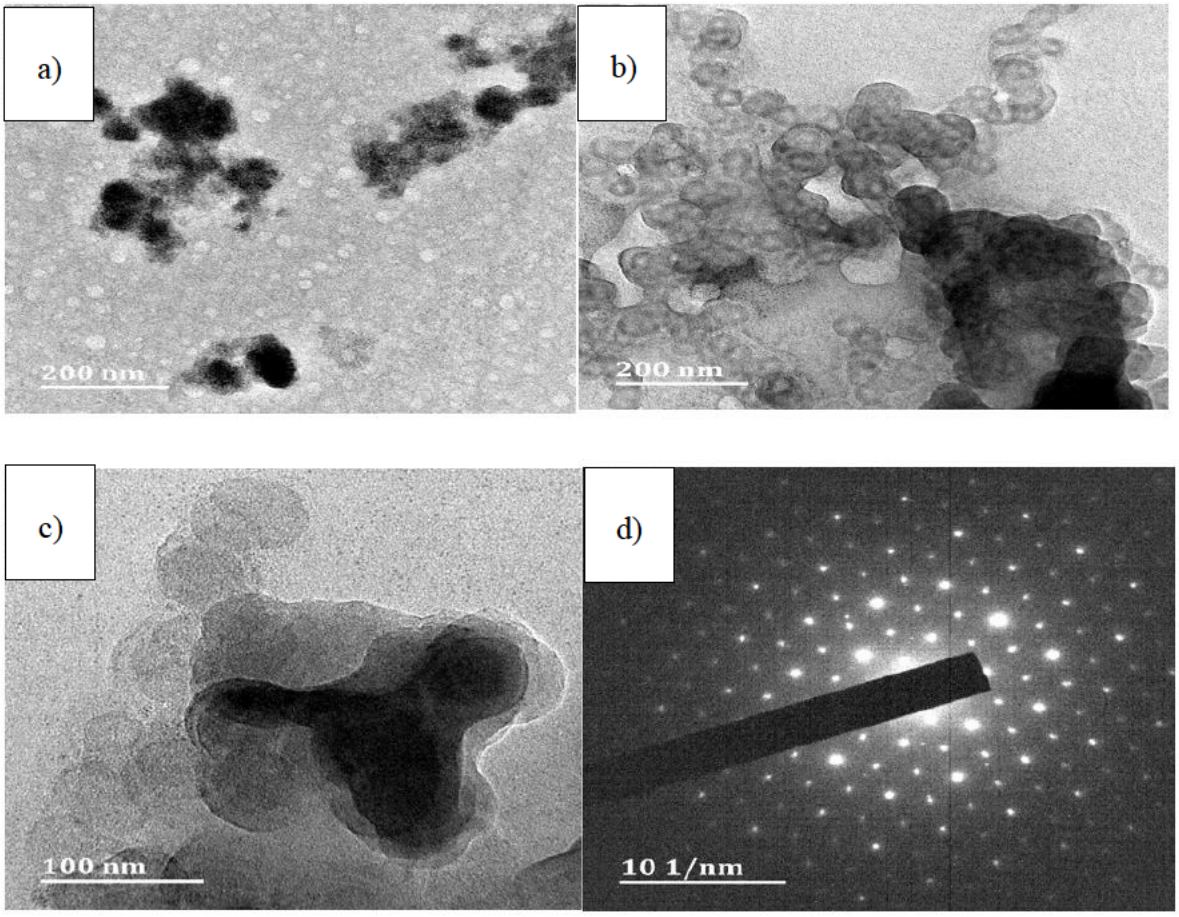

Figure 4.3: HR (a-c) and electron diffraction images (d) of pure AFFF concentrate.

It can be observed from Figure 4.3 (d) that the electron diffraction image of pure AFFF concentrate provides numerous spots that are aligned in a particular direction. This is a demonstration that the concentrate in a pure state has a single crystalline structure. This shows that the concentrate has uniform properties and is more stable in its pure form [79]. Moreover, Figure 4.3 (a-c) reveals that the particles of pure AFFF concentrate are scattered along the concentrate. This might be caused by the collision of two or more repelling particles within the concentrate [80]. Figures 4.4–4.6 depict the HR and electron diffraction images when various materials were immersed in AFFF concentrate.

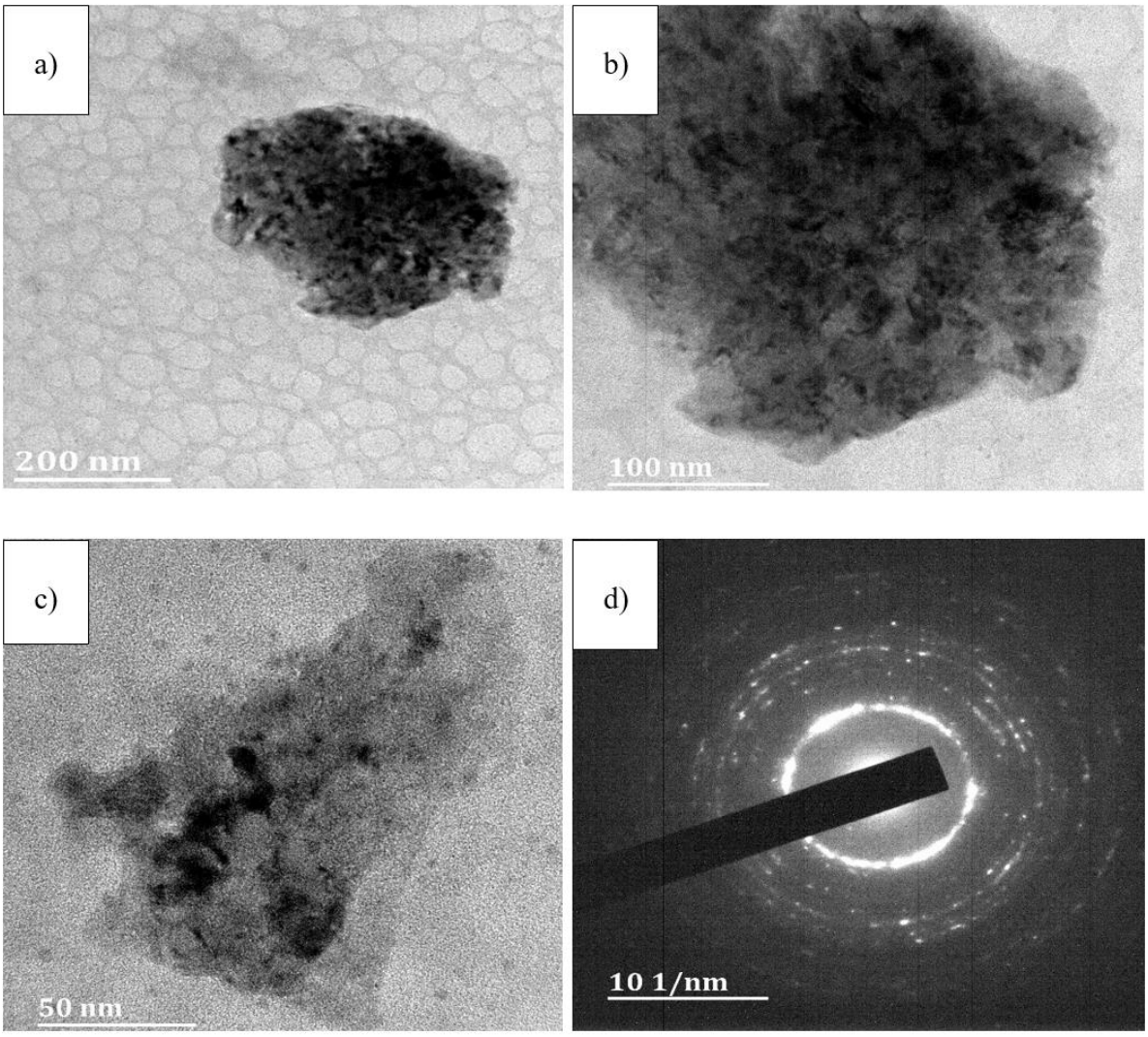

Figure 4.4: HR (a-c) and electron diffraction images (d) of AFFF concentrate immersed in mild steel.

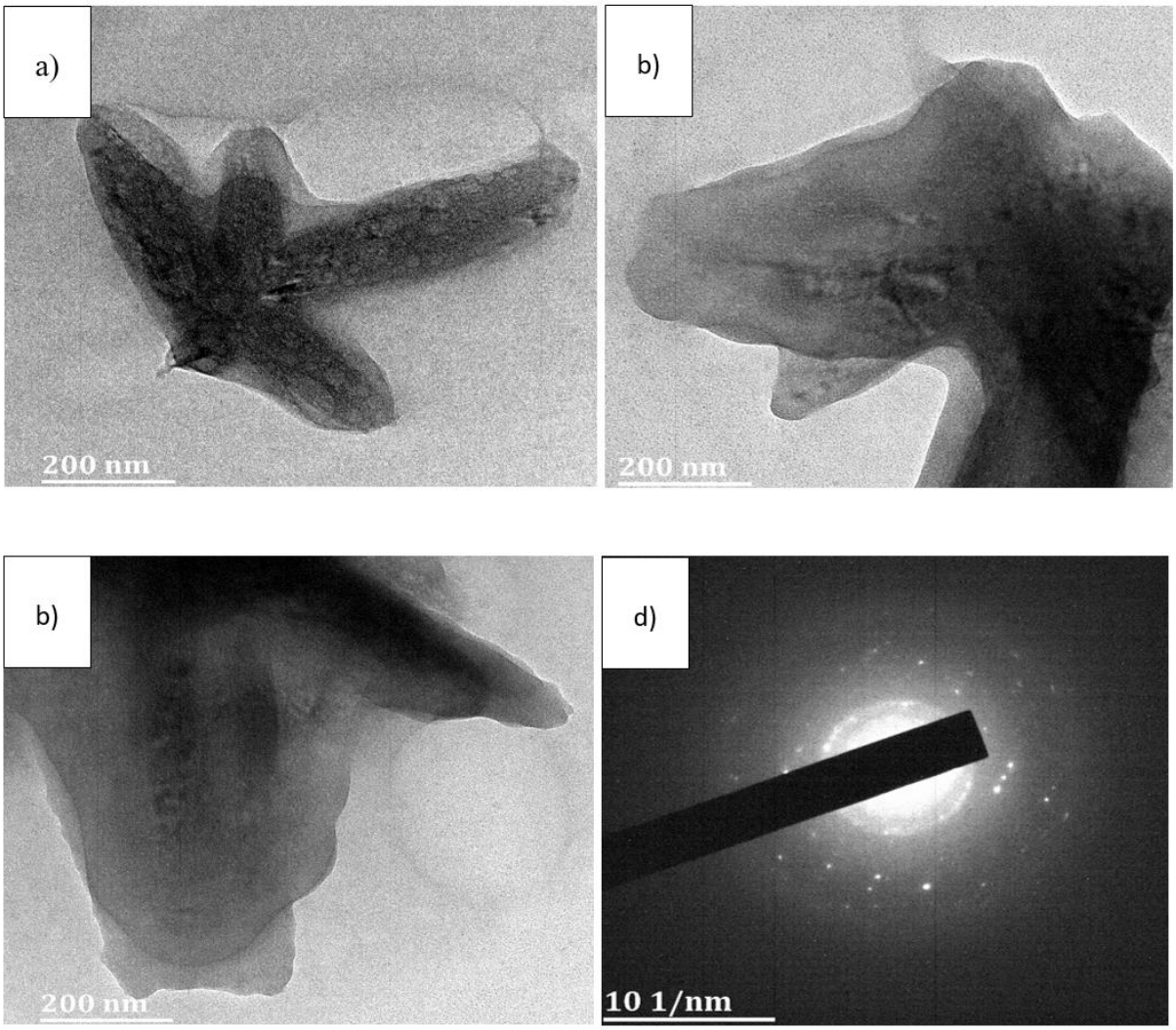

Figure 4.5: HR (a-c) and electron diffraction images (d) of AFFF concentrate immersed in stainless steel.

The overall crystal structure and the difference in particle shape for the three samples compared to a pure AFFF sample were studied. Although the present TEM analyses are not able to provide the precise particle sizes of the samples, they nonetheless provide a significant overall change in the crystal structure. Figure 4.3 revealed that in a pure state, AFFF concentrate possesses a single crystalline structure. However, when studying Figures 4.4–4.6, it is observed that the exposed AFFF concentrate has critically changed to a polycrystalline structure. When closely inspecting the electron diffraction images of these samples, this is seen in Figures 4.4–4.6 (d).

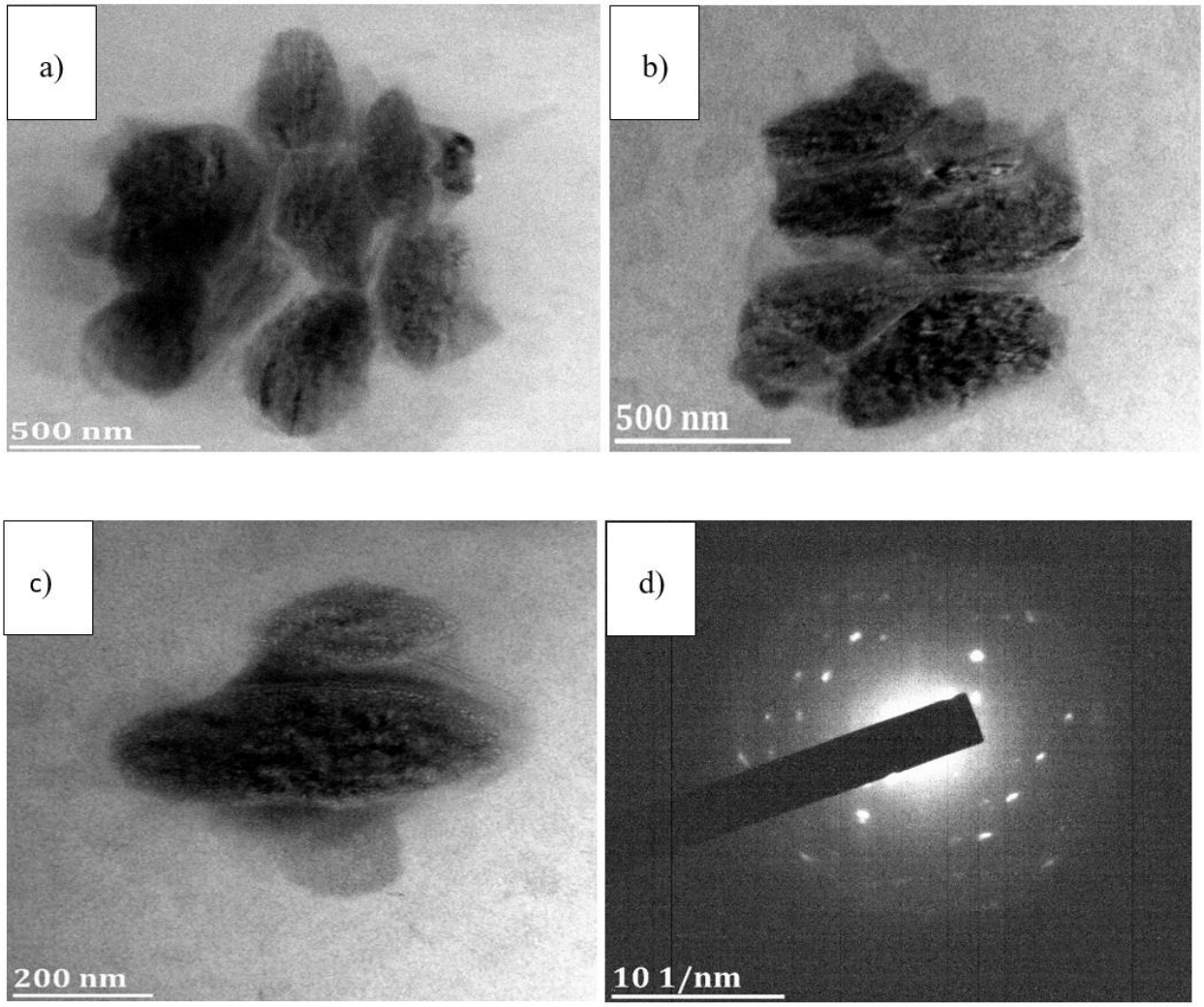

Figure 4.6: HR (a-c) and electron diffraction images (d) of AFFF concentrate immersed in HDPE.

The concentrated circular rounds imply that all these materials are polycrystalline. This is confirmed by the morphology (particles, grains, and crystallites), as several grains are observed in Figures 4.4–4.6. These grains are separated by grain boundaries and have random crystallographic_orientations. It can be further observed that Figure 4.4 has more grains compared to Figures 4.5 and 4.6. Consequently, this implies that most of the crystal structural changes occurred when mild steel was immersed in AFFF concentrate.

When comparing the differences topographically (structure and shape), it can be observed in Figure 4.3 that the particles for pure AFFF concentrate are scattered and distributed along the concentrate. However, when closely observing Figures 4.4–4.6, it can be seen that the particles for these samples are concentrated in one area, especially in Figure 4.4. As a result, this

demonstrates that when the materials of interest were immersed in AFFF concentrate, there was a structural and shape particle change. The alteration in crystal structure and particle shape in AFFF concentrate complements the shifts in functional groups obtained using FTIR. Zhuoqing An et al. [81] experimentally investigated the effect of the particle shape on the viscosity of the liquid. Their results indicated that the spherical particles have a lower viscosity, and any other particle shape will result in a higher viscosity. In addition, a change in any additives in AFFF concentrate will affect the foam drainage time. It should be noted that the causes of these alterations are not known as of yet. However, conclusive results and interpretations are detailed in Sections 4.5 and 4.6 using the DLS and elementary analysis to validate the vital information provided by FTIR and TEM.

4.5 Dynamic Light Scattering (DLS)

4.5.1 Particle size analyses

Table 4.1 shows the summary of the results for average particle sizes for the four samples used during the experimental work in nanometer (nm). All the samples are AFFF concentrates, depending on which materials was immersed.

Table 4.1: Summary of average particle sizes.

SAMPLE ID (AFFF CONCENTRATE)	Z-AVERAGE (D)
1 – When mild steel was immersed	660.7 nm
2 – When stainless steel was immersed	4.892 nm
3 – When HDPE was immersed	4.036 nm
4 – Pure	3.586 nm

It can be observed from Table 4.1 that there have been changes in particle diameter. The pure AFFF concentrate has an average particle size of 3.586 nm, which is a very small particle size. However, when comparing this to samples 2 and 3, it can be observed that there is a slight difference or change. To be precise, the change in Z-average is around 1.306 nm at most. At this point, it is not known if these changes are slight enough to not affect the properties of AFFF concentrate. Sample 1, in Table 4.1, shows a major change in particle size. Sample 1 has an

average particle size of 660.7 nm, which is way above the other three samples by about 655.808 nm at most. This difference is extremely surprising and has some implications. Koca et al. [82] studied the effect of particle size on the properties of nanofluids. They discovered that larger particles have a slower diffusion speed than smaller ones.

As a matter of fact, for AFFF stability, rapid diffusion of fluorosurfactant molecules is required. The rate of diffusion is inversely proportional to the particle size [83]. However, it also depends on the surface area and temperature. This is a demonstration that once AFFF concentrate has been in contact with mild steel, it decreases its diffusion rate rapidly and thus decreases the foaming stability of AFFF. On the other hand, the Z-average (particle size diameter) results demonstrate that when stainless steel and HDPE have been immersed in AFFF concentrate, there are slight differences in particle diameter when compared to pure AFFF concentrate. When visually observing the numbers, the difference looks slight. On the contrary, the quantitative analysis in terms of the percentage increase calculations demonstrates a relatively large difference. The fundamental equation is given as:

$$\%Increase = \frac{D_S - D_O}{3.586} \times 100 \tag{4.1}$$

$$= \frac{4.892 - 3.586}{3.586} \times 100$$

$$= 36.419\%$$

It is possible to calculate the percentage increase in particle size for the AFFF concentrate when stainless steel was immersed.

Where,

D_s *is the particle size diameter of sample* 2 *in nm*

D_O *is the particle size diameter of sample* 4 *in nm*

The same formula employed in Equation (4.1) can be used to calculate the percentage increase in particle diameter for the AFFF concentration when HDPE was immersed.

$$\%Increase = \frac{D_H - D_O}{D_O} \times 100 \quad (4.2)$$

$$= \frac{4.036 - 3.586}{3.586} \times 100$$

$$= 12.549\%$$

Where,

D_s *is the particle size diameter of sample* 2 *in nm*

D_O *is the particle size diameter of sample* 4 *in nm*

It can be seen from Equation (4.1) that the particle size percentage change is 36.419% when stainless steel is immersed in AFFF concentrate. This can be regarded as a huge increase since there is more than a quarter (1/4) difference between the two particles. When analyzing Equation (4.2), it can be observed that when HDPE was immersed in AFF concentrate, the particle size had an average change of 12.549 nm. This is a much smaller percentage compared to 36.419 nm, with a difference of 23.87 nm. However, it cannot be guaranteed that it does not affect the foaming ability of AFFF concentrate. At this moment, there are still doubts regarding the effects of these materials on AFFF concentrate. However, the analysis of the particle size distribution (PSD) and element composition will be conducted in Sections 4.5.2 and 4.6, respectively, for further validation.

4.5.2 Particle size distribution (PSD) analyses

The PSD curve of the pure AFFF concentrate plotted by intensity is shown in Figure 4.7. This PSD curve is used to compare and analyse the alteration in PSD of AFFF concentrate when various materials were immersed.

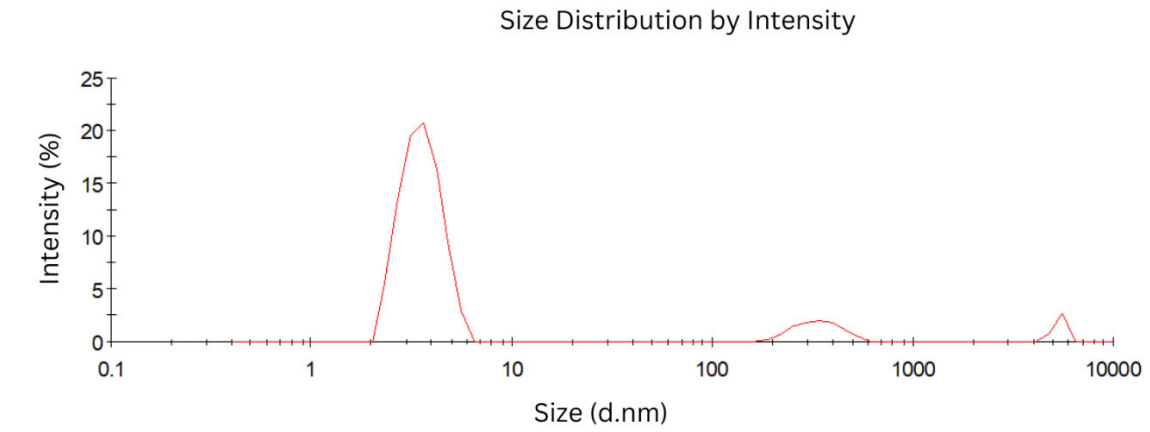

Figure 4.7: Particle size distribution of pure AFFF concentrate.

It can be observed from Figure 4.7 that the particle size distribution curve shows that the peaks are divided into three intensities. It was expected that the major peak would be at a particle size of 3.586 nm since it was previously demonstrated in Table 4.1, and the second and third peaks can be estimated at 350 and 5500 nm, respectively. De la Calle et al. [83] studied the particle size distribution of aqueous concentrate. They demonstrated that the aqueous concentrate with a narrow PSD was able to disperse easily. Similarly, it can be seen from Figure 4.7 that the first peak is very narrow. As expected, this is evidence that, in a pure state, AFFF concentrate can disperse or spread rapidly over a large surface area.

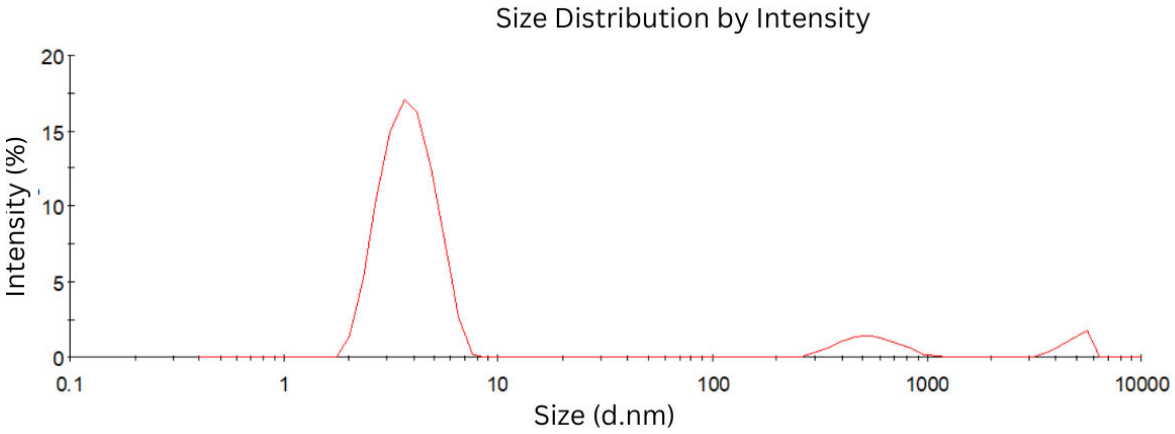

Figure 4.8: Particle size distribution of AFFF concentrate when stainless steel was immersed.

Referring to Figure 4.8, it is observed that the AFFF concentrate possesses three peaks. This is precisely the same observation as in Figure 4.7. The main peak can be attributed to a particle size of 4.892 nm. Moreover, it can be seen from Figure 4.8 that the main peak has a narrow PSD. However, when closely observed, it is slightly wider compared to Figure 4.7. This

demonstrates that stainless steel did not cause any critical alteration of PSD within the AFF concentrate, as it is still able to disperse easily. This is validation that stainless steel does not influence the spreading ability of AFFF. This further concludes that the minor particle size alteration discussed in Section 4.5.1 and Equation (4.1) does not have a significant impact on the diffusion rate of fluorosurfactant molecules.

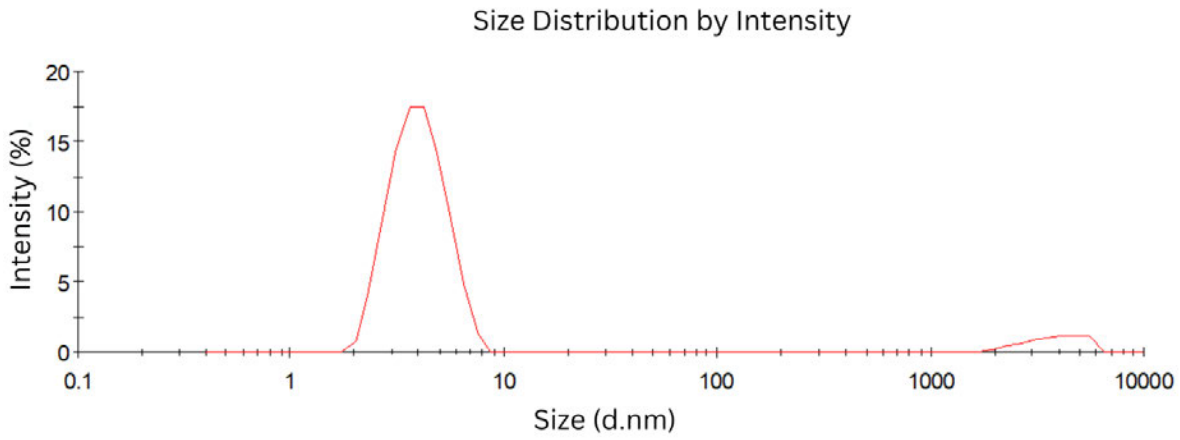

Figure 4.9: Particle size distribution of AFFF concentrate when HDPE was immersed.

It can be observed from Figure 4.9 that the PSD curve consists of peaks that are divided into two intensities. This is in contrast to Figures 4.7 and 4.8, where the peaks were divided into three intensities. The major peak can be associated with a particle size of 4.036 nm, whereas the other peak can be estimated at 5000 nm. When observing the broadness of the major peak, it can be noticed that it is wider than the peak in Figure 4.7 and almost the same size as Figure 4.8. This, however, can be considered a narrow peak. Moreover, this provides sufficient evidence that HDPE does not alter the PSD within the pure AFFF concentrate, which suggests that the dispersion rate is not affected. This further concludes that the minor particle size alteration discussed in Section 4.5.1 does not have a significant impact on the diffusion rate of fluorosurfactant molecules.

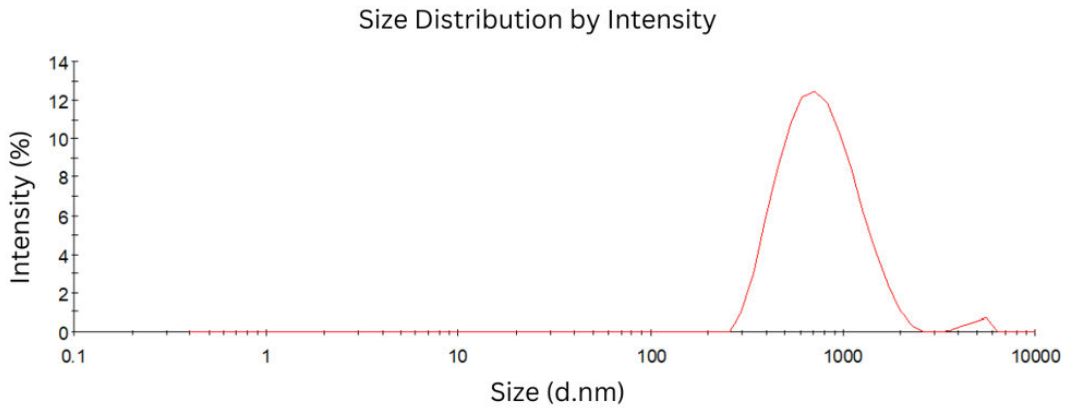

Figure 4.10: Particle size distribution of AFFF concentrate when mild steel was immersed.

Surprisingly, Figure 4.10 depicts a distinct PSD compared to Figures 4.7–4.9. It can be observed that Figure 4.10 reveals peaks that are divided into two intensities. These peaks can be associated with particle sizes of 660.7 nm, whereas the other peak can be estimated at 5500 nm. Due to the large difference in size between these two peaks, they can be generally regarded as major and minor peaks, respectively. It is interesting to note that Figure 4.10 possesses a wide major peak compared to all previous peaks illustrated in Figures 4.7–4.9. This is an indication that there has been a sensitive reaction between mild steel and AFFF concentrate. Moreover, this demonstrates that the spreading ability of the concentrate has been reduced. This could be caused by several parameters, such as an increase in viscosity that causes the concentrate to be slightly thicker. However, it is well known that viscosity is largely dependent on the shape of the particles, and any deviation from the spherical shape of the particle increases viscosity [84]. Nevertheless, it is noticed in Figure 4.10 that the alteration in PSD can have a slight impact on the spreading capability of the aqueous concentrate.

4.6 Wet chemical analyses

As aforementioned, the ICP-AES was used to identify both the amounts and major concentrations of elements within the exposed AFFF concentrate and benchmark these with the standard quantities and qualities. The alterations in elements or composition can immensely affect the properties, hence the performance of AFFF during firefighting circumstances. The concrete results are provided in this section, and conclusive information is drawn regarding the severity of mild steel, stainless steel, and HDPE on the performance parameters of AFFF. In addition, the elementary results are more reliable as they provide the precise elements that are

present within the AFFF concentrate before and after the materials were immersed. Thus, they validate the previous results of the analyses conducted using FTIR, TEM, and DLS.

4.6.1 Elemental composition analyses

For the present research, the elements were analyzed based on the importance of the role they possess within the AFFF concentrate. Table 4.2 depicts the elemental composition results of the pure AFFF concentrate and those obtained when mild steel, stainless steel, and HDPE were immersed. The entire elemental composition results are depicted in Figures F.1 and F.2 in the appendices for validation purposes.

Referring to Table 4.2, samples 1-3 are the AFFF concentrate after mild steel, stainless steel, and HDPE were immersed, respectively, with sample 4 being the pure AFFF concentrate. From Table 4.2, it can be observed that in a pure state, AFFF concentrate has 2354 and 94.7 parts per million (ppm) of sodium and sulphur, respectively. When observing closely, it is seen that the sodium in pure AFFF concentrate (sample 4) decreases gradually. To be precise, the sodium is reduced by 5, 22, and 52 ppm, respectively, from the pure AFFF concentrate. This indicates that the sodium composition of the AFFF concentrate is reduced when it is exposed to the materials of interest. Moreover, it can be observed that the amount of sodium reduction is diverse in all samples. This further demonstrates that the severity of the effects caused by the materials on the foam's stability varies greatly.

Table 4.2: Chemical elements of AFFF concentrate.

Element	Chemical symbol	Composition in PPM			
		Sample ID:			
		1	2	3	4
Sodium	Na	2302	2332	2349	2354
Sulphur	S	92	89	94.2	94.7

Similar occurrences can be observed with sulphur. Referring to Table 4.2, it is observed that the elemental composition of sulphur in pure AFFF decreases when it reacts with various materials. Consequently, it is evident that the reaction of the three materials with the AFFF

concentrate reduces the surfactants (sodium alkyl sulfate). This increases the surface tension of the water within the concentrate, reducing the stability of the foam. Moreover, it can be seen that the sodium alkyl sulphate was immensely reduced when the AFFF concentrate was in contact with mild steel (Sample 1). These findings correlate with FTIR analyses, which confirmed the presence of isothiocyanate N=C=S stretching on the triple bond region at bands 2056 and 2060 cm^{-1}. This functional group confirmed the presence of sulphur in the AFFF concentrate when HDPE and stainless steel were immersed, but sulfur did not appear in the AFFF concentrate when mild steel was immersed.

In addition, the elementary findings further correlate with the gradual diffusion rate of surfactants due to the large particles discussed in 4.5.1. These findings are evidence that stainless steel and HDPE have a minimal effect on the foam ability and foam stability of AFFF. They further demonstrate that mild steel has a severe impact on the two performance parameters of AFFF due to the chemical elements' reactions with surfactants. However, further studies should be conducted to determine the precise causes of the negative effects of these materials, as this research is limited to the impacts or effects of the materials in AFFF concentrate. In this way, it will be uncomplicated to optimize these materials in such a way that they are compatible with the AFFF concentrate.

The ICP-AES used for the present research was not able to detect organic compounds. However, the functional groups revealed by FTIR spectra were sufficient to provide the key variations of the elements within the AFFF concentrate. The shifting of the C-F stretch observed in Section 4.2 confirmed that the materials of interest also affect the fluorine content that is present within the PFAS in AFFF concentrate. This alteration of fluorine is a huge setback for the performance parameters of AFFF. PFAS are responsible for forming an aqueous film on fire fuels, which effectively suffocates them by creating a barrier to any oxygen and cooling them to prevent hot fuels from reigniting [3]. Consequently, the alteration of fluorine within the AFFF concentrate greatly reduces the blanketing capabilities during firefighting. It is well known that PFAS are harmful to the environment and humans (carcinogenic). However, the AFFF is primarily chosen for its effective extinguishing capabilities due to PFAS. This implies that any alteration of fluorine within the AFFF concentrate yields unfavourable outcomes. Other

vital elements that influence the performance of AFFF are listed in Table 4.3 and concisely discussed.

Table 4.3: Chemical elements of AFFF concentrate.

Element	Chemical symbol	Composition in PPM Sample ID:			
		1	2	3	4
Aluminium	Al	0.9	0.2	0.5	1.1
Calcium	Ca	46	07	10	6.9
Iron	Fe	132	58	3.7	2.5
Potassium	K	04	03	2.8	2.4
Magnesium	Mg	27	03	2.4	2.3
Silicon	Si	07	07	11	10.6

Referring to Table 4.3, it is noticed that the iron content observed in pure AFFF concentrate increased when various materials were immersed. Initially, the iron concentration was 2.5 ppm; it then increased to 3.7 ppm, 58 ppm, and 132 ppm when HDPE, stainless steel, and mild steel were immersed, respectively. In general, the increase in the iron element predominantly implies the degradation or wearing of the material [28]. Consequently, this demonstrates that mild steel degrades immensely when in contact with the AFFF concentrate, as the iron element increases by 129.5 ppm. This is evidence that there is a severe reaction between AFFF concentrate and mild steel. The obvious reason for this could be the initiation of corrosion in mild steel when it was first exposed to environmental conditions before immersion in AFFF concentrate. On the other hand, HDPE and stainless steel underwent a similar process, with severity being the major difference. The iron element increased by 1.2 and 55.5 ppm when HDPE and stainless steel reacted with AFFF concentrate, respectively.

The other elements, such as calcium, potassium, and magnesium, are typically water additives. However, the concern is the variation of these elements across the four samples. Subsequently, the degradation of the materials made the AFFF concentrate impure, possibly influencing its firefighting capabilities. This is drawn from visual observation of the various AFFF

concentrates during the post-experimental work. Figure 4.11 depicts the state of pureness of the AFFF concentrate after the immersion of materials.

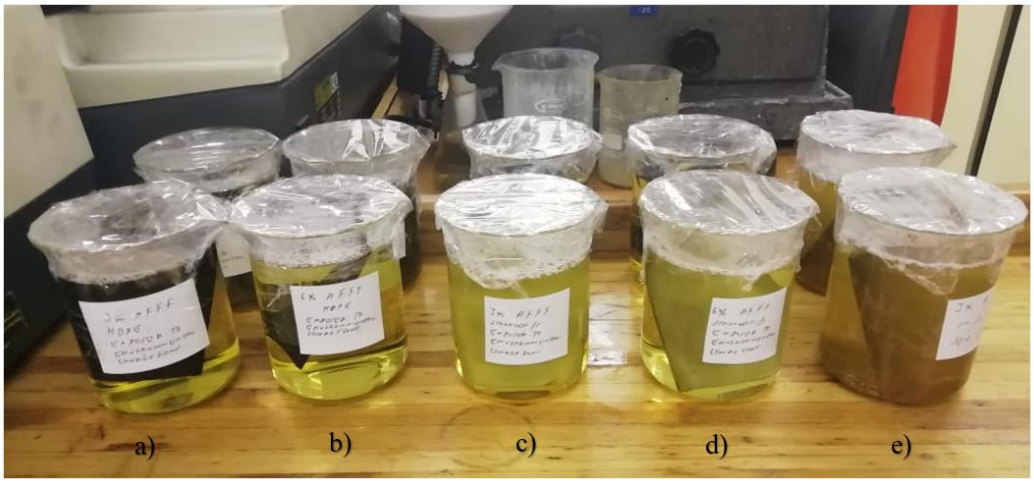

Figure 4.11: Pureness of AFFF concentrate after immersion of the materials.

It can be observed from Figure 4.11 that the purity of the samples varies greatly. Samples (a-b) are AFFF concentrates when HDPE was immersed, and samples (c-d) are when stainless steel was immersed. It is clear from these samples that there was no significant degradation of the materials. This is because the AFFF concentrate was able to maintain its pure yellowish colour during the interaction with these materials. However, when observing closely, it is noticed that samples a–b are purer than samples c–d. This is evidence that stainless steel also underwent the degradation process due to the increase in iron by 55.5 ppm, as suggested by Table 4.3. In contrast, sample (e) is the AFFF concentrate when mild steel was immersed. It can be visually observed that mild steel is immensely degraded when it interacts with AFFF concentrate. The AFFF concentrate's transition from a yellowish to a brownish colour serves as visual evidence of this. This is further justified by the large increase in iron of 129.5 ppm observed in Table 4.3. Although the precise performance parameters affected by this degradation cannot be determined, the reaction between mild steel and AFFF concentrate remains severe.

4.7 Conclusion

This chapter documented the results obtained using the FTIR, TEM, DLS, and ICP-AES instruments. Tests were conducted to determine the impact of mild steel, stainless steel, and HDPE on the performance parameters of AFFF. The analyses entangled the function groups,

particle shape, and size distribution, as well as the elemental composition of AFFF concentrate. Most of the tests conducted can be classified as successes concerning reliability. For each test, the results are illustrated in the form of graphs, pictures, calculations, or tables, as well as a discussion of any relevant observations or concerns arising from the results. AFFF performance parameters such as foam ability, foam stability, surface tension, foam drainage, and viscosity were all found to be statistically significant during the analyses. Among the three materials tested, mild steel was found to have the greatest impact on AFFF performance parameters. While stainless steel was the second 'severe' material, HDPE was the compatible material with only the ESC concerns.

CHAPTER 5: CONCLUSIONS AND FURTHER STUDIES

5.1 Introduction

This chapter presents the conclusion and recommendations for future work on this study. The impact of using mild steel, stainless steel, and HDPE as storage facilities for AFFF concentrate was analyzed. This was achieved by performing various tests on the materials and, therefore, conducting thorough analyses. The relevant literature review and findings were used to draw conclusions and make recommendations for future studies.

5.2 Findings from the Primary Research

Findings from the primary research were presented in relation to research questions that this study strived to answer.

- The functional group of C-F stretch shifted when mild steel, stainless steel, and HDPE were immersed. The largest shift was observed when the AFFF concentrate interacted with mild steel. The elemental analyses further support this reaction.

- In a pure state, AFFF concentrate possesses a single crystalline structure, whereas when the three materials were immersed, it critically changed to a polycrystalline structure. Most of the crystal structural changes occurred when AFFF concentrate reacted with mild steel.

- The spherical particle shape of AFFF concentrate was not altered by reacting with mild steel, stainless steel, or HDPE. This implies that the AFFF concentrate can retain its viscosity after reacting with the three materials.

- The diameter of the particles in the pure AFFF concentrate was altered when it reacted with the materials of interest. The particle size had a percentage increase of 36.419% and 12.549% when stainless steel and HDPE were immersed, respectively. On the other hand, when mild steel was immersed, the particle size increased immensely by 655.808 nm. Based on this, it was discovered that the reaction of mild steel with AFFF concentrate reduces the diffusion rate of fluorosurfactant molecules, which has a significant impact on AFFF's foaming ability.

- Narrow peaks observed in the PSD when AFFF concentrate reacts with stainless steel or HDPE do not have a vital impact on the diffusion rate of fluorosurfactant molecules. It further demonstrated that the two materials do not influence the spreading ability of AFFF during firefighting.

- When AFFF concentrate reacted with mild steel, the PSD revealed a wide peak. This demonstrated that the spreading ability of AFFF might have been slightly reduced. This suggests that the alteration of PSD can cause a slight impact on the spreading capability of any aqueous concentrate [72].

- The elemental analyses demonstrated that the reaction of the AFFF concentrate with the materials of interest reduced the sulphur and sodium content of the concentrate. Consequently, this increases the surface tension of water with the AFFF solution and thus decreases the stability of foam during firefighting. However, the FTIR spectra analyses confirmed the presence of N-C-S when AFFF concentrate reacted with stainless steel and HDPE, but it did not appear when it reacted with mild steel.

- The fluorine element was reduced in the AFFF concentrate. This was confirmed by the FTIR spectra when observing the C-F stretch. This alteration is very harmful, as it reduces the blanketing capabilities of AFFF during firefighting.

- There was a massive degradation or wearing of mild steel when it interacted with AFFF concentrate. This was caused by the critical increase of the iron element during the chemical reaction. Additionally, the elemental report showed that stainless steel and HDPE also underwent the degradation process, but it was far less severe than in mild steel.

- The visual observation during the post-experimental work showed that the degradation of the materials influences the pureness of AFFF concentrate, thus possibly influencing the fighting capabilities.

5.3 Concluding Remarks

Based on the findings, it is clear that mild steel is not compatible with the AFFF concentrate. Although it is a relatively cheap option when selecting a storage tank for AFFF concentrate, some alterations within the tank should be made to avoid the degradation of AFFF. Stainless

steel could be an option as well, as it has minimal effects on the AFFF. The huge concern is that it is not economical, making it an unfeasible option. As a result, HDPE is a viable option for storing AFFF concentrate. However, as aforementioned, it has the setback of suffering from ESC. This is normally avoided by cross-linking the HDPE to produce cross-linked polyethene (XLPE). Nonetheless, more research should be conducted to validate its resistance to ESC. In addition, plastic materials have the fundamental advantage of being inexpensive.

In the 21st century, storage tanks are constructed using fibreglass. This material is gradually replacing the materials used for constructing the storage tanks due to several benefits, including being resistant to numerous chemicals [85]. As a consequence, fibre glass is undoubtedly a material to consider when selecting a storage tank for AFFF concentrate.

5.4 Areas for Further Research

The objectives of this research work were achieved. However, the outcome of the previous studies has shown that further studies should be conducted to improve on what has been done thus far. The following avenues were recommended for future studies:

- The study was limited to the impact of the three materials on any performance parameters of AFFF. It did not focus on the causes of these effects. Further research work should be conducted to thoroughly investigate the causes of the interaction between AFFF and mild steel, stainless steel, and HDPE. In this way, it will be uncomplicated to optimize these materials in such a way that they are compatible with the AFFF concentrate.

- Further research should focus on other materials that are also utilized to construct the tanks for storing the AFFF concentrate, such as fibreglass and cross-linked polyethene (XLPE). This will establish several alternatives for storing AFFF concentrate without causing any harm.

- Further studies should focus on the fabrication methods used to construct the AFFF concentrate storage facility. These methods may include welding, bolting, screwing, and moulding. The evaluation of these methods could be an essential optimization process, as the connection joints may greatly affect the product stored in the storage tank. Besides, the connection joints may further contribute to the failure of the storage tank.

- Based on the relevant literature provided in the primary research, further studies should be able to investigate the precise heat treatment methods that will alter the properties of these materials, especially mild steel, as it is inexpensive. This will ensure their compatibility with AFFF concentrate and be economical concurrently.

5.5 Conclusion

This chapter concluded the study and suggested areas for further research. Achieving the objectives and answering the research questions fulfilled the overall aim of the study. The study utilized critical data from a theoretical and practical base to determine the impact of the storage facility on the performance parameters of AFFF. Evaluation of the impact of mild steel, stainless steel, and HDPE in the AFFF concentrate storage tank was experimentally performed. The critical performance parameters of AFFF affected by these materials were determined. Based on the scientific phenomena and relevant literature, the study demonstrated how these parameters influence the performance of AFFF during firefighting circumstances in aviation fire protection.

REFERENCES

[1] D. N. Meldrum, J. R. Williams, and C. J. Conway, "Storage life and utility of mechanical fire-fighting foam liquids," *Fire Technol.*, vol. 1, no. 2, pp. 112–121, 1965, doi: 10.1007/BF02588481.

[2] R. Oguike, "Study of Fire Fighting Foam Agent From Palm Oil for Extinguishing of Petrol Fires," *Sci. Postprint*, vol. 1, no. 1, 2013, doi: 10.14340/spp.2013.12a0002.

[3] P. Adhikari, *Understanding Firefighting Foams*, no. April. 2018.

[4] X. Dauchy, V. Boiteux, C. Bach, C. Rosin, and J. Munoz, "Chemosphere Per- and poly-fluoroalkyl substances in firefighting foam concentrates and water samples collected near sites impacted by the use of these foams," *Chemosphere*, vol. 183, pp. 53–61, 2017, doi: 10.1016/j.chemosphere.2017.05.056.

[5] I. Tureková and K. Balog, "The Environmental Impacts of Fire-Fighting Foams," *Fire Sci. Technol.*, vol. 18, no. 29, pp. 111–120, 2010, doi: 10.2478/v10186-010-0033-z.

[6] J. L. Scheffey, R. L. Darwin, and J. T. Leonard, "Evaluating firefighting foams for aviation fire protection," *Fire Technol.*, vol. 31, no. 3, pp. 224–243, Aug. 1995, doi: 10.1007/BF01039193.

[7] HM Fire Service Inspectorate, "Fire Service Manual. Volume 1 Fire Service Technology, Equipment and Media," 2000.

[8] S. Wang, "Research on aqueous film-forming foam concentrate formulations and properties," *IOP Conf. Ser. Earth Environ. Sci.*, vol. 295, no. 3, pp. 1–4, 2019, doi: 10.1088/1755-1315/295/3/032072.

[9] AFFF Foam Concentrates - Chemguard, "Foaming properties." https://www.chemguard.com/fire-suppression/catalog/foam-concentrates/aqueous-film-forming-foam-afff/C306-MS.aspx (accessed Apr. 04, 2020).

[10] A. J. Laundess, M. S. Rayson, B. Z. Dlugogorski, and E. M. Kennedy, "Suppression Performance Comparison for Aspirated, Compressed-Air and In Situ Chemically Generated Class B Foams," *Fire Technol.*, vol. 48, no. 3, pp. 625–640, 2012, doi: 10.1007/s10694-010-0155-z.

[11] Z. Xi, "Experimental Investigation of the Innovative Foaming Device Using Gasas the Sole Power for Firefighting," *Environ. Sci. Saf. Eng.*, vol. 25, no. 4, pp. 326– 330, 2016, doi.org/10.1002/prs.11834.

[12] H. S. Mukunda and C. S. B. Dixit, "Phenomenological Model and Experimental Comparisons on Static Foam Drainage for Fire Fighting Foams," *Fire Sci. Technol.*, vol. 35, no. 1, pp. 1–17, 2016, doi: 10.3210/fst.35.1.

[13] D. Rie, J. Lee, and S. Kim, "applied sciences Class B Fire-Extinguishing Performance Evaluation of a Compressed Air Foam System at Different Air-to-Aqueous Foam Concentrate Mixing Ratios," *Appl. Sci.*, vol. 6, p. 191, 2016, doi:

10.3390/app6070191.

[14] Xiaoyang Yu, Ning Jiang, Xuyang Miao, Ruowen Zong, You-Jie Sheng, Changhai Li, Shouxiang Lu, "Formation of stable aqueous foams on the ethanol layer: Synergistic stabilization of fluorosurfactant and polymers," *Colloids and Surfaces A: Physicochemical and Engineering Aspects*, vol. 591, 2020, 124545. Doi:10.1016/j.colsurfa.2020.124545.

[15] H. Persson, *Fire Extinguishing Foams: Resistance Against Heat Radiation: project 609-903*. Swedish National Testing and Research Institute, SP-RAPP: Statens provningsansalts, 1992.

[16] T. J. Martin, "Fire-Fighting Foam Technology," in *Foam Engineering: Fundamentals and Applications*, 2nd ed., P. Stevenson, Ed. John Wiley and Sons, Incorporated, 2012, pp. 411–457.

[17] G. B. Geyer, *Evaluation of Aircrafts Ground Firefighting Agents and Techniques*. Department of Transport, Federal Aviation Administration, 1972.

[18] G. B. Geyer, L. M. Nert, and C. H. Urban, "Comparative evaluation of firefighting foam," United States Patent 790928043, 1979.

[19] K. M. Hinnant, M. W. Conroy, and R. Ananth, "Colloids and Surfaces A : Physicochemical and Engineering Aspects Influence of fuel on foam degradation for fluorinated and fluorine-free foams," *Colloids Surfaces A Physicochem. Eng. Asp.*, vol. 522, pp. 1–17, 2017, doi: 10.1016/j.colsurfa.2017.02.082.

[20] K. Osei-bonsu, N. Shokri, and P. Grassia, "Colloids and Surfaces A : Physicochemical and Engineering Aspects Foam stability in the presence and absence of hydrocarbons : From bubble- to bulk-scale," *Colloids Surfaces A Physicochem. Eng. Asp.*, vol. 481, pp. 514–526, 2015, doi: 10.1016/j.colsurfa.2015.06.023.

[21] H. Do, M. Brady, D. P. Telionis, P. P. Vlachos, and R. Yoon, "Numerical modelling and experiments of coarsening foam," *Int. J. Miner. Process.*, vol. 98, no. 1–2, pp. 66–73, 2011, doi: 10.1016/j.minpro.2010.10.008.

[22] M. Zhao *et al.*, "Improving the performance of fluoroprotein foam in extinguishing gasoline pool fires with addition of bromofluoropropene," *Fire Mater.*, vol. 40, no. November 2014, pp. 261–272, 2016, doi: 10.1002/fam.

[23] S. A. Milley, I. Koch, P. Fortin, J. Archer, D. Reynolds, and K. P. Weber, "Estimating the number of airports potentially contaminated with per fl fluoroalkyl and poly-fluoroalkyl substances from aqueous film forming foam : A Canadian example," vol. 222, no. May, pp. 122–131, 2018, doi: 10.1016/j.jenvman.2018.05.028.

[24] H. Person, B. Lonnermark, and A. Persson, "FOAMSPEX: Large Scale Foam Application—Modelling of Foam Spread and Extinguishment," *Fire Technol.*, vol. 39, pp. 347–362, 2003.

[25] E. Minay and A. Boccaccini, "Metals," in *Biomaterials, Artificial Organs and Tissue Engineering*, 1st, Ed. United States: Woodhead Publishing, 2005, pp. 15–25.

[26] M. G. Ceruti, “States of Matter and States of information,” in *International Society for Computers and their Applications (ICSA)*, 2002.

[27] R. Timings, “Engineering materials and heat treatment,” in *Fabrication and Welding Engineering*, Oxford: Elsevier Ltd, 2008, pp. 69–81.

[28] H. Mcarthur and D. Spalding, “Metal and alloys,” in *Engineering Materials and Science Properties, Uses, Degradation, Remediation*, Woodhead Publishing Limited, Ed. Cambridge: Horwood Publishing Limited, 2004, pp. 316–363.

[29] S. Mridha, “Metallic materials,” in *Materials Science and Materials Engineering*, Glasgow: Elsevier Inc., 2016, pp. 1–7.

[30] R.M.C Molabe, “Determining the optimum welding material of 3CR12 stainless steel,” University of Johannesburg, 2018.

[31] D. Torrington, “Metallic bonding,” *Siyavula Technology powered-learning*, 2020. https://www.siyavula.com/read/science/grade-10/chemical-bonding/06-chemical-bonding-05 (accessed Jun. 27, 2020).

[32] Jim Clark, “Metallic bonding,” *Chemistry libreTexts*, 2020. https://chem.libretexts.org/Bookshelves/Physical_and_Theoretical_Chemistry_Textbook_Maps/Supplemental_Modules_(Physical_and_Theoretical_Chemistry)/Chemical_Bonding/Fundamentals_of_Chemical_Bonding/Metallic_Bonding (accessed Jun. 28, 2020).

[33] A. M. Helmenstine, “Metallic Bond: Definition, Properties, and Examples,” *ThoughtCo.*, 2019. https://www.thoughtco.com/metallic-bond-definition-properties-and-examples-4117948 (accessed Jun. 28, 2020).

[34] W.Callister and D. Rethwisch, “Materials and Structure,” in *Materials Science & Engineering*, 9th ed., United States: John Wiley and Sons, 2014, p. 905.

[35] L. Li, M. Mahmoodian, C. Li, and D. Robert, “Effect of corrosion and hydrogen embrittlement on microstructure and mechanical properties of mild steel,” vol. 170, pp. 78–90, 2018, doi: 10.1016/j.conbuildmat.2018.03.023.

[36] R. Sadeghi, M. Amirnasr, S. Meghdadi, and M. Talebian, “Carboxamide derivatives as corrosion inhibitors for mild steel protection in hydrochloric acid concentrate,” *Corros. Sci.*, vol. 151, no. February, pp. 190–197, 2019, doi: 10.1016/j.corsci.2019.02.019.

[37] D. Olsen, “How To Evaluate Materials - Properties To Consider,” *Metal Tek International*, 2016.https://marketing.metaltek.com/smart-blog/how-to-evaluate-materials-properties-to-consider (accessed Jul. 06, 2020).

[38] M. Khebra, “AISI 1018 Mild / Low Carbon Steel.” AZO Materials, p. 3, 2019, https://www.azom.com/article.aspx?ArticleID=6115. (accessed Jun. 30, 2020).

[39] J. Abou-Jahjah and J. Dobránszky., “Mechanical Properties Improvement of Low Carbon Steel by Combined Heat Treatments,” *Metals Technology*. pp. 1–15, 2001, Available: real.mtak.hu/5650/1/1155611.pdf. (accessed July. 7, 2020).

[40] Y. A. Cengel, “Heat conduction equation,” in *Heat transfer, A practical approach*, 2nd ed., Boston, Mass: WBC McGraw-Hill, 1995, pp. 61–113.

[41] S. Islam, K. Otani, and M. Sakairi, “Effects of metal cations on mild steel corrosion in 10 mM Cl − aqueous concentrate,” *Corros. Sci.*, vol. 131, no. November 2017, pp. 17–27, 2018, doi: 10.1016/j.corsci.2017.11.015.

[42] T. Sourmail and H. K. D. H. Bhadeshia, “Stainless steels,” *University of Cambridge*, 2005. https://www.phase-trans.msm.cam.ac.uk/2005/Stainless_steels/stainless.html (accessed Jul. 07, 2020).

[43] G. George and H. Shaikh, *Introduction to Austenitic Stainless Steels*. Alpha Science International Ltd, 2002.

[44] H. Bhadeshia and R. Honeycombe, “Stainless Steel,” in *Steels: Microstructure and Properties*, 4th ed., United States of America: Elsevier Ltd, 2017, pp. 343–376.

[45] R. Gunn, “Physical and Mechanical Properties,” in *Duplex Stainless Steels: Microstructure, Properties and Applications*, R. . Gunn, Ed. Cambridge: Woodhead Publishing Limited, 1997, pp. 56–67.

[46] A. I. Karayan and H. Castaneda, “Weld decay failure of a UNS S31603 stainless steel storage tank,” *Eng. Fail. Anal.*, vol. 44, pp. 351–362, 2014, doi: 10.1016/j.engfailanal.2014.05.008.

[47] W. Grzesik, “MACHINABILITY OF ENGINEERING MATERIALS,” in *Advanced Machining Processes of Metallic Materials*, 2nd ed., Heather Cain, Ed. Amsterdam: Joe Hayton, 2008, pp. 183–196.

[48] S. A. H. Roslan, “Mixing Ratio on the Tensile Strength of High Density,” 2013.

[49] P. Nugent, “Rotational Molding,” in *Applied Plastics Engineering Handbook*, Second Edi., Reading, United States: Elsevier Inc., 2017, pp. 321–344.

[50] S. Kurtz and M. Manley, “Cross-Linked Polyethylene,” *Surg. Treat. Hip Arthritis Reconstr. Replace. Revis.*, no. November 2004, pp. 456–467, 2009, doi: 10.1016/B978-1-4160-5898-4.00061-6.

[51] L. H. Gabriel, “Non-metallic materials, ” *History and Physical Chemistry of HDPE*(accessed Sept. 16, 2020).

[52] S. T. Tamboli and S M. Mhaske, “Cross-Linked Polyethylene Cross-Linked Polyethylene,” *Encycl. Chem. Process.*, no. January, pp. 577–587, 2005, doi: 10.1081/E-ECHP-120007720.

[53] A. G. Andreopoulos and E. M. Kampouris, “Mechanical Properties of Crosslinked Polyethyelene,” *Appl. Polym. Sci.*, vol. 31, no. 4, pp. 1061–1068, 1986, doi: https://doi.org/10.1002/app.1986.070310407.

[54] H. L. R. Patrerson and A. Kandelbauer, “Crosslinked Thermoplastics,” in *Handbook of Thermoset Plastics*, 3rd ed., H. D. and S. H. Goodman, Ed. Oxford: Elsevier Inc., 2014.

[55] G. M. Carlomagno, “Cross-Linked Polyethylene Cross-Linked Polyethylene,” no. January 2015, 2005, doi: 10.1081/E-ECHP-120007720.

[56] D. Houston, “Test Methods for Evaluation of ESCR of Plastics,” 2016. https://docplayer.net/21098298-3-test-methods-for-evaluation-of-escr-of-plastics.html (accessed Jun. 19, 2021).

[57] M. Gao, et al. "Nanostructured metal chalcogenides: synthesis, modification, and applications in energy conversion and storage devices." *Chemical Society Reviews* 42.7 (2013): 2986-3017.

[58] B. Borisova and K. Jörg, "Environmental stress-cracking resistance of LDPE/EVA blends." *Macromolecular Materials and Engineering* 288.6 (2003): 509-515.

[59] J.R Brady and F. Robert, "A fracture mechanical analysis of fouling release from nontoxic antifouling coatings." *Progress in organic coatings* 43.1-3 (2001): 188-192.

[60] Al-Saidi, F. Lutfi, M. Kell, and A. Kristoffer. "Environmental stress cracking resistance. Behaviour of polycarbonate in different chemicals by determination of the time-dependence of stress at constant strains." *Polymer Degradation and Stability* 82.3 (2003): 451-461.

[61] J. Cazenave, et al. "Short-term mechanical and structural approaches for the evaluation of polyethylene stress crack resistance." *Polymer* 47.11 (2006): 3904-3914.

[62] S.M. Henrichs, "Early diagenesis of organic matter: the dynamics (rates) of cycling of organic compounds." *Organic Geochemistry: Principles and Applications*. Boston, MA: Springer US, 1993. 101-117.

[63] T. Liang, N. Constanze, and R. Tobias, "Introduction of fluorine and fluorine-containing functional groups." *Angewandte Chemie International Edition* 52.32 (2013): 8214-8264.

[64] M. Fan, D. Dasong and H. Biao, "Fourier transform infrared spectroscopy for natural fibres." *Fourier transform-materials analysis* 3 (2012): 45-68.

[65] N. Jaggi, and D. R. Vij. "Fourier transform infrared spectroscopy." *Handbook of Applied Solid State Spectroscopy*. Boston, MA: Springer US, 2006. 411-450.

[66] M.S. Wheal, O.F. Teresa, and T. P Lyndon, "A cost-effective acid digestion method using closed polypropylene tubes for inductively coupled plasma optical emission spectrometry (ICP-OES) analysis of plant essential elements." *Analytical Methods* 3.12 (2011): 2854-2863.

[67] J.P. Coates, ‘The Interpretation of Infrared Spectra: Published Reference Sources’, *Appl. Spectrosc. Rev.*, 31(1 – 2), 179 – 192 (1996).

[68] H. C. Kolb, M. G. Finn, and K. B. Sharpless, "Click chemistry: diverse chemical function from a few good reactions." *Angewandte Chemie International Edition* 40.11 (2001): 2004-2021.

[69] A. Karau, C. Benken, J. Thömmes, and M. R. Kula, “The Influence of Particle Size

Distribution and Operating Conditions on the Adsorption Performance in Fluidized Beds" *Biotechnology and Bioengineering*, vol. 55, no. 1, pp. 54-64, 2000, doi.org/10.1002/(SICI)1097-0290(19970705)55:1<54::AID-BIT7>3.0.CO;2-W

[71] K.L. Klein, I.M. Anderson, and N. de Jonge, "Transmission electron microscopy with a liquid flow cell," *J. Microsc*. 242 (2) (2011) 117–123.

[73] M.J. Baker et al., "Using Fourier transform IR spectroscopy to analyze biological materials." *Nature protocols* 9.8 (2014): 1771-1791.

[74] P. Gans, *Vibrating Molecules: an Introduction to the Interpretation of Infrared and Raman Spectra*, Chapman & Hall, London, 1975.

[75] L.J. Bellamy, *Advances in Infrared Group Frequencies, Infrared Spectra of Complex Molecules*, Chapman & Hall, New York, vol. 2, 1980.

[76] N.B. Colthrup, L.H. Daly, and S.E. Wiberley, *Introduction to Infrared and Raman Spectroscopy*, Academic Press, San Diego, CA, 1990.

[77] I.A. Mudunkotuwa, A. Al Minshid, and V.H. Grassian, ATR-FTIR spectroscopy as a tool to probe surface adsorption on nanoparticles at the liquid-solid interface in environmentally and biologically relevant media., Analyst. 139 (2014) 870–81. doi:10.1039/c3an01684f.

[78] J.S. Gaffney, N.A. Marley, and D.E. Jones, Fourier Transform Infrared (FTIR) Spectroscopy, Charact. Mater. (2012) 1104–1135. doi:10.1002/0471266965.

[79] S. Bandyopadhyay, "Characterization of Metal Nanoparticles." in *Fabrication and Application of Nanomaterials*. 1st ed. New York: McGraw-Hill Education.,2019

[80] W.D. Pyrz and D.J. Buttrey, "Particle size determination using TEM: a discussion of image acquisition and analysis for the novice microscopist, " *Langmuir 24* (2008) 11350–11360, doi: 10.1021/la801367j.

[81] Zhuoqing An, Yanling Zhang, Qi Li, Haoran Wang, Zhancheng Guo, and Jesse Zhu, "Effect of particle shape on the apparent viscosity of liquid-solid suspensions," *Powder Technology*, vol. 328, pp.199-206, 2018, doi.org/10.1016/j.powtec.2017.12.019.

[82] H. D. Koca, S. Doganay, A. Turgut, I. H. Tavman, R. Saidur, and I. M. Mahbubul, "Effect of particle size on the viscosity of nanofluids: A review" *Renewable and Sustainable Energy Reviews*, vol.82, pp. 1664-1674, 2018,

[83] I. De la Calle, P. Pérez-Rodríguez, D. Soto-Gómez, and J. E. López-Periago, "Detection and characterization of Cu-bearing particles in throughfall samples from vine leaves by DLS, AF4-MALLS (-ICP-MS) and SP-ICP-MS," *Microchemical Journal*, vol.133, pp. 293-301,2017, doi.org/10.1016/j.microc.2017.03.034.doi.org/10.1016/j.rser.2017.07.016.

[84] L. M. F. Ramirez, C. Rihouey, F. Chaubet, D. Le Cerf, and L. Picton, "Characterization of dextran particle size: How frit-inlet asymmetrical flow field-flow fractionation (FI-AF4) coupled," *Chromatography A*, vol.1653, pp. 462404, 2021,

doi.org/10.1016/j.chroma.2021.462404.

[85] A. Avdeeva, I. Shlykova, M. Perez, M. Antonova, and S. Belyaeva, “Chemical properties of reinforcing fiber glass in aggressive media,” *Engineering and Technology*, vol. 53, 2016, doi:10.1051/matecconf/20165301004.

APPENDICES

Appendix A: Specifications of AFFF.

AQUA FILM FORMING FOAM - A.F.F.F

- Filmosin 1060, Filmosin 1060 Cold
- Filmosin 1030, Filmosin 1030 Cold
- Filmosin 1010

Filmosins are aqua film forming fire fighting foam concentrates produced carefully controlled blend of high activity selective special fluorocarbon and hydrocarbon surfactants with various solvents, preservatives and stabilizers.

Specification	Filmosin 1060		Filmosin 1030		Filmosin 1010	
Appearance	Yellow Clear liquid		Yellow Clear liquid		Yellow Clear liquid	
Density g/ml. at 20 °C	1.01 min.		1.02 min.		1.04 min.	
pH Value at 20 °C	6.00 - 9.50		6.00 - 9.50		6.00 - 9.50	
Viscosity $mm^2/sec.$ at 20 °C	3.00 min.		5.00 min.		10.00 min.	
Pour Point °C	- 5.00 min.		- 5.00 min.		- 10.00 min.	
Sedimentation v/v %	0.05		0.05		0.05	
Expansion	7.00 min.		7.00 min.		7.00 min.	
50 % Drainage Time minute	5.00 min.		5.00 min.		6.50 min.	
Surface Tension mN/m	20.00 approx.		19.00 approx.		19.00 approx.	
Proportioning %	6.0		3.0		1.0	
Film Forming	+		+		+	
Properties	**Low**	**Medium**	**Low**	**Medium**	**Low**	**Medium**
Covering Effect	++	++	++	++	++	++
Flowability	++	++	++	++	++	++
Gas Tightness	++	++	++	++	++	++
Re-Ignitions	++	++	++	++	++	++
Adhesiveness	-	-	-	-	-	-
Isolating Effect	0	0	0	0	0	0
Cooling Effect	++	+	++	+	++	+
Extinguishing Time	++	++	++	++	++	++
Foam Weight	++	0	++	0	++	0
Foam High	-	0	-	0	-	0
Wetting Effect	++	++	++	++	++	++
Film Formation	++	++	++	++	++	++
Alcohol Resistance	-	-	-	-	-	-
Polymer Film Formation	-	-	-	-	-	-
Non-Toxicity	0	0	0	0	0	0
Non-Corrosiveness	+	+	+	+	+	+
Biodegradability	+	+	+	+	+	+
Applicability With Every Kind of Water	+	+	+	+	+	+

► ++ Good ► + Medium ► 0 Low ► - Not

Figure A.1: Original specifications of AFFF concentrate [3].

Appendix B: Properties and specifications of steels.

Carbon Steel

Material	Condition	Yield Strength [ksi]	Ultimate Strength [ksi]	Elongation %	Elastic Modulus [psi]	Density [lb/in^3]	Poisson's Ratio
AISI 1020	Hot Rolled	32	50	25	29e6	0.283	0.32
	Cold Worked	60	70	5			
	Stress Relieved	50	65	10			
	Annealed	28	48	30			
	Normalized	34	55	22			
AISI 1045	Hot Rolled	45	75	15	29e6	0.283	0.32
	Cold Worked	80	90	5			
	Stress Relieved	70	80	8			
	Annealed	35	65	20			
	Normalized	48	75	15			
ASTM A36		36	58	21	29e6	0.283	0.3
ASTM A516	Grade 70	38	70	17	29e6	0.283	0.3

Figure B.2: Mechanical and physical properties of mild steel (AISI 1020) [37]

Designation	Cr	Ni	C	Mn	Si	P	S	Other	UTS / MPa	Elongation / %
Type 329	28.0	6.0	0.10	2.0	1.0	0.04	0.03	1.5 Mo	724	25
Type 326	26.0	6.5	0.05	1.0	0.6	0.01	0.01	0.25 Ti	689	35
2RE60	18.5	4.5	0.02	1.5	1.6	0.01	0.01	2.5 Mo	717	48
IC378	21.8	5.5	0.03	1.38	0.40	0.03	0.01	3.0 Mo 0.18 Cu 0.07 V 0.14 N		
IC381	22.1	5.8	0.02	1.92	0.48	0.03	0.01	3.2 Mo 0.07 Cu 0.13 V 0.14 N		
A219	25.6	9.4	0.03	0.70	0.60	0.02	0.01	4.1 Mo 0.27 N		

Figure B.3: Weighed composition of duplex stainless steel [42]

Stainless Steel

Material	Class	Condition	Yield Strength [ksi]	Ultimate Strength [ksi]	Elongation %	Elastic Modulus [psi]	Density [lb/in^3]	Poisson's Ratio
AISI 201	Austenitic	Annealed	40	75	40	28e6	0.289	0.27
AISI 202	Austenitic	Annealed	40	75	40	28e6	0.289	0.27
AISI 302	Austenitic	Annealed	30	75	40	28e6	0.289	0.27
AISI 304	Austenitic	Annealed	30	75	40	28e6	0.289	0.29
AISI 304L	Austenitic	Annealed	25	70	40	28e6	0.289	0.28
AISI 316	Austenitic	Annealed	30	75	40	28e6	0.289	0.26
AISI 316L	Austenitic	Annealed	25	70	40	28e6	0.289	0.26
AISI 405	Ferritic		25	60	20	29e6	0.282	0.28
AISI 410	Martensitic	Annealed	40	70	16	29e6	0.282	0.28
		Quenched & Tempered	80	100	12			
AISI 430	Ferritic		30	60	20	29e6	0.282	0.28
AISI 446	Ferritic	Annealed	40	65	16	29e6	0.282	0.28
15-5PH	Martensitic precipitation hardenable	H900	170	190	10	28.5e6	0.283	0.27
		H1025	145	155	12			
		H1150	105	135	16			
17-4PH	Martensitic precipitation hardenable	H900	170	190	10	28.5e6	0.282	0.27
		H1025	145	155	12			
		H1150	105	135	16			
17-7PH	Semiaustenitic precipitation hardenable	TH1050	150	177	6	29e6	0.276	0.28
A-286	Austenitic precipitation hardenable		95	140	15	29.1e6	0.287	0.31
Alloy 2205	Duplex Austenitic-Ferritic		65	95	25	28.5e6	0.287	0.27
Ferrallium 255	Duplex Austenitic-Ferritic		80	110	15	28.5e6	0.287	0.27

Figure B.4: Mechanical and physical properties of stainless steel [44]

Appendix C: Role of microstructural constituents.

Microstructural constituents	Dependent on/characteristics (selection)	Responsible for (examples)
Vacancies	Temperature, deformation	Hardening at low temperatures; diffusion processes at elevated temperatures; diffusional creep
Dislocations	Deformation, temperature, recovery and recrystallization processes; at elevated temperatures edge dislocations may climb, and leave their slip planes	Plastic deformation; strength is controlled by their number and motion; driving force for recrystallization; dislocation creep
Stacking faults	Crystal structure, alloying	Mobility of dislocations, for example, climb of edge dislocations and cross-slip of screw dislocations is hampered
Mechanical twins	Stacking fault energy, deformation, temperature	Additional deformation mechanism at low temperatures and/or high strain rates
Subgrains/domains	Deformation, temperature, stacking fault energy/ordered crystal structure; antiphase boundary energy	Work hardening, creep, creation of antiphase boundaries
Grain boundaries	Lattice orientation between neighboring grains; subdivision in small-angle, medium-angle and high-angle grain boundaries	Work hardening by acting as barriers to slip from one grain to the next; segregation site of impurity atoms
Phase boundaries	Alloy system, composition, phase stability at elevated temperatures	Strengthening effects, for example, in duplex or multiphase steels
Grains	Alloy system, type of nucleation, processing, deformation, heat treatment, recrystallization	Strengthening (see grain boundaries) but ductility is maintained; grain boundary sliding at elevated temperatures (creep, superplasticity)
Annealing twins	Stacking fault energy; characteristic of face-centered cubic materials exhibiting a low stacking fault energy	Lowering of total boundary energy during grain growth
Precipitates/ dispersoids	Alloy system, composition, heat treatment, processing; the interface between particle and matrix can be coherent, semicoherent, or incoherent	Increase in strength by the interaction of moving dislocation; dislocations can loop, cut through or cross-slip the particles at ambient temperatures; at elevated temperatures the dislocations can surmount the particles by climb processes

Figure C.5: Role of microstructural constituents on metallic materials [58].

Appendix D: Full annealing temperature cycle.

AISI steel	Annealing Celsius temperature	Cooling cycle from Celsius	To	Hardness range HB
1018	855–900	855	705	111–149
1020	855–900	855	700	111–149
1025	855–900	855	700	111–187
1030	845–885	845	650	126–197
1040	790–870	790	650	137–207
1050	790–870	790	650	156–217
1060	790–845	790	650	156–217
1070	790–845	790	650	167–229
1080	790–845	790	650	167–229
1090	790–830	790	650	167–229

Figure D.6: Full annealing temperature cycle of popular steel and hardness range [66]

Appendix E: Effect of changing various substances in PE.

EFFECTS OF CHANGES IN DENSITY, MELT INDEX AND MOLECULAR WEIGHT DISTRIBUTION			
Property	As Density Increases, Property:	As Melt Index Increases, Property:	As Molecular Weight Distribution Broadens, Property:
Tensile Strength (At Yield)	Increases	Decreases	
Stiffness	Increases	Decreases Slightly	Decreases Slightly
Impact Strength	Decreases	Decreases	Decreases
Low Temperature Brittleness	Increases	Increases	Decreases
Abrasion Resistance	Increases	Decreases	
Hardness	Increases	Decreases Slightly	
Softening Point	Increases		Increases
Stress Crack Resistance	Decreases	Decreases	Increases
Permeability	Decreases	Increases Slightly	
Chemical Resistance	Increases	Decreases	
Melt Strength		Decreases	Increases
Gloss	Increases	Increases	Decreases
Haze	Decreases	Decreases	
Shrinkage	Decreases	Decreases	Increases

Figure E.7: The effect of changes in density, melt index, and molecular weight distribution on the properties of PE [75]

CELL CLASSIFICATIONS (SEE ASTM D 3350)			
Property	**ASTM Specification**	**Classification**	**Classification Requirement**
Density	**ASTM D 1505** – Test Method for Density of Plastics by the Density-Gradient Technique	**3**	0.941-0.955 gm/cm3
Melt index (MI)	**ASTM D 1238** – Test Method for Flow Rates of Thermoplastics by Extrusion Plastometer	**3**	0.4 > MI ≥ 0.15
Flexural modulus (E_f)	**ASTM D 790** – Test Method for Flexural Properties of Unreinforced and Reinforced Plastics and Electrical Insulating Materials	**5**	758 ≤ E_f <1103 MPa 110,000 ≤ E_f< 160,000 psi
Tensile strength (f_t)	**ASTM D 638** – Test Method for Tensile Properties of Plastics	**4**	21 ≤ ft < 24 MPa 3000 ≤ f_t< 3500 psi
Slow crack growth resistance Environmental stress crack resistance (ESCR)	**ASTM D 1693** – Test Method for for Environmental Stress-Cracking of Ethylene Plastics	**2**	test condition B, 24 hr duration 50% failure (max)
Hydrostatic Strength Classification Hydrostatic Design Basis (HDB)	**ASTM D 2837** – Obtaining Hydrostatic Design Basis for Thermoplastic Pipe Materials	**0**	(not pressure rated)
Color (C)	(not specified by ASTM)	**C**	2% ≤ C ≤ 5%

Figure E.8: Cell classifications for PE [76].

Appendix F: Chemical elements report.

SCROOBY'S LABORATORY SERVICE (PTY) Ltd

Spectrographic, Chemical and Mechanical Testing of Materials

Established 1999 TEL: 011 425 1074 / 0116 P O Box 13401
21 O'Reilly Merry St CELL: 082 925 0115 Northmead
Rynfield Benoni 1501 1511
VAT No: 4390188391 / REG No: 2022/711019/07 www.scroobyslab.co.za

CERTIFICATE of ANALYSIS

Durban University of Technology (DUT)
P.O. Box 4995
King Dinizulu
Eshowe
ATTENTION: Mr Nhlanhla Khanyi

Date Received: 06 October 2022
Date Tested: 11 October 2022
Date Reported: 26 October 2022
Order No:
Reference No: 32059/1

ELEMENT	Reported As:	Composition in PPM Sample ID: #1	#2	#3
Silver	Ag	≤ 0.1	≤ 0.1	≤ 0.1
Aluminium	Al	0.9	0.2	0.5
Arsenic	As	≤ 0.1	≤ 0.1	≤ 0.1
Boron	B	≤ 0.1	0.3	0.2
Barium	Ba	≤ 0.1	≤ 0.1	0.9
Berrylium	Be	≤ 0.1	≤ 0.1	≤ 0.1
Bithmuth	Bi	≤ 0.1	0.4	0.3
Calcium	Ca	46.0	7.0	10.0
Cadmium	Cd	≤ 0.1	≤ 0.1	≤ 0.1
Cobalt	Co	≤ 0.1	≤ 0.1	≤ 0.1
Chrome	Cr	≤ 0.1	≤ 0.1	≤ 0.1
Copper	Cu	≤ 0.1	0.3	0.5
Iron	Fe	132	158	3.7
Mercury	Hg	≤ 0.1	≤ 0.1	≤ 0.1
Potasium	K	4.0	3.0	2.8
Lithium	Li	≤ 0.1	≤ 0.1	≤ 0.1
Magnesium	Mg	27.0	3.0	3.4
Manganese	Mn	2.0	3.0	≤ 0.1
Molybdenum	Mo	≤ 0.1	≤ 0.1	≤ 0.1
Sodium	Na	2302	2332	2349
Noibium	Nb	≤ 0.1	2.0	≤ 0.1
Nickel	Ni	≤ 0.1	≤ 0.1	0.2
Phosphorous	P	≤ 0.1	≤ 0.1	0.7
Lead	Pb	≤ 0.1	0.2	0.2
Sulphur	S	92.0	89.0	94.2
Antimony	Sb	≤ 0.1	≤ 0.1	≤ 0.1
Selenium	Se	≤ 0.1	2.0	0.8
Silicon	Si	7.0	7.0	11.0
Tin	Sn	≤ 0.1	≤ 0.1	≤ 0.1
Strontium	Sr	≤ 0.1	≤ 0.1	≤ 0.1

Figure F.9: Chemical elements of samples 1-3.

SCROOBY'S LABORATORY SERVICE (PTY) Ltd

Spectrographic, Chemical and Mechanical Testing of Materials

Established 1999 TEL: 011 425 1074 / 0116 P O Box 13401
21 O'Reilly Merry St CELL: 082 925 0115 Northmead
Rynfield Benoni 1501 1511
VAT No: 4390188391 / REG No: 2022/711019/07 www.scroobyslab.co.za

CERTIFICATE of ANALYSIS

Durban University of Technology (DUT)
P.O. Box 4995
King Dinizulu
Eshowe
ATTENTION: Mr Nhlanhla Khanyi

Date Received: 06 October 2022
Date Tested: 11 October 2022
Date Reported: 26 October 2022
Order No:
Reference No: 32059/2

ELEMENT	Reported As:	Composition in PPM Sample ID: #4	#5
Silver	Ag	≤ 0.1	≤ 0.1
Aluminium	Al	1.1	≤ 0.1
Arsenic	As	≤ 0.1	≤ 0.1
Boron	B	0.2	≤ 0.1
Barium	Ba	0.7	1.1
Berrylium	Be	≤ 0.1	≤ 0.1
Bithmuth	Bi	0.2	0.3
Calcium	Ca	6.9	6.2
Cadmium	Cd	≤ 0.1	≤ 0.1
Cobalt	Co	≤ 0.1	≤ 0.1
Chrome	Cr	≤ 0.1	≤ 0.1
Copper	Cu	0.4	≤ 0.1
Iron	Fe	2.5	2.4
Mercury	Hg	≤ 0.1	≤ 0.1
Potasium	K	2.4	3.0
Lithium	Li	≤ 0.1	≤ 0.1
Magnesium	Mg	2.3	2.3
Manganese	Mn	≤ 0.1	≤ 0.1
Molybdenum	Mo	≤ 0.1	≤ 0.1
Sodium	Na	2354	2324
Noibium	Nb	≤ 0.1	0.6
Nickel	Ni	≤ 0.1	≤ 0.1
Phosphorous	P	≤ 0.1	≤ 0.1
Lead	Pb	0.4	≤ 0.1
Sulphur	S	94.7	94.1
Antimony	Sb	≤ 0.1	≤ 0.1
Selenium	Se	1.1	0.6
Silicon	Si	10.6	7.4
Tin	Sn	≤ 0.1	≤ 0.1
Strontium	Sr	≤ 0.1	≤ 0.1

Figure F.10: Chemical elements of sample 4.